

ASSOCIATION AND INTERACTION OF SERUM
ALBUMIN WITH LUNG SURFACTANT EXTRACT

CENTRE FOR NEWFOUNDLAND STUDIES

**TOTAL OF 10 PAGES ONLY
MAY BE XEROXED**

(Without Author's Permission)

SANGEETHA VIDYASANKAR

Association and Interaction of Serum Albumin with Lung Surfactant Extract



Sangeetha Vidyasankar (B.Sc. Hons)

Oct. 2004, Memorial University of Newfoundland

Submitted in partial fulfillment of the requirements for the degree of Master of Science

Department of Biochemistry

Memorial University of Newfoundland

St. John's, NL A1B 3X9

2004



Library and
Archives Canada

Published Heritage
Branch

395 Wellington Street
Ottawa ON K1A 0N4
Canada

Bibliothèque et
Archives Canada

Direction du
Patrimoine de l'édition

395, rue Wellington
Ottawa ON K1A 0N4
Canada

0-494-06666-0

Your file *Votre référence*
ISBN:
Our file *Notre référence*
ISBN:

NOTICE:

The author has granted a non-exclusive license allowing Library and Archives Canada to reproduce, publish, archive, preserve, conserve, communicate to the public by telecommunication or on the Internet, loan, distribute and sell theses worldwide, for commercial or non-commercial purposes, in microform, paper, electronic and/or any other formats.

The author retains copyright ownership and moral rights in this thesis. Neither the thesis nor substantial extracts from it may be printed or otherwise reproduced without the author's permission.

AVIS:

L'auteur a accordé une licence non exclusive permettant à la Bibliothèque et Archives Canada de reproduire, publier, archiver, sauvegarder, conserver, transmettre au public par télécommunication ou par l'Internet, prêter, distribuer et vendre des thèses partout dans le monde, à des fins commerciales ou autres, sur support microforme, papier, électronique et/ou autres formats.

L'auteur conserve la propriété du droit d'auteur et des droits moraux qui protègent cette thèse. Ni la thèse ni des extraits substantiels de celle-ci ne doivent être imprimés ou autrement reproduits sans son autorisation.

In compliance with the Canadian Privacy Act some supporting forms may have been removed from this thesis.

While these forms may be included in the document page count, their removal does not represent any loss of content from the thesis.

Conformément à la loi canadienne sur la protection de la vie privée, quelques formulaires secondaires ont été enlevés de cette thèse.

Bien que ces formulaires aient inclus dans la pagination, il n'y aura aucun contenu manquant.


Canada

ABSTRACT

Lung surfactant (LS) stabilizes the alveoli during normal respiration by reducing surface tension of the alveolar air-water interface. Among other diseases, dysfunction of the material occurs in acute respiratory distress syndromes (ARDS). During ARDS, plasma proteins leaked from capillaries inhibit LS surface activity. As models for ARDS, bovine lipid extract surfactant (BLES) and dipalmitoylphosphatidylcholine (DPPC) in monolayer and bilayer dispersions, with and without bovine serum albumin (BSA), were studied. The studies were conducted using Langmuir and adsorption surface balances (monolayer), atomic force microscopy (AFM), differential scanning calorimetry (DSC), transmission electron microscopy (TEM) and Fourier transform infrared spectroscopy (FTIR). Surface balance studies suggested that BSA inhibited surfactant adsorption to the air-water interface to form monolayer films, and such films did not reach low surface tension upon compression. AFM showed the appearance of well defined gel-like or condensed domains in films of BLES alone, but with BSA added, these domains appeared less defined, more numerous, and other fluid-like new domains were also detected. With DSC, BLES (2 mgs/ml) bilayer dispersions showed a broad gel to liquid crystalline phase transition between 20-40°C, and addition of BSA (12.5-250 wt % of BLES lipids) to BLES (or DPPC) made the transition more diffuse suggesting protein interactions with the bilayer. TEM studies showed elongation of BLES multilamellar vesicles and only minor alterations of such structures with the addition of BSA. FTIR of similar BLES/BSA dispersions suggested that BSA associated with the head group

regions of the phospholipid and also affected the hydrophobic tail regions, as monitored from CH_2 , $\text{C}=\text{O}$ and PO_4^- vibrational stretching modes. This study suggests that albumin inhibits surfactant by perturbing surfactant lipid packing in monolayers and bilayers. Such alterations may lead to poor surface activity of LS as found in ARDS and other diseases.

ACKNOWLEDGEMENTS

I would like to thank my supervisor Dr. Nag for his guidance, support, advice, and consideration during the course of my Masters project. I would also like to thank Dr. Keough for being my co-supervisor, and a member of my supervisory committee, and providing me advice and guidance with my experiments and thesis. In addition, I would like to thank my other supervisory committee member Dr. Davis for the guidance and help he has provided me in writing this thesis.

I would like to thank Dr. Nathan Rich for his help with the monolayer balance, and Dr. Joe Banoub for his assistance in mass spectrometry. Furthermore, I would like to thank Lisa Lee for her assistance in electron microscopy, and Linda Windsor and Kai Zhang for their assistance in FTIR and mass spectrometry. As well, a special thank you to Dr. Robert Harbottle for providing the AFM and TOF-SIMS images. I would also like to thank Dr. Mike Morrow, Dr. Valerie Booth, and Dr. David Heeley for their suggestions.

A special thank you goes out to June Stewart, Marie Codner, and Donna Jackman of the Keough lab for all their help with DSC, and many other lab techniques.

I would like to thank the former and present members of the Nag lab: Pam, Erin, Ravi, Kylie, Stephanie, and Lynn for their support, assistance, and most of all friendship during my program.

Furthermore, I'd like to thank the School of Graduate Studies and the Department of Biochemistry for allowing me this opportunity.

This study was supported by grants from a CIHR-New Investigator award to K. Nag and Health Canada to K. Keough. The research was also supported in part by grants from the Regional Partnership Programme by CEDA Newfoundland, Technology Development Programme, and Health and Community Services of Newfoundland. The grant for the purchase of a Raman and atomic force microscope was from CFI new opportunity research grants to K. Nag. We (K. Nag and I) would also especially like to thank Dr. David Bjarnson of BLES Biochemicals for his generous gifts of BLES for research used in the study.

Last, but not least, I would like to thank my family and friends for their support.

TABLE OF CONTENTS

Abstract	i
Acknowledgements	iii
Table of Contents	v
List of Figures	vii
List of Abbreviations and Symbols used	ix
Chapter 1: INTRODUCTION	1
1.1. Surfactant	1
1.2. Composition of Surfactant	2
1.2.1. Lipids	2
1.2.2. Proteins	4
1.3. Surfactant Life Cycle	8
1.4. Acute Respiratory Distress Syndrome	11
1.5. Lung Surfactant and ARDS	15
1.6. Bovine Lipid Extract Surfactant	19
1.7. Albumin	20
1.8. Present Study	24
Chapter 2: MATERIALS AND METHODS	25
2.1. Materials	25
2.2. Organic Extraction of BLES lipids and proteins	26
2.3. Preparation of Buffer	27
2.4. Techniques	27
2.4.1. Mass Spectrometry	27
2.4.2. Surface Balance (Monolayer) Studies	29
2.4.3. Atomic Force Microscopy	30
2.4.4. Differential Scanning Calorimetry	32
2.4.5. Electron Microscopy	33
2.4.6. Fourier Transform Infrared Spectroscopy	33
Chapter 3: RESULTS	35
3.1. Mass Spectrometry	35

3.2 Monolayer Experiments	38
3.3 AFM Experiments	52
3.4 TOF-SIMS	63
3.5 DSC Experiments	66
3.6 Transmission Electron Microscopy	77
3.7 FTIR Experiments	77
Chapter 4: DISCUSSION	93
4.1 Mass Spectrometry	98
4.2 Surface Balance (Monolayer) Studies	100
4.3 AFM and TOF-SIMS	103
4.4 Differential Scanning Calorimetry	105
4.5 Transmission Electron Microscopy	108
4.6 Fourier Transform Infrared Spectroscopy	109
4.7 Summary and Conclusions	114
4.8 Future Directions	115
References	117

LIST OF FIGURES

Figure 1: Transmission Electron Micrographs (TEMs) of lavaged rat surfactant large aggregate.	9
Figure 2: TEM's of Normal LS rat lavage (LB and TM) and a dysfunctional LS from a hyperventilation injured rat.	17
Figure 3: Topographical cartoon structure of serum albumin.	21
Figure 4: Mass spectrum profiles showing the composition of Bovine Lipid Extract Surfactant.	36
Figure 5: Adsorption isotherms (surface tension vs time) of BLES dispersion (0.25 mg/ml) with varying concentrations of BSA at $23 \pm ^\circ\text{C}$.	39
Figure 6: Surface tension vs relative pool area isotherms for compression expansion cycles of BLES, and BLES + BSA (250% w/w), mixed dispersions adsorbed onto a ddH ₂ O subphase.	42
Figure 7: Surface tension vs relative pool area (γ -A) isotherms for compression expansion cycles of solvent-spread monolayers of BLES and BLES + 250% BSA (w/w).	44
Figure 8: Surface tension vs relative pool area isotherms of the first compression-expansion cycle of solvent-spread monolayers of BLES, and BLES + BSA.	46
Figure 9: Surface tension vs pool area graph of multiple cycles of solvent-spread monolayers of BLES, and BLES + 250% BSA (w/w).	50
Figure 10: AFM images of deposit of BLES films on mica taken at a γ of 40mN m^{-1} , and one of BLES + BSA (100% w/w) film taken at the same γ .	53
Figure 11: Line section through an AFM image from a BLES deposited film; a molecular model showing the compacted BLES lipids when they are in condensed domains.	55
Figure 12: AFM images of BLES/BSA films of BLES + BSA at 100% w/w, 500% w/w, and 2000% w/w taken at a γ of 50 mN/m.	59

Figure 13: Three dimensional view of AFM images of deposit of BLES, BLES + BSA (100% w/w), and BLES + BSA (250% w/w) taken at a γ of 30 mN/m.	61
Figure 14: Time of Flight- Secondary Ion Mass Spectrometry (TOF-SIMS) positive ion images of BLES films, and BLES + 10% BSA films deposited at a γ of 40 mN/m.	64
Figure 15: DSC melting profiles of DPPC (2mg/ml), and DPPC + 100% BSA (w/w) dispersions.	67
Figure 16: DSC melting profiles of BLES (2mg/ml), and BSA (20mg/ml).	70
Figure 17: DSC melting profiles of BLES (2mgs/ml) , BLES + 25% BSA (w/w), BLES + 100% BSA (w/w), and BLES + 250% BSA (w/w).	72
Figure 18: DSC scans of BLES, BLES + 250% BSA added to the preformed vesicles, and BLES vesicles formed by reconstitution in the presence of 250% (w/w) BSA; DSC scans of BLES + 250% BSA (w/w) diluted in ddH ₂ O, and BLES + 250% BSA (w/w) added to Tris HCl/NaCl Buffer with 2mM CaCl ₂ .	74
Figure 19: TEMs of BLES vesicles and BLES + 250% BSA (w/w) where BSA was added to the preformed BLES dispersions.	78
Figure 20: Diagram of the DPPC phospholipid molecule, showing the vibrational bands observed by FTIR.	80
Figure 21: Complete FTIR spectra of dispersions of 27mg/ml DPPC, 27mg/ml BLES, and 27mg/ml BSA.	82
Figure 22: Spectra of comparison of transmittance and absorbance modes for 27 mgs/ml BLES.	85
Figure 23: FTIR graphs focusing on the PO ₂ ⁻ asymmetric stretching mode, C=O stretching mode, CH ₂ symmetric stretching mode, CH ₂ asymmetric stretching mode of mixtures of BLES/BSA at low BSA concentrations.	87
Figure 24: FTIR spectra of BLES focusing on the addition of high concentrations of BSA.	90
Figure 25: Molecular model of a BLES monolayer (a) and bilayer (b) with BSA.	96

LIST OF ABBREVIATIONS AND SYMBOLS USED

AFM	atomic force microscopy
ALI	acute lung injury
API-MS	atmospheric pressure ionization mass spectrometry
ARDS	acute respiratory distress syndrome
ATPase	adenosine triphosphatase
ATR	attenuated total reflection
BLES	bovine lipid extract surfactant
BSA	bovine serum albumin
CLSE	calf lipid surfactant extract
CRP	C-reactive protein
Da	daltons
ddH ₂ O	double distilled H ₂ O
DOPC	dioleoylphosphatidylcholine
DPPC	dipalmitoylphosphatidylcholine
DPPG	dipalmitoylphosphatidylglycerol
DSC	differential scanning calorimetry
EM	electron microscopy

ESI-MS	electrospray ionization mass spectrometry
FTIR	Fourier transform infrared spectroscopy
γ	surface tension
γ -A	surface tension- pool area
IR	infrared spectroscopy
LA	large aggregate
LB	lamellar bodies
LBPA	lyso-bis-phosphatidic acid
LPC	lysophosphatidylcholine
LS	lung surfactant
M.W.	molecular weight
mg/ml	milligrams/milliliter
mN/m	millinewtons/meter
m/z	mass/charge
MALDI-TOF MS	matrix assisted laser desorption ionization- time of flight mass spectrometry
MLV	multilamellar vesicles
μ l	microliters
PC	phosphatidylcholine
PE	phosphatidylethanolamine
PG	phosphatidylglycerol
pI	isoelectric point

PI	phosphatidylinositol
PMPC	1-palmitoyl-2-myristoyl-phosphatidylcholine
POPC	palmitoyloleoylphosphatidylcholine
POPG	1-palmitoyl-2-oleoyl-phosphatidylglycerol
PS	phosphatidylserine
PSPC	1-palmitoyl-2-stearoyl-phosphatidylcholine
RDS	respiratory distress syndrome
SA	small aggregate
SEM	scanning electron microscopy
SM	sphingomyelin
SP-A	surfactant protein A
SP-B	surfactant protein B
SP-C	surfactant protein C
SP-D	surfactant protein D
TEM	transmission electron microscopy
TM	tubular myelin
TOF-SIMS	time of flight-secondary ion mass spectrometry
w/w	weight by weight

INTRODUCTION

1.1 Surfactant

Lung surfactant (LS) is a complex mixture of lipids and proteins lining the hypophase of the alveolar epithelium and maintaining lung stability by reducing the surface tension (γ) of the lung air-water interface. LS is secreted by alveolar type II cells, which form part of the outer cellular interface of the alveoli along with other epithelial cells and macrophages (Clements, 1957; Goerke, 1974; King and Clements, 1972). In the alveolar hypophase, surfactant forms vesicles and tubular myelin (TM), and at the air/liquid interface, LS is adsorbed as putative mixed lipid-protein films. The major functions of LS are to prevent alveolar collapse at low lung volume and to preserve bronchiolar patency (air-way opening) during normal respiration. Also, its major immunological functions are to protect the lungs from injuries and infections caused by inhaled particles and micro-organisms (reviewed by Griese, 1999).

To work properly, LS must be fluid enough to adsorb rapidly to the alveolar interface to form monolayer films. These films must be rigid enough to promote near zero surface tensions (γ) during the alveolar compression. The ability of LS films to attain a γ of close to 0 mN/m during lateral compression, stabilizes the lung alveoli at end expiration by counteracting forces at alveolar collapse (Goerke, 1998). Alteration and inactivation of LS in the lung may lead to several respiratory syndromes such as acute respiratory distress syndrome (ARDS), hyaline membrane disease, and acute lung injury

(ALI) (reviewed by Floros and Phelps, 1997; Griese, 1999; Lewis and Jobe, 1993; and Possmayer *et al.*, 2004).

1.2 Composition of Surfactant

Biochemically, mammalian LS is composed of approximately 90% lipid by weight and 10% protein. The lipid component is made up of phospholipids and neutral lipids. The protein component contains the surfactant proteins (SP-) SP-A, SP-B, SP-C, and SP-D, which have been studied for structure and properties, and how they interact with surfactant lipids (reviewed by Johansson *et al.*, 1994; Possmayer *et al.*, 2001; Veldhuizen *et al.*, 1998).

1.2.1 Lipids

About 90% by weight of the lipid fraction of LS is phospholipids, 80% of which is phosphatidylcholine (PC) (Veldhuizen *et al.*, 1998; Yu *et al.*, 1983).

Dipalmitoylphosphatidylcholine (DPPC) is the most abundant PC, making up about 65% of the weight of the phospholipid component in most mammals. DPPC is important in the function of LS, and plays an essential role in decreasing γ . This is the only component of LS which can be packed tightly into condensed films at 37°C, and such packing can lower the γ of an air-water interface to near zero values. There is also a significant portion of phosphatidylglycerol (PG) in LS. PG abundance in LS varies considerably from species to species and during fetal lung development. PG can be replaced by another negatively charged phospholipid, phosphatidylinositol (PI), without

affecting the surface properties of lowering the γ at the air water interface (reviewed by Robertson *et al.*, 1992). DPPC and PG are unusual phospholipids and are not found in most mammalian membranes (Veldhuizen *et al.*, 1998). Other minor phospholipids present in LS are phosphatidylethanolamine (PE), phosphatidylserine (PS), sphingomyelin (SM), lysophosphatidylcholine (LPC), and lyso-bis-phosphatidic acid (LBPA) (Body, 1971; Notter and Finkelstein, 1984; Shelley *et al.*, 1984). Not much is known about the function of these lipids; however, some of them are important constituents of biological membranes. Some studies have shown that the lamellar body (LB) limiting membrane of LS may contain higher levels of PE and SM. As well the minor phospholipid components could be involved in signaling events related to LS metabolism (reviewed by Veldhuizen *et al.*, 1998).

The non-phospholipid components of LS include neutral lipids such as cholesterol and triglycerides. Cholesterol has been known to enhance the adsorption rate of DPPC vesicles, presumably by increasing fluidity and improving film respreading (Fleming and Keough, 1988). It is also known to regulate the crystallization behavior of LS (Larsson *et al.*, 2003). However, by increasing fluidity, cholesterol limits the minimum γ obtainable during compression, because the sterol cannot be squeezed out easily from DPPC-cholesterol mixed films at high packing densities (Notter *et al.*, 1980). This is a reason why cholesterol is removed from some modified natural surfactants for clinical therapies. Other studies with neutral lipids combined with DPPC and PG mixtures stated that the mixtures adsorbed well, but were not effective in attaining low γ (Veldhuizen *et al.*, 1998).

Bovine Lipid Extract Surfactant (BLES) is a modified natural surfactant extracted from repeated cow lung washings (lavage), modified from the extensively studied bovine pulmonary surfactant (Yu *et al.*, 1983). It has the water soluble surfactant proteins SP-A and SP-D and the neutral lipids such as cholesterol and triglycerides removed for better surface activity. BLES was the surfactant used for the present study, due to its consistent composition, availability, and success as the only clinical replacement surfactant developed in Canada (see section 1.7).

1.2.2 Proteins

SP-A and SP-D make up the hydrophilic surfactant protein pool, and SP-B and SP-C are the hydrophobic surfactant proteins, associated with surfactant lipids.

The most abundant protein by weight in LS is SP-A, which has a mass of approximately 32 -35 kDa (depending on glycosylation) per monomer. It is a glycoprotein with three distinct structural domains. A long stretched collagenous domain is connected via a linking region to a globular domain. This is the site where calcium dependent binding occurs to lipids (Haagsman *et al.*, 1989). SP-A consists of 18 monomers organized by covalent disulphide bonds and non-covalent interactions, having an octadecameric mass of 640 kDa. SP-A has been shown to accelerate the adsorption of LS phospholipids at the air-water interface (King and Clements, 1972; Palaniyar *et al.*, 2000; Schurch *et al.*, 1992), and reverse inhibition of LS by serum proteins (Cockshutt *et al.*, 1990). It is also involved in the structural organization of LS, and is an essential

component in the formation of tubular myelin. As well, it stimulates the defense system which depends on macrophages (Wright, 1997).

SP-D is the second hydrophilic protein, with a mass of 37-50 kDa per monomer (depending on glycosylation and species). It is also a collagenous carbohydrate-binding lectin glycoprotein, such as SP-A. It has a larger collagenous domain than SP-A, and is attached directly without a connecting region to the calcium dependent carbohydrate recognition domain. The lectin SP-D exhibits calcium dependent carbohydrate binding activity to receptors, however does not bind any lipids except phosphatidylinositol, which is not present in lung surfactant in any significant amount (Floros and Phelps, 1997). SP-D does not contain cysteine residues and this prohibits interhelical disulphide crosslinks, like those in SP-A. SP-D has 12 monomers, 4 of which form a cross-like structure which may bind to bacterial lipopolysaccharides and to cell surfaces forming large networks of cells or bacteria (Crouch, 1998). SP-D is an aqueous protein found in alveolar fluid, whereas SP-A, SP-B and SP-C are almost entirely found in association with LS lipids. SP-D has been suggested to counteract the inhibitory effect of SP-A on phospholipid secretion (Floros and Phelps, 1997). As well, SP-D binds PI and ceramides in a calcium dependent manner. Not much else is known about SP-D, however. Some studies suggest that SP-D is not a “surfactant-associated protein”, considering it does not show major surface activity with surfactant lipids (Taneva *et al.*, 1997). SP-D gene knockout mice show no altered γ of extracted LS but do show high LS lipid secretion, or a condition called alveolar lipoidosis (Ikegami *et al.*, 2000).

Although SP-A and SP-D have minimal effect on the surface activity of LS phospholipids, SP-B and SP-C have significant effects. SP-B and SP-C are both hydrophobic proteins and are thought to be responsible for rapid formation of LS monolayers at the air-water interface (Possmayer, 1990; Yu and Possmayer, 1990). The proteins also help in the insertion and removal of phospholipids during the expansion and compression of the LS film (reviewed by Pérez-Gil and Keough, 1998). As well, they both increase the uptake of phospholipids into type II pneumocytes (reviewed by Griese, 1999).

SP-B is a cysteine-linked homodimer with a monomeric molecular weight (M.W.) of 8.7 kDa. It consists of 4 amino acid repeats with a conserved periodicity of cysteine residues in each repeat. The repeats are linked by regions rich in proline and glycine. The third repeat contains an additional cysteine residue that may be involved in inter chain disulphide bond formation (reviewed by Johansson *et al.*, 1994). SP-B has many functions. Like SP-A, it is important for the formation of TM (Floros and Phelps, 1997). TM is the material in LS thought to be the most surface active. As well, SP-B induces bilayer contact sites and subsequent lipid mixing in the presence of negatively charged phospholipids, divalent or monovalent cations, or lowered pH. Also, SP-B increases the size of small unilamellar vesicles and causes vesicle fusion (Rice *et al.*, 1989). In addition, SP-B accelerates the formation of a surface active film composed of phospholipids at the air water interface by means of an increase in adsorption rate of LS lipids (reviewed by Johansson *et al.*, 1994), and this is affected by the presence of calcium ions. As well, SP-B appears to affect the squeeze out of unsaturated lipids from

the surface film of LS, resulting in a DPPC- enriched monolayer (Floros and Phelps, 1997; Nag *et al.*, 1999). In addition, SP-B interacts with phosphatidylglycerol at the surface of the bilayer membrane in a concentration-dependent manner (Batz *et al.*, 1990). SP-B increases order in the lipid head group region of a lipid bilayer and not in the membrane interior (Batz *et al.*, 1990). Genetic knock-out of the SP-B protein is lethal, and the animals die within a few hours of birth (Clark *et al.*, 1995; Melton *et al.*, 2003; and reviewed by Johansson *et al.*, 1994).

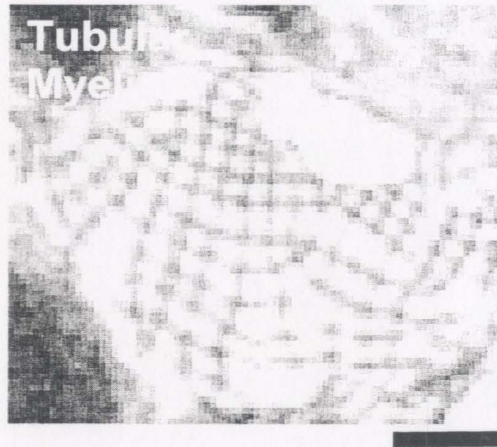
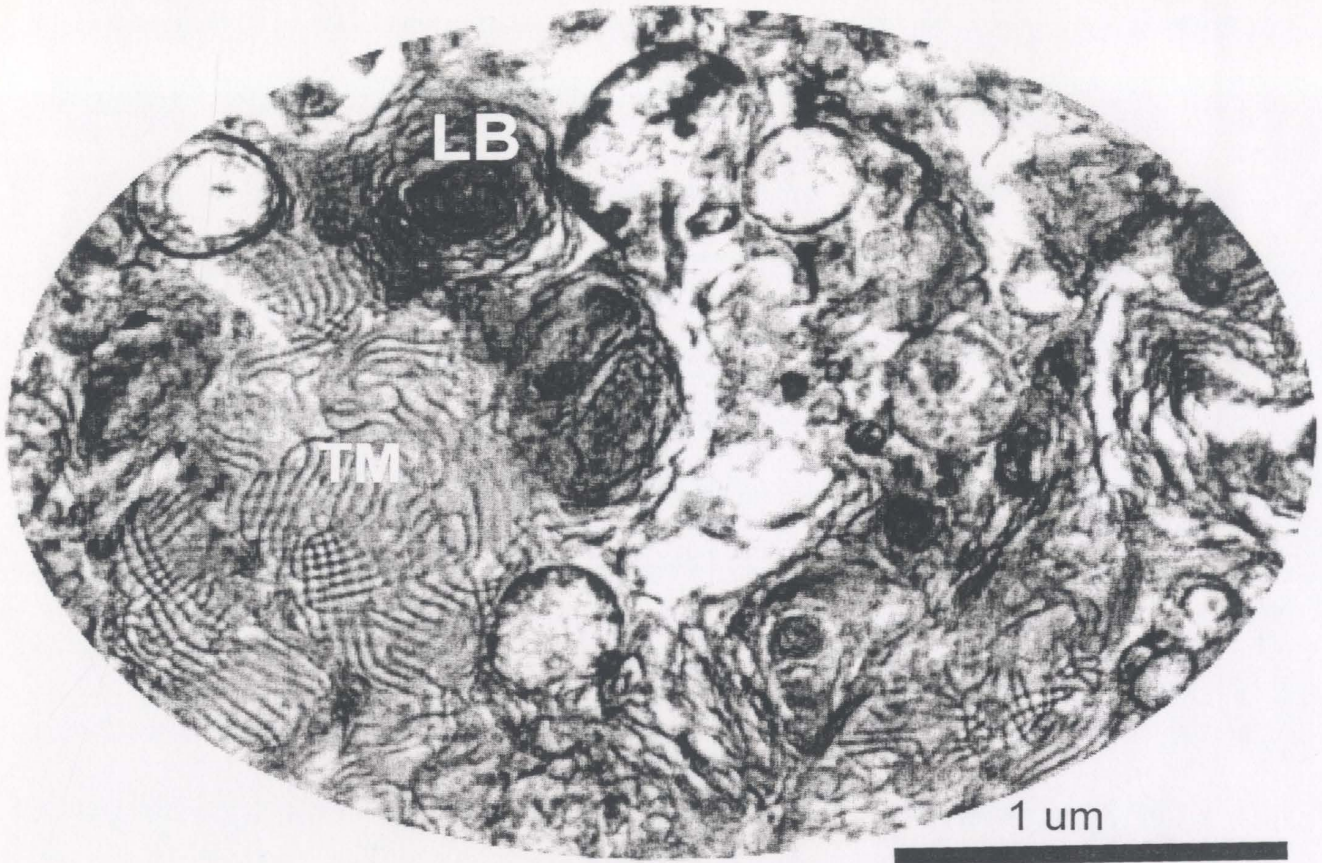
SP-C is the only surfactant protein expressed exclusively by type II cells in the mature lung. It is one of the most hydrophobic natural monomeric peptides with its carboxy-terminus being extremely hydrophobic, and it has a M.W. of 4.2 kDa. It is a mainly α -helical membrane-spanning molecule and has two covalently linked palmitic acid residues attached to the cysteines near the N-terminus (Beers and Fisher, 1992). The hydrophobic helix and acylation are important for anchoring the protein to the membrane (Floros and Phelps, 1997), and can act as a transmembrane protein. The main known function of SP-C is to enhance the surface activity of the surfactant lipids. This occurs through acceleration of the rate of adsorption of lipids at the air-water interface. SP-C also allows for an increase in the resistance of LS to inhibition by serum proteins (Holm *et al.*, 1988). As well, SP-C stabilizes the surface activity of the LS film during the expansion and compression involved in breathing by possibly forming multilayer structures (reviewed by Pérez-Gil and Keough, 1998). In addition, SP-C disturbs the ordering of the acyl chain region or lipid packing of DPPC in bilayer models, and broadens the gel-fluid phase transition temperature (Johansson, 1998). SP-C knock-out

mice however do not show any significant altered surface activity although they develop other problems such as altered lung fluid-balance, and eventually perish a few weeks after birth (Glasser *et al.*, 2001). Both SP-B and SP-C are normally present in lipid extracts of LS used for clinical treatment (such as BLES) because of their hydrophobicity.

1.3 Surfactant Life Cycle

LS assumes several structural and morphologic forms during its life span in the type II alveolar cell and in the hypophase. After synthesis by type II cells, LS is secreted into the alveolar space. Secretion of LS from type II cells is assumed to be induced by deep sighing breaths and the resulting large increases in lung surface area (Wirtz and Dobbs, 2000). After secretion, it undergoes several processes such as adsorption, surface film formation, film refining, self assembly, and monolayer-bilayer-multilayer transformation. It also undergoes phase transitions at an air-water interface *in vitro* (reviewed by Nag *et al.*, 2000). During secretion, lamellar bodies (LB) are formed, which can transform into lattice bound tubes called tubular myelin (TM), in the presence of calcium, SP-A, and SP-B (Wright and Hawgood, 1989). **Figure 1** shows structures of LB and TM in lavaged rat LS. LB have concentric layers of unit bilayer membranes that have similar structural features to multilamellar liposomes or vesicles (Goerke, 1998). The TM is thought to be the precursor of the surface active film and is present in high amounts in the large aggregate (LA) [**Fig. 1(a)**] form of LS (Floros and Phelps, 1997; Veldhuizen *et al.*, 1996). TM structures are nano-tubules that have a square lattice

Figure 1: Transmission Electron Micrographs (TEMs) of lavaged rat surfactant large aggregate, with tubular myelin (TM) and lamellar bodies (LB) identified. The LB are the secretory materials which transform into TM. In disease and dysfunction, TM structures are absent (see Fig. 2). The electron micrographs were done by embedding rat LS in Lowicryl and staining using uranyl acetate. The black lines are of typical bilayer (40-50 Å) thickness. [The TEM were a generous gift from Stephen Hearn, Cold Spring Harbour Laboratory, New York (Unpublished Data)].



100 nm

network where the bilayer membranes intersect at a perpendicular angle and form the walls of these tubes (Groniowski and Walski, 1979). LS monolayers possibly reside at the alveolar interface for hundreds of breathing cycles before replacement by further secretion (Pison *et al.*, 1996). LS vesicles are presumably created in the hypophase from cycling of large aggregates, and the smaller vesicles (small aggregates) are taken up preferentially by the type II pneumocytes and reutilized for LS synthesis (Gross, 1995). It is presumed that the LA or TM forms a surface active layer or film, and the film, after recycling (due to breathing cycles), is converted into small aggregates (SA). The LA and SA forms are different in composition of surfactant proteins (Gross, 1995). Approximately 50% by weight of the LS is present in the alveolar space, in the form of LA, and 50% is in the form of SA (Griese *et al.*, 1996), however this ratio changes dramatically in lung disease (Veldhuizen *et al.*, 2002). The typical LA form of LS from rat lungs is shown in **Figure 1**.

1.4 Acute Respiratory Distress Syndrome

The first studies on lungs and the alveolar lining materials were carried out in the 1950s and 1960s (Ashbaugh *et al.*, 1967; Avery and Mead, 1959; Clements, 1957; Pattle, 1955, 1958). John A. Clements first discovered the surface tension reducing properties of lung lavage (Clements, 1957). The surface tension-area (γ -A) behaviour of lung derived surfaces was first studied using the Langmuir-Wilhemmy surface balances by these authors (King and Clements, 1972). They were the first to suggest that LS probably existed at the lung air-water interface as monolayer films, since most of the molecules of LS were

amphipathic. They noted that the γ of the lung derived surface varied from 46 to 10mN/m, and that the surface exhibited hysteresis and provided a characteristic elasticity to the fluid surface (Goerke, 1974, 1998). Schurch *et al.* (1976) measured the γ of the lung interface *in situ*, and substantiated that the values were very close to those found by King and Clements (1972), at near 1mN/m at end expiration.

Acute Respiratory Distress Syndrome was first described by Ashbaugh *et al.* (1967). They observed 12 patients who weren't responding to the usual modes of therapy, and were exhibiting clinical, physiological and pathological courses of events that were similar to infant respiratory distress syndrome (otherwise known as hyaline-membrane disease) (Avery and Mead, 1959). Hyaline (shiny-appearance) membrane disease was found to be due to lack of ample secretion of LS (Avery and Mead, 1959). In ARDS the patients exhibited severe dyspnoea, tachypnoea, cyanosis that is refractory to oxygen therapy, loss of lung compliance, and diffuse alveolar infiltration (Ashbaugh *et al.*, 1967; reviewed by Lewis and Jobe, 1993). In all patients, ventilation was assisted or controlled by a respirator and measurements were made when the patient was in a relaxed or steady state. As well, the minimum γ observed in patients was 24 mN/m whereas in normal situations it was less than 10 mN/m, when LS from such lungs were studied *in vitro*. Other features noticed were the presence of a patchy bilateral alveolar infiltrate visible in the x-ray of the chest, as well as the presence of protein-rich layers in the microscopic appearance of the lungs. All this led Ashbaugh and his colleagues to collectively define the symptoms of these patients as adult respiratory distress syndrome, and today it is defined as acute respiratory distress syndrome (ARDS).

In 1994, the American-European Consensus Conference Committee defined ARDS, and ALI as a syndrome of inflammation and increased capillary permeability that is associated with a constellation of clinical, radiologic, and physiologic abnormalities that cannot be explained by left atrial or pulmonary capillary hypertension (Bernard *et al.*, 1994). The Conference Committee also mentioned several risk factors for ARDS. They include aspiration, diffuse pulmonary infection, near-drowning, toxic inhalation, lung contusion, sepsis syndrome, and cardiopulmonary bypass. Ware and Matthay (2000) mentions that sepsis is associated with the highest risk of progression to ALI or ARDS, by approximately 40%.

The annual incidence of the disease in the US is about 75 per 100,000 population according to the National Institutes of Health (NIH) (Murray, 1977), whereas the consensus mentions approximately 150,000 cases per year (Bernard *et al.*, 1994). The mortality rate is approximately 40-60%, and the majority of deaths are attributable to sepsis or multi organ dysfunction rather than primary respiratory causes (Doyle *et al.*, 1995).

The acute phase of ARDS is characterized by the influx of protein rich edema fluid into air spaces as a consequence of increased permeability of the alveolar-capillary barrier or leakage of blood vessels (Pugin *et al.*, 1999). There are two types of cells present in the alveolar epithelium of adult lungs. Flat type I cells, which make up 90% of the surface area, are easily injured. However, the cuboidal type II cells make up the remaining 10% and are more resistant to injury. The functions of the type II cells include surfactant production, ion transport, and proliferation (reviewed by Ware and Matthay,

2000). Increased permeability of the epithelium can contribute to alveolar flooding. As well, the loss of epithelial integrity and injury to type II cells disrupt normal epithelial fluid transport, impairing the removal of edema fluid from alveolar space (Sznajder, 1999). Also, injury to type II cells reduces the production and turnover of LS, contributing to surfactant abnormalities. In addition, loss of the epithelial barrier can lead to septic shock in patients with bacterial pneumonia (reviewed by Ware and Matthay, 1999). In ARDS, inflammation gives rise to phospholipases, proteases, and other mediators within lung tissue. Damage to the alveolo-capillary membrane allows for these compounds, along with cellular degradation products and blood derived lipids and proteins, access to the alveoli where they can impair the surface-active function of LS (Holm *et al.*, 1999). Another mechanism of injury is evident when neutrophils predominate in pulmonary edema fluid obtained from affected patients, suggesting neutrophil dependent lung injury (Pittet *et al.*, 1997). Other mechanisms included injury by cytokines, ventilator-induced lung injury due to high volumes and pressures of mechanical ventilation, and abnormalities in the production, composition, and function of LS (Ware and Matthay, 2000).

To resolve the cause of this disease, many suggestions have been made. Alveolar edema can be resolved by the transport of sodium and chloride from the distal air spaces into the lung interstitium (Matalon *et al.*, 1996). As well, in clinical studies, clearance of alveolar fluid can cause improved oxygenation, a shorter duration of mechanical ventilation, and an increased likelihood of survival. As well the removal of insoluble

protein is important since hyaline membranes provide a framework for growth of fibrous tissue (reviewed by Griese, 1999; and Ware and Matthay, 2000).

Several approaches to treatment have been discussed. These include prophylaxis, supplementation with oxygen and positive end-expiratory pressure, mechanical ventilation, pharmacologic therapy through the use of corticosteroids, and nonsteroidal anti-inflammatory drugs, fluid and hemodynamic management, synthetic and natural surfactant therapy, and inhaled nitric oxide and other vasodilators (Bernard and Brigham, 1986; Spragg and Lewis, 2003; reviewed by Ware and Matthay, 2000). Although these may help, there is still an onset of the disease, with a 40-60% mortality rate, so more studies have to be carried out to understand the mechanisms of dysfunction and surfactant replacement for more effective modes of therapy.

1.5 Lung Surfactant and ARDS

Jacobson *et al.* (1993) found an occurrence of free surfactant particles in the tracheal aspirates of 30 patients without and 23 with ARDS. They also found the presence of fibrinogen in the aspirates of only 5 of 30 patients without, but in 20 out of 21 patients with ARDS. The surfactant particles are identical to those found in the type II cells of the alveolar epithelium. There are several studies, which show the importance of LS in lung activity, and the inactivation causing ARDS (reviewed by Griese, 1999). Studies have shown that phospholipid composition was altered (decreased PC and PG with increased PI and PE), surfactant associated proteins were decreased (SP-A), and alveolar LS aggregate forms were altered (reviewed by Lewis and Jobe, 1993). Changes

in alveolar surfactant aggregate metabolism leads to a decrease in the functionally active aggregate pool size within the air space. Increased alveolar phospholipase activity may also enhance surfactant aggregate conversion (Veldhuizen *et al.*, 1996).

Plasma proteins have been known to inhibit LS function which in turn leads to ARDS. **Figure 2** shows TEM's of normal and dysfunctional LS forms from rat lung lavage. The lung injury here was induced using hyperventilation *ex vivo* (Panda *et al.*, 2004; Veldhuizen *et al.*, 1998). The general concentration of plasma proteins in the normal rat lungs was ~300 $\mu\text{g/lung pair}$, whereas in injured lungs, the concentration was ~830 $\mu\text{g/lung pair}$, almost a three fold increase (Panda *et al.*, 2004). Also, the γ of such ventilation injured surfactant did not reach below 20mN/m. Holm *et al.* (1988) found that at low surfactant concentrations, plasma proteins significantly inhibit LS adsorption, resulting in an increase in the equilibrium γ . At low surfactant concentration of 0.5 mg/ml, plasma proteins prevent the LS suspension from reaching γ below 21 mN/m, a value that is generally considered incompatible with normal physiological function (Goerke, 1998; Enhorning, 1977).

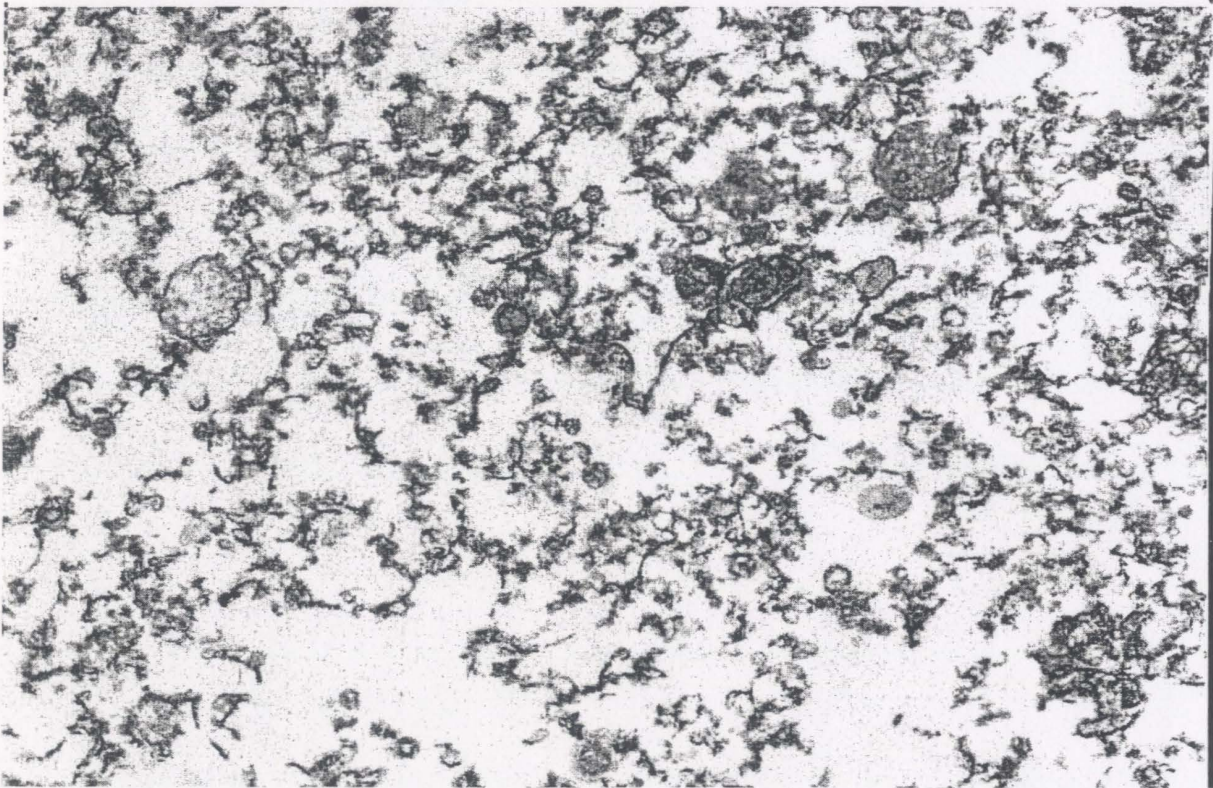
There are possibly many mechanisms by which protein may inhibit LS. It can inhibit either by interactions with surfactant phospholipids in the bulk phase or surface layer, by inserting into the intact surface film, or by competing with surfactant molecules for space at the air-liquid interface during adsorption (Holm *et al.*, 1999). Holm *et al.* (1988) found that large amounts of plasma proteins injected beneath a preformed surfactant film do not affect equilibrium γ , the opposite of the phenomenon that was

Figure 2: TEM's of Normal LS rat lavage (LB and TM) and a dysfunctional LS from a hyperventilation injured rat LS (Panda *et al.*, 2004). Lamellar bodies and tubular myelin formation is completely disrupted, and small aggregates and other unknown structures (Veldhuizen *et al.*, 2002) are mostly found in such lavaged LS from injured lungs. [The EM's were a generous gift from Stephen Hearn, Cold Spring Harbour Laboratory, New York (Unpublished Data)].



500 nM

NORMAL



500 nM

DYSFUNCTIONAL

observed when proteins are added simultaneously with the surfactant suspension. Keough *et al.* (1989) found that the plasma proteins albumin, globulin, and fibrinogen detract from the ability of LS to adsorb to the air-water interface using a pulsating bubble surfactometer. As well, in surface balance studies, each of the proteins altered some of the γ -A properties of the isotherms of surfactant films. The proteins decreased the minimum γ which the surfactant films attained on compression, and decreased the areas occupied per molecule of the lipid. The proteins also reduced the areas of hysteresis between compression and expansion isotherms, and decreased the rate of change of γ with area at the point of initial expansion of the monolayers (Keough *et al.*, 1988).

Various studies reviewed by Holm, (1988) mentioned that when injected beneath the surface of a stirred subphase, albumin adsorbed to an equilibrium γ of only 50 mN/m. When albumin and surfactant were combined in dispersion and injected together, there was a substantial reduction both in adsorption rate and rise in final equilibrium γ compared to the surfactant alone. They hypothesized that albumin acted primarily through competitive adsorption and blocking of the air water interface for lipid molecules of LS to adsorb. As well, it has been stated that plasma proteins may also impair LS adsorption by associating with surfactant aggregates in the subphase during lung injury (Holm, 1999, and references there in).

1.6 Bovine Lipid Extract Surfactant

The modified LS used in this study was Bovine Lipid Extract Surfactant (BLES™) obtained from BLES Biochemicals Inc., in London, Ontario. BLES is a

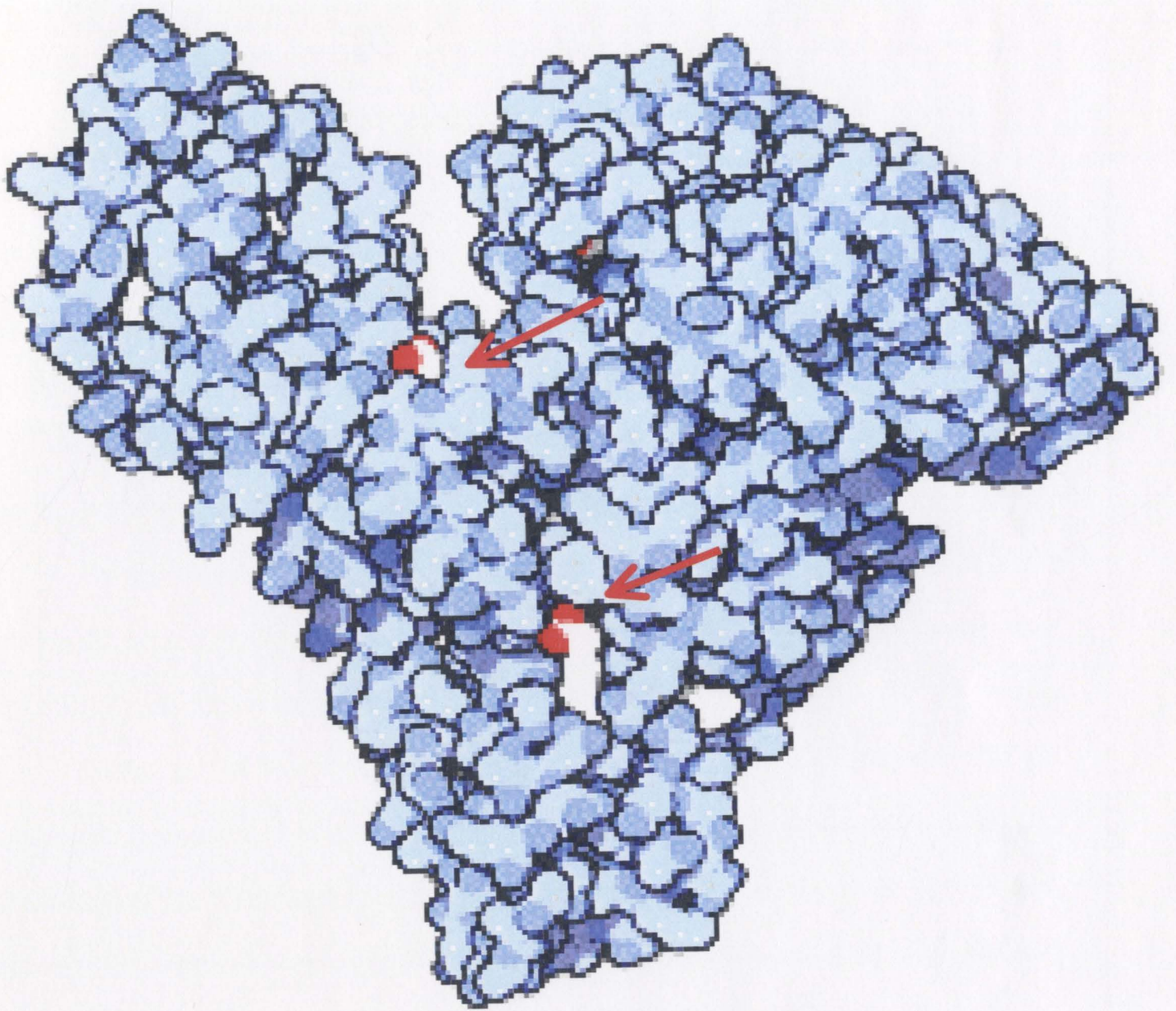
modified natural LS hydrophobic extract from bovine lung lavage. It contains mainly ~50% DPPC, 35% unsaturated PC, ~10% acidic phospholipids such as PG, and at 2% of the weight of lipids, SP-B and SP-C, among other minor phospholipids of surfactant (Yu *et al.*, 1983). BLES was used as a standard model of natural LS due to its consistent composition and surface activity, its availability in large amounts, and its cost effectiveness as a Canadian product. Previous studies using various extracted surfactant preparations have suggested contradictory results due to various extraction artifacts, contaminants, and compositions quite different from their natural surfactants (Holm, 1992). SP-A, SP-D, and neutral lipids (cholesterol) are removed from the surfactant for better surface activity, however, BLES contains all other lipids and the hydrophobic proteins SP-B and SP-C as found in bovine lavaged LS.

1.7 Albumin

Albumin (**Figure 3**) is one of the most structurally defined plasma proteins and is one of the most abundant proteins in the circulatory system, with a concentration of approximately 40g/l in human plasma (Rosenoer *et al.*, 1977). Albumin contributes to 80% of the colloid osmotic blood pressure (Carter and Ho, 1994). Serum albumin is chiefly responsible for the maintenance of blood pH as well as a carrier for fatty acids (Figge *et al.*, 1991).

Albumin is first synthesized in the liver as prealbumin. The signal peptide is then removed, and a 6-residue pro-peptide is cleaved from the N-terminus to give mature albumin.

Figure 3: Topographical cartoon structure of serum albumin. Arrows point to the lipid binding regions of the molecule. Taken from the Protein Data Bank (<http://www.rcsb.org/pdb/molecules/1e7i>- icon.gif)



Bovine serum albumin (BSA) is a single polypeptide of about 600 AA's (Brown, 1975). It has an approximate M.W. of 66,000 Da. Albumin's pI is about 4.7 in 0.15 M NaCl. It is a highly water soluble protein with a strong negative charge of -17 per residue at pH 7 (Peters, 1985). The protein is composed of 3 homologous domains divided into 9 loops by 17 disulphide bonds. About 67% of the protein is α -helical, and the remaining polypeptide is made up of turns and loops connecting the domains. There are very few β -sheets in the structure. Disulphide pairing is located mostly between helical segments. This suggests that the disulphides are protected from reducing agents at neutral pH (Peters, 1985).

The denaturation temperature of bovine serum albumin (BSA) is around 65 °C (Wetzel *et al.*, 1980). Upon denaturation, there appears to be a loss in α -helical structure and increase in antiparallel β -sheets.

There are 4 buried clusters embedded within the structure, which appear to be the lipid binding domains. These clusters are favorable for hydrophobic interactions with lipids such as free fatty acids (Bardos-Nagy and Galantai, 2003). These areas are rich in hydrophobic amino acids such as phenylalanine, leucine, methionine, alanine, valine, and isoleucine. These hydrophobic regions may suggest a propensity of albumin to interact with LS lipids.

Albumin has many functions such as binding and transporting fatty acids, maintenance of colloid osmotic blood pressure, free radical scavenging, platelet function inhibition, and anti-thrombic effects. It also affects capillary membrane permeability, is involved in foaming when interacting with other proteins (Poole *et al.*, 1984), forms

soluble aggregates (Matsudomi *et al.*, 1993), and is involved in reversible ligand binding (Goodman, 1958).

1.8 Present Study

This study tested the interaction and association of LS with one of the serum proteins: albumin. The hypothesis for this work is based upon whether albumin interacts with specific lipid molecules of BLES and if this can be biophysically observed. The study focuses on testing the hypothesis that albumin would insert or at least affect the headgroup region of the bilayer or monolayer, and that the effect is translated deep into the hydrophobic part of the bilayer. Biophysical studies were performed on monolayer films, as well as bilayer vesicle dispersions of BLES. The techniques used were Langmuir and adsorption surface balances (Monolayer), differential scanning calorimetry (DSC), atomic force microscopy (AFM), transmission electron microscopy (TEM), and Fourier transform infrared spectroscopy (FTIR) (reviewed by Nag *et al.*, 2002a, 2004b). Surfactant monolayers were used in the surface balance and AFM studies, and bilayer dispersions were used in DSC, FTIR, and TEM studies.

MATERIALS AND METHODS

2.1 Materials

Bovine Lipid Extract Surfactant (27mgs/ml in 5ml vials) was a generous gift from Dr. Dave Bjarnson of BLES® Biochemicals Inc. (London, Ontario). 1, 2-dipalmitoyl-*sn*-glycero-3-phosphatidylcholine (DPPC) was purchased from Sigma-Aldrich (St. Louis, MO). Chloroform and methanol were HPLC grade solvents (99%) purchased from Fisher Scientific (Ottawa, ON). Delipidated bovine serum albumin (BSA) (Protease-free, Fraction V, 99%, catalogue number - A3059-50G) in crystallized form was purchased from Sigma-Aldrich Inc., (St. Louis, MO).

All experiments were carried out in doubly distilled water (ddH₂O) at pH of 7, unless otherwise stated. All glassware used in the monolayer experiments were chromic acid washed, rinsed thoroughly, and baked at 180°C for 2 hours prior to use, to remove any organic and surface active contaminants, as discussed previously (Nag *et al.*, 1996, PhD Thesis).

BLES was combined with 12.5-250 % (w/w) of BSA for DSC, FTIR, and monolayer studies. These concentrations are physiologically/pathologically relevant to what occurs in ARDS and lung injury (1:1 protein: lipid ratios). Extremely high concentrations of 2000-3000% (w/w) of BSA (10:1 and 20:1) were also used, as previously used in some *in vitro* studies in the laboratory of others (Holm *et al.*, 1999). These high concentrations are laboratory-assigned to show maximal inhibition, however

this may not be physiologically relevant, except in certain cases such as RDS where most of the surfactant secretion does not occur.

2.2 Organic extraction of BLES lipids and proteins

For some film, mass spectrometry, and AFM studies, BLES was extracted in hydrophobic solvents from aqueous dispersions (as supplied by BLES ® Biochemicals Inc.) by the method of Bligh and Dyer (1959). Briefly, 0.8 volume of BLES dispersion in saline (27mg/ml), two volumes of methanol and one volume of chloroform were added. This mixture was vortexed and shaken vigorously. This was followed by one volume of chloroform, and more vortexing and shaking to mix the solvents thoroughly. Then one volume of ddH₂O was added, and the mixture was vortexed and shaken again. The mixture was then centrifuged at 1000 rpm for 1 minute to separate the organic and aqueous layers. The bottom organic phase was extracted with a Pasteur pipette, done carefully as to not mix the layers, and placed in a glass vial. The aqueous phase was extracted again as described above with chloroform and then with 2:1 chloroform:methanol (C:M). The subsequent organic layer extractions were pooled with the previous organic layer. This was then dried under nitrogen gas, and redissolved in 3:1 C:M to appropriate concentrations required for the specific experiments.

The concentration of phosphorus in extracted BLES was obtained by a modified version of the Bartlett analysis of organic phosphorus in surfactant (Keough and Kariel, 1987; Bartlett, 1959). The estimated weight of the phospholipids in BLES was

determined by multiplying the total phosphorus concentration by 25 [(M.W. of P= 31), where 31x25 is the approximate M.W. of the phospholipids].

2.3 Preparation of Buffer

For certain DSC studies the buffer was prepared with 145 mMol NaCl, 5 mMol Tris-HCl, and 2 mMol CaCl₂ dissolved in ddH₂O. The pH was then adjusted to 6.9 using a pH meter and titration with 0.1 M HCl until the desired pH was reached. For most other studies ddH₂O was used, since specific ions can dramatically alter the LS structure and function, as well as affect the structure of albumin. Future studies with specific ions (Na⁺, Ca²⁺) are underway in our laboratory, with these systems.

2.4 Techniques

Biophysical studies on BLES +/- BSA were carried out using mass spectrometry, surface balance (monolayer) studies, atomic force microscopy (AFM), differential scanning calorimetry (DSC), electron microscopy (EM), and Fourier transform infrared spectroscopy (FTIR).

2.4.1 Mass Spectrometry

For the compositional analysis of the phospholipids of BLES, electrospray ionization mass spectrometry (ESI-MS) was performed on hydrophobic extracts. An Atmospheric Pressure Ionization-Mass Spectrometer (API-MS) was used. This mass spectrometer is part of an Agilent 1100 series LC/MSD chromatographic system (Model

No. GC-G1946A, Agilent, Mississauga, ON). Some initial studies were conducted in the facilities at the Department of Fisheries and Oceans under the supervision of Dr. Joseph Banoub, whose expertise in this system of lipid analysis was utilized. In the FIA mode (flow injection analysis) chloroform: methanol (C:M) sample solutions are injected into a quadrupole mass analyzer with a mass range of m/z 50-3000 and a mass accuracy of 0.1 amu. About 100 μ l of extracted BLES (1mg/ml) in C:M (3:1 vol:vol) was added to 50 μ l of NH_4OH (10 mM), and this was injected into the mass spectrometer after mixing. The NH_4OH removed all the sodiation in the sample, so that only non-sodiated peaks appeared (Harbottle *et al.*, 2003). Spectra in the positive as well as negative ion modes were obtained. The negative ion mode spectrum was obtained without the addition of NH_4OH to BLES. All data is displayed as the molecular weight (M.W.) (as mass/charge or m/z where $z=1$) in Daltons.

For analysis of the hydrophobic proteins in BLES a matrix-assisted laser desorption-time of flight mass spectrometer (MALDI-TOF MS) was used, available in our university's C-CART (Centre for Chemical Analysis, Research and Training) facility. The instrument is an Applied Biosystems Voyager DE- PRO [(modified from DE-RP) (Serial No. 5-2437, Foster City, California)] equipped with a reflectron, delayed ion extraction and high performance N_2 laser (337 nm). Both positive and negative ion detection was available. In the linear mode an upper mass range of 350 kDa with a resolution of 1,000 (for m/z 17,000) was used in the positive ion mode. A solvent solution of 10 μ l of extracted BLES (250mgs/300 μ l) was diluted to 200 μ l of C:M 35:65, 20 μ l H_2O , and 20 μ l acetic acid, as previously discussed by Gustafsson *et al.* (2001).

This solution was combined with sinapinic acid, dried to form a matrix, and then analyzed by the mass spectrometer, using laser desorption, at a time of flight spectrometer detection range of 3000 - 17,000 Da.

2.4.2 Surface Balance (Monolayer) Studies

A custom designed Langmuir surface balance with a teflon ribbon barrier (leak proof) was used, the construction and operation of which have been described previously (Nag *et al.*, 1990). The dimensions of the Teflon trough give a surface area of 165 cm², which is used as 100% of pool area in the isotherms. Surface tension-pool area (γ -A) was used in all studies, as accurate area/molecule information can not be calculated for adsorbed films. However, approximately 40 nmoles of BLES phospholipids were used in each monolayer study. A motorized Teflon barrier compresses and expands the monolayer. Surface tension is measured by a roughened Wilhelmy platinum dipping plate hanging on a force transducer (Nag *et al.*, 1990). A subphase of ddH₂O was added to the trough before spreading or adsorbing the films. When needed, BSA was dissolved directly in the subphase before the experiments. The BLES monolayer (in C:M 3:1) was spread on top of the subphase for the compression-expansion experiments with and without BSA. In other studies, dispersions of BLES + BSA were adsorbed to a desired γ . The monolayer was initially spread or adsorbed to a γ of 65 mN/m before compression. Compression-expansion was done at a speed of 506 mm²/sec. By compressing the monolayer, the transition of the lipids from fluid to condensed (gel-like) phase was initiated, and this is measured as a surface tension-pool area (γ -A) isotherm in our studies

(Nag *et al.*, 1998). In this study, only 80% compression was possible due to 20% of the area being occupied by the Wilhelmy plate and a circular window for optical observation. In certain studies similar monolayers were deposited on to mica slides using Langmuir-Blodgett techniques for structural studies using AFM (Nag *et al.*, 1999). All experiments were performed at an ambient but monitored temperature of $23 \pm 1^\circ\text{C}$, due to the lack of heating and cooling controls on our instrument (Nag *et al.*, 1990).

Adsorption experiments were carried out in a small cylindrical teflon cup (volume of 6.28 cm^3 , and surface area of 6.28 cm^2). BLES/BSA dispersions were injected underneath the surface of the ddH₂O in the cup, and were consistently stirred, using a magnetic stirrer. Adsorption to the surface (determined by surface tension drop) was measured as a function of time (sec), using a Wilhelm platinum plate as discussed in a previous study (Nag *et al.*, 1998).

2.4.3 Atomic Force Microscopy

AFM allows for imaging structures of monolayers deposited on an atomically flat surface such as mica or glass, and suggests topographical variation of a surface as in the case of scanning electron microscopy (SEM). However with AFM, height difference and surface topography are determined from the movement of a small tip (20nm in diameter), supported by a cantilever and no sample coating and electron beams are required as in SEM (Nag *et al.*, 2004b). In principle, the tip can tap or be in constant contact with the surface of the material. Movement of the cantilever with the tip are from the sample surface, seen as a deflection of a sensor laser, which then reports the surface topography

(or the variation of the signal coming from the movement of the cantilever in contact with the surface) of the object or monolayer. The experiments in this study were carried out on a Langmuir-Blodgett surface balance (Kibron Scientific, Helsinki, Finland) (Harbottle *et al.*, 2003). BLES was solvent spread or adsorbed onto the ddH₂O or BSA subphase. The material was absorbed to a γ close to 55mN/m, and then compressed at 0.04 nm²/molecule/min (an approximation from the amount of 40 nmoles lipids adsorbed). The film was then deposited onto freshly cleaved mica plates at a γ of 50, 40, and 20 mN/m by a slow lifting of mica from the subphase (Blodgett deposits). The AFM was then performed, using the contact mode, on these freshly deposited samples using a Nanoscope IIIa (Digital Instruments, Santa Barbara, CA) at the University of Western Ontario. Details of the AFM methodology are discussed elsewhere (Nag *et al.*, 2004b). The AFM images were displayed in two or three dimensions, and further processing using line sections were performed using the Nanoscope IIIa software (Harbottle *et al.*, 2003; Nag *et al.*, 2004b).

The deposited films were also imaged using a time of flight-secondary ion mass spectrometer (TOF-SIMS) (details described by Harbottle *et al.*, 2003). The method required sputtering of the surface of the film by an inert beam of gallium ions, with detection of fragments of the specific molecules in a TOF tube at different molecular masses. These fragments were simultaneously mapped in a 10 x 10 μ m region, and their intensities were plotted to show the two dimensional distribution.

2.4.4 Differential Scanning Calorimetry

DSC is a technique that measures the thermodynamic melting properties of phospholipids bilayers, as they undergo a phase transition from gel to liquid crystalline phase upon heating. Studies were performed on a MC-2 Differential Scanning Calorimeter (Serial No. 025, Microcal, LLC Inc., Northhampton, Massachusetts) and data analyses were performed using Origin Software (Microcal LLC Inc.). Water was used as a reference in one of the cells, and the samples were inserted into the other cell. The volume in both cells was 1.192 ml. Experiments were run over a temperature range of 10-50 °C at a scan speed of 60 °C/hr. The sample, at an initial temperature of 10°C, was heated to the desired end temperature. Only heating could be performed due to instrumental limitations. A total of three heating scans were performed for each sample, with a 60-minute break in between to cool back to the initial temperature of 10°C. Slower scan rates did not show any appreciable difference with the ones performed in the fast rates, and were not pursued further. The scans were performed and were plotted as heat capacity as a function of temperature, and were later baseline normalized to kcal/mole of phospholipids (which was performed by the Origin Software). All experiments were done in triplicate. Normally, the second or third scan out of the three cycles was displayed in the data, as previously described by others (Keough and Kariel, 1987).

2.4.5 Electron Microscopy

Transmission electron micrographs were obtained for BLES/BSA dispersions. Samples were fixed in 4% glutaraldehyde and water, and stained with 1% OsO₄. The sample was then pelleted by centrifugation and left overnight. The sample was then dehydrated with acetone, and embedded in an epoxy TAAB 812 resin, followed by ultrathin (100nm) sectioning of the resin block using a Reichert OmU2 ultra microtome to 90 nm thicknesses. It was then counterstained with uranyl acetate and lead citrate, and examined with a Zeiss EM109 transmission electron microscope, and photographs of the images were obtained. Details of such methods applied to LS are discussed by others (Nag *et al.*, 1997a).

2.4.6 Fourier Transform Infrared Spectroscopy

FTIR experiments were performed with a Bruker Tensor 27 infrared spectrometer (Bruker, Billerica, Massachusetts). This instrument is equipped with a MIRacle Attenuated Total Reflection (ATR) accessory allowing rapid and easy Fourier transform analysis of liquid and solid samples. BLES dispersions (27mgs/ml) mixed with different concentrations of BSA were added to the surface of a zinc crystal, from which an infrared laser beam was reflected. Samples were not degassed prior to addition to the crystal. The sample was exposed to the infrared laser, and a sensor detected the frequency shifted wavelengths of the beam. The frequency shift of the incident light occurs due to the molecular vibrations of the C-H, C-C etc. bonds of the phospholipids of the sample (Dluhy and Mendelsohn, 1988). The spectra appears as a series of peaks in either

transmittance or absorbance mode, as a function of wavenumber (in $\pm 1 \text{ cm}^{-1}$). Studies with different concentrations of BLES suggested CH_2 , CH_3 and $\text{C}=\text{O}$ signals could be obtained from dispersions above 60 mgs/ml concentration. However, due to specific alignment of the zinc crystal (experimental limitation) it couldn't be resolved if the CH_2 and CH_3 stretching vibrations were from the phospholipid chains or the headgroup regions as the signal intensity did not alter with higher concentration of the samples.

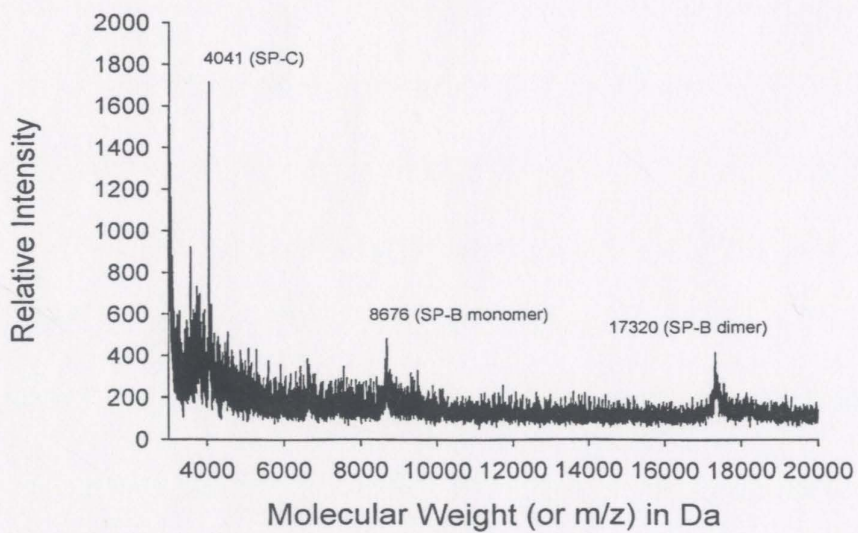
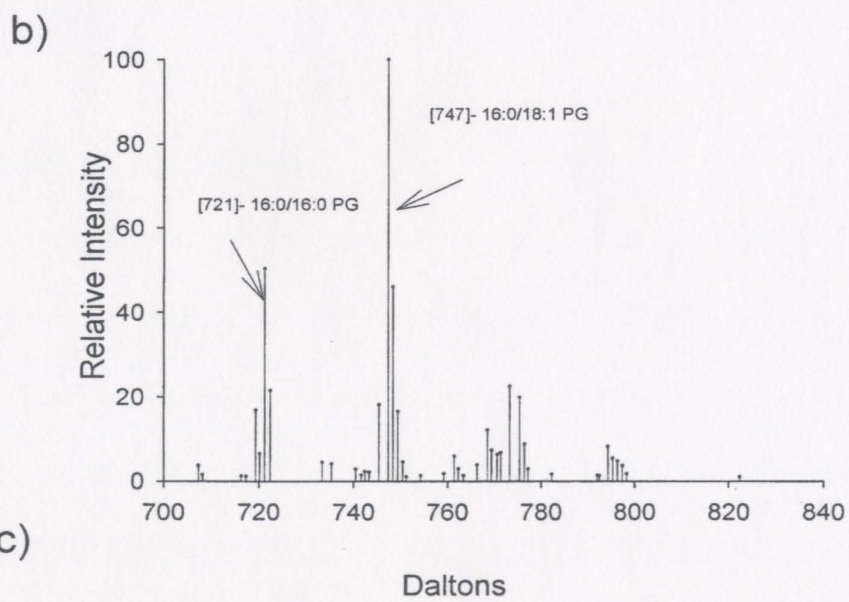
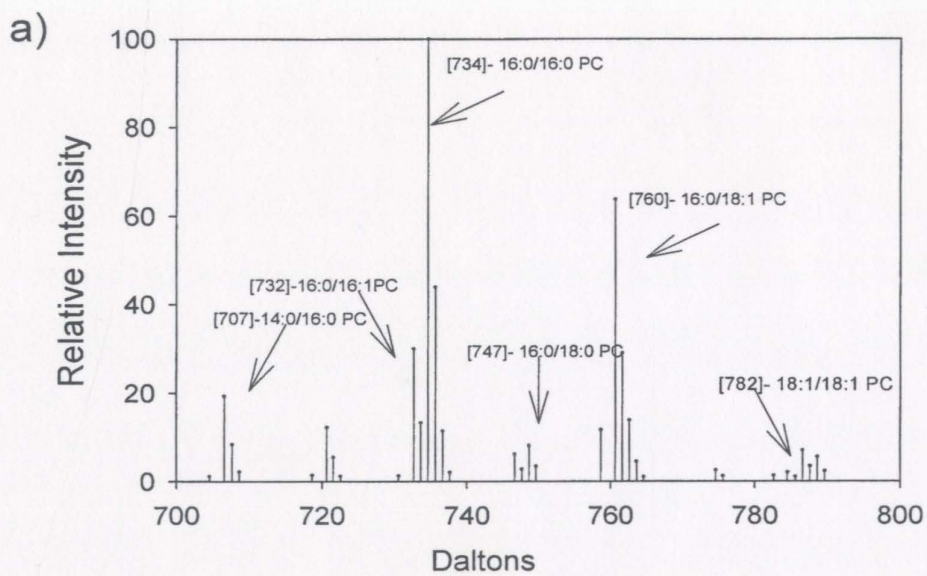
RESULTS

3.1 Mass Spectrometry

Different types of mass spectrometry were performed on BLES to determine the accurate and detailed composition of the lipids and proteins. Electrospray ionization mass spectrometry (ESI-MS) was done to determine the phospholipid composition of BLES. NH_4OH was added to the BLES (in C:M 3:1) as mentioned in the materials and methods, to remove the sodiated peaks (Harbottle *et al.*, 2003). **Figure 4** shows the positive ion **(a)** and negative ion **(b)** ESI spectra of the phospholipids. In the positive ion mode, DPPC (16:0/16:0 PC) was the most abundant phospholipid at 734 Da (mass in Daltons/charge where charge = 1), and the next most abundant was palmitoyl-oleoylphosphatidylcholine (POPC) (16:0/18:1 PC) at 760 Da. Other prominent peaks were 1-palmitoyl-2-myristoyl-phosphatidylcholine (PMPC) (16:0/14:0 PC) at 707 Da, 1-palmitoyl-2-palmitoyl-oleoylphosphatidylcholine (16:0/16:1 PC) at 732 Da, 1-palmitoyl-2-stearoyl-phosphatidylcholine (PSPC) (16:0/18:0 PC) at 747 Da, and dioleoylphosphatidylcholine (DOPC) (18:1/18:1 PC) at 782 Da. In the negative ion mode, 1-palmitoyl-2-oleoyl-phosphatidylglycerol (POPG) (16:0/18:1 PG) was the most prominent peak (at 747 Da) and the next was dipalmitoylphosphatidylglycerol (DPPG) (16:0/16:0 PG) at 721 Da. The other peaks were probably less abundant negatively charged phospholipids present in BLES such as PI, and other phosphatidylglycerols (PG).

MALDI-TOF was done to determine the hydrophobic protein compositions of BLES. **Fig. 4 (c)** shows the peaks of the lipid associated proteins of BLES. There is a

Figure 4: Mass spectrum profiles showing the composition of bovine lipid extract surfactant. The profile in (a) is the ESI mass spectra in positive ion mode of the phospholipids of BLES, with dipalmitoylphosphatidylcholine (16:0/16:0 PC) being the most abundant, and 1-palmitoyl-2-oleoylphosphatidylcholine (16:0/18:1 PC) being the next most abundant. Other phospholipids visible are 14:0/16:0 PC, 16:0/16:1 PC, 16:0/18:0 PC, and 18:1/18:1 PC. The profile in (b) is in the negative ion mode, with 16:0/18:1 PG being the most abundant, and 16:0/16:0 PG also present in significant amounts. The m/z (mass/charge where $z = +1$, and thus $m = \text{M.W.}$ in Daltons) of the lipids is shown in the brackets [] in the figures. The spectrum in (c) is the MALDI-TOF mass spectra of the hydrophobic proteins (SP-B & SP-C) of BLES.



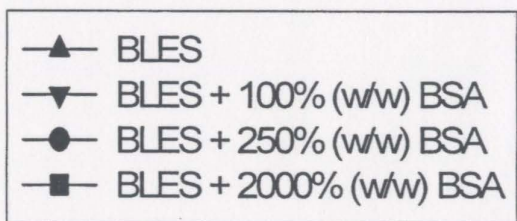
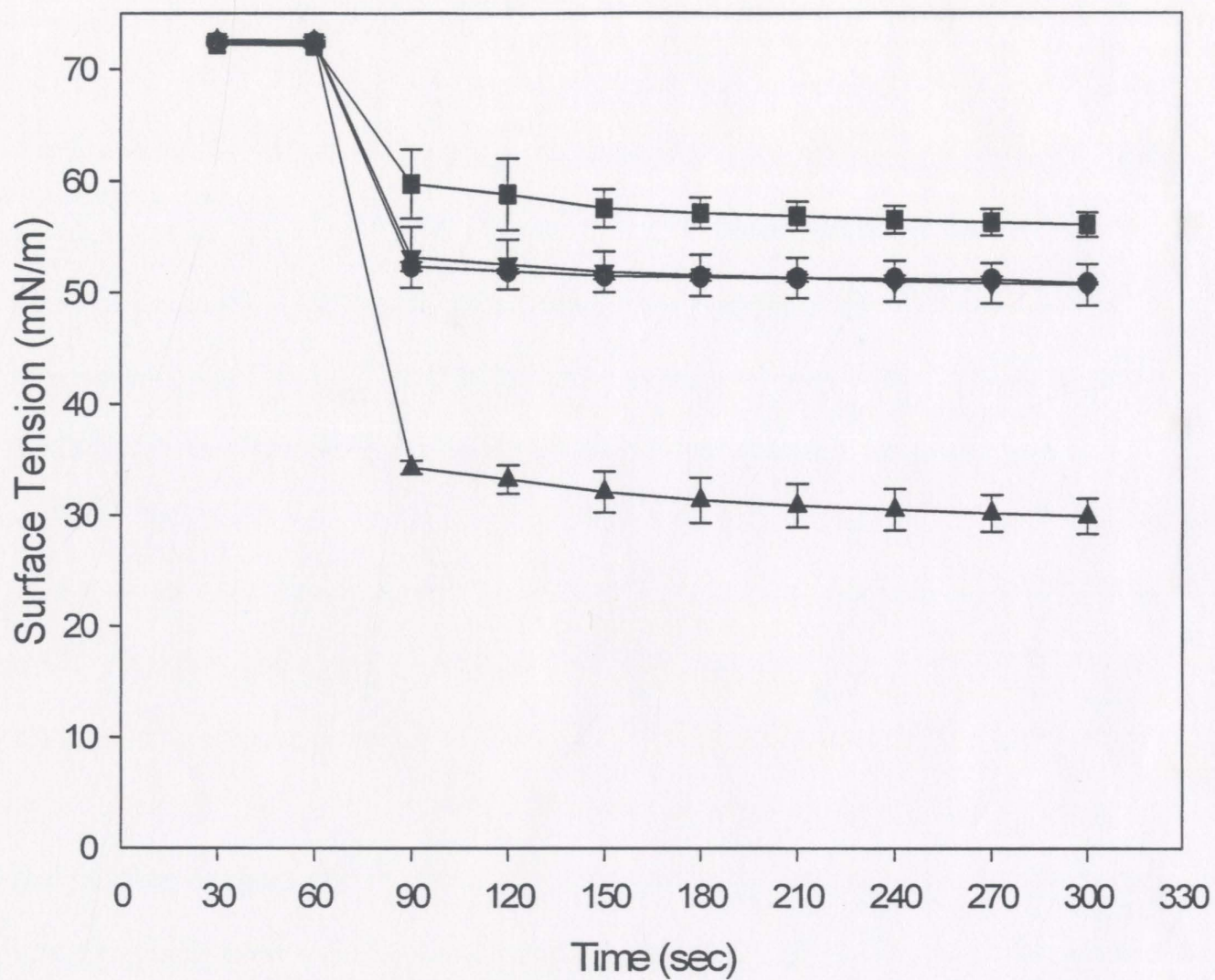
prominent peak at 4041 m/z which corresponds to SP-C, and two peaks at 8676 and 17320 m/z which correspond to the SP-B monomer and dimer respectively. The data of MALDI-TOF of BLES suggests SP-C is present in a higher amount than SP-B, in bovine surfactant.

These lipid and protein compositions of BLES are in agreement with previous studies performed using other assay methods on bovine lavaged LS (Yu *et al.*, 1983), but are more accurate in mass resolution. Also, this lipid profile was in close agreement with those of ESI-MS of human LS performed by Postle, (2000) and on isolated SP-B/C from porcine lungs (Nag *et al.*, 1997b).

3.2 Monolayer Experiments

Adsorption experiments were carried out in which BLES or BLES+BSA dispersions were injected beneath the interface at a concentration of 0.25 mg/ml, and the adsorption of the lipids to the surface was measured as a function of time (in seconds), monitored by a change in γ . Concentrations of 0.25 (100% w/w), 0.625 (250% w/w), and 5 mg/ml (2000% w/w) of BSA were added to BLES dispersions (0.25 mg/ml) while the total volume was kept constant, and the mixtures were incubated at 37°C for one hour. **Figure 5** shows the adsorption curves for BLES, and BLES + BSA mixtures. These experiments are repeatable, and each curve is an average of three independent experiments, with the standard deviations noted by the error bars. BLES alone adsorbed rapidly to a minimum γ of 30 mN/m (near the equilibrium γ of 25mN/m), whereas in mixtures with BSA, a decrease in the magnitude of the drop in γ in the same

Figure 5: Adsorption isotherms (surface tension vs time) of BLES dispersion (0.25 mg/ml) with varying concentrations of BSA in the dispersions at $23 \pm ^\circ\text{C}$. The first sixty seconds of the curve was used in monitoring the γ of the clean air-water interface before injecting the samples. The curves are an average of 3 different sets of experiments, with standard deviations, shown by the bars of the $n=3$ experiments. BSA has been shown to be adsorbing to a γ of 45-50 mN/m under these conditions by others (Taneva and Paniaotov, 1984).

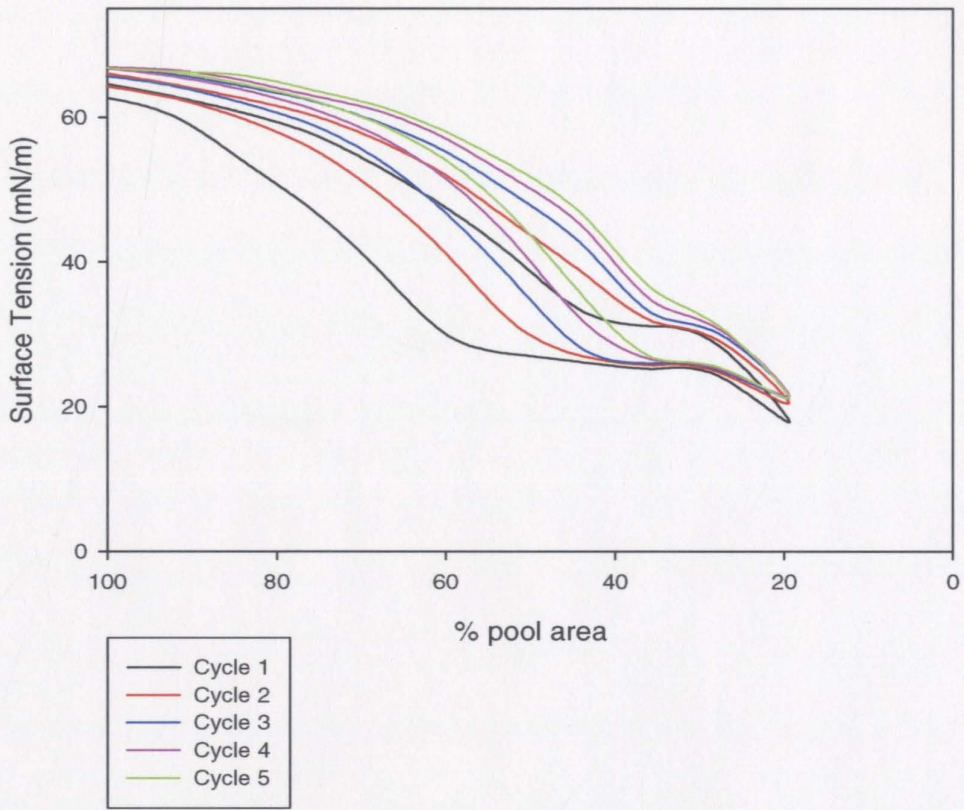


time period was observed. Pure BSA adsorbs to a γ of about 45-50 mN/m as determined in a number of previous studies (Taneva and Panaiotov, 1984). BLES + 2000% BSA (w/w) showed the least drop in γ , with a final γ of approximately 55mN/m, significantly higher than the equilibrium γ of 30mN/m for BLES alone. This suggests that BSA does not allow the BLES dispersion to adsorb as well to the air-water interface.

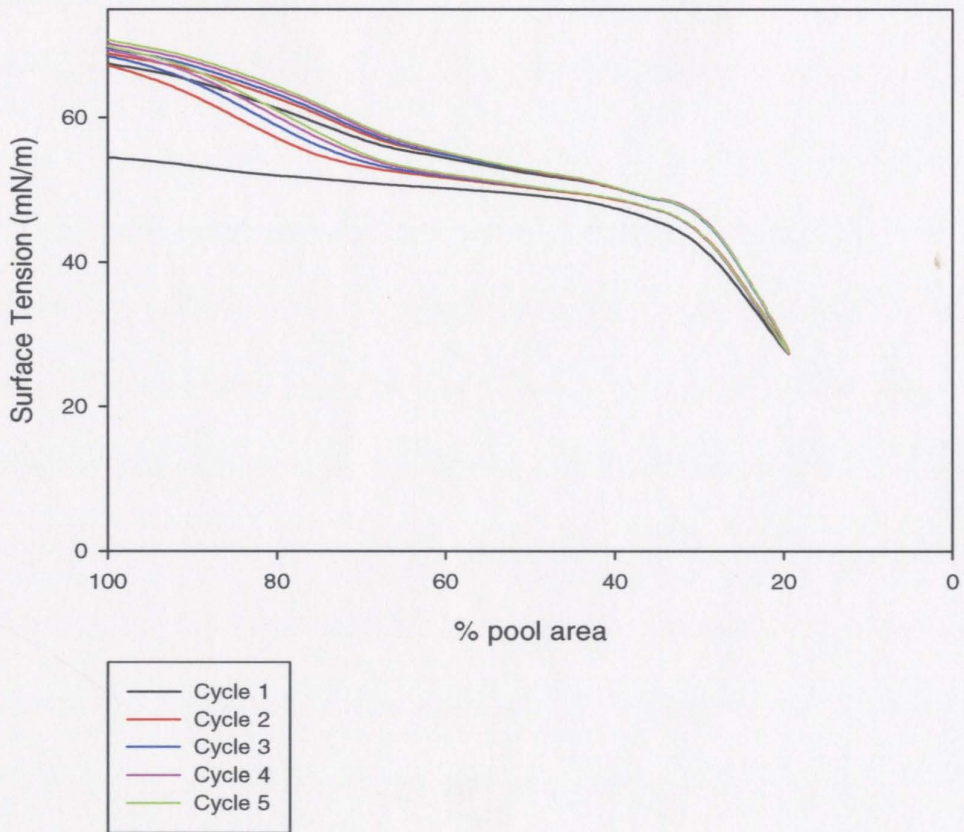
Compression-expansion experiments were done with BLES + BSA mixed dispersions spread onto a ddH₂O subphase. **Figure 6** compares multiple compression-expansion cycles of adsorbed films of BLES (40 nmoles) **(a)** with multiple cycles of BLES + 250% BSA **(b)**. Cycles were carried out at a fast speed of 506 mm²/sec. BLES alone showed a reduction of γ to a minimum of 17.9 mN/m, whereas when BSA was added to the dispersion, there was a drop to 27.9 mN/m, at least at 80% of film area compression. This suggested that when BSA was added to the BLES dispersions, and the film was compressed, BSA interfered with lipid packing and deterred BLES from reaching low minimum γ . A low γ was not reached even at larger area compression, since BSA may have occupied more space in the films and was difficult to squeeze-out. As in **(a)**, for BLES alone, multiple cycles seemed to reduce the plateau area (30% in the first cycle) with successive cycles (30% to 15%). This suggested possibly some sort of loss of material from the films (“squeeze-out”) over multiple cycles (called film refining). Previous studies have shown that pure BSA films show a broad transitional plateau at about 50 mN/m, and collapse at 35mN/m (Taneva and Panaiotov, 1984). In our BLES + BSA film **(b)** the plateau was seen to be prominent over 5 cycles in the BLES + BSA

Figure 6: Surface tension vs relative pool area isotherms for compression expansion cycles of BLES (a) and BLES + BSA (250% w/w) (b) mixed dispersions adsorbed onto a ddH₂O subphase. Total pool area (100%) was 165 cm² and only 80% compression was possible due to 20% of the area being occupied by the Wilhelmy plate and a circular window for optical observation. Multiple cycles were performed for each. The concentration of BLES dispersion used was 0.09 mg/ml of lipid plus 0.225 mg/ml BSA. All experiments were performed at an ambient but monitored room temperature of 23 ± 1°C. All compression-expansion experiments were repeated 3 times for reproducibility, and only a representative plot is shown for clarity.

a)



b)



films. With successive cycles, there was no change in the plateau region (50% area), suggesting that BSA could not be removed from these films by squeeze-out, through multiple cycling. This suggests that BLES lipids and BSA mix together very well and such mixtures cannot be easily separated out even with expansion.

Compression-expansion experiments were further performed where BLES (in C:M 3:1) (1mg/ml) was solvent-spread on the surface of the ddH₂O subphase. BSA was dissolved in to the subphase, before the addition of BLES. Cycles were carried out at a speed of 506 mm²/sec. **Figure 7** compares the first cycle of BLES with the first cycle of BLES (40 nmoles) + 250% BSA (w/w). BLES films alone reduced γ to 7.9 mN/m when compressed, whereas BLES + 250% BSA (w/w) dropped to a minimum γ of 31.1 mN/m. This result suggests that albumin adsorbs onto the BLES monolayers and can interfere with the packing of lipids at the surface during compression. This is possible if BSA adsorbs separately and inserts into the BLES films in the chain hydrocarbon region of the lipids.

Figure 8 compares solvent-spread BLES film isotherms with increasing concentrations of BSA dissolved in the subphase. Once again, the first cycle of the compression-expansion experiments were compared. The films were compressed and expanded at 506 mm²/sec. It was evident that with increasing concentrations of BSA, there was less of a reduction in the minimum γ . This implies that with more BSA added, the ability of the films to reach low γ is disrupted in a step-wise fashion. There was also a change in the surface tension and length of the plateau with increasing BSA; eventually the plateau was lowered to ~52 mN/m at the maximum amount of BSA.

Figure 7: Surface tension vs relative pool area (γ -A) isotherms for compression expansion cycles of solvent-spread monolayers of (-) BLES and (---) BLES + 250% BSA (w/w) (0.225 mgs/ml in the subphase). The amount of BLES spread on the surface was about 40 nmoles of phospholipid as assayed using the phosphorus assay of the hydrophobic extract of BLES. Arrows indicate the direction of compression (>) and expansion (<).

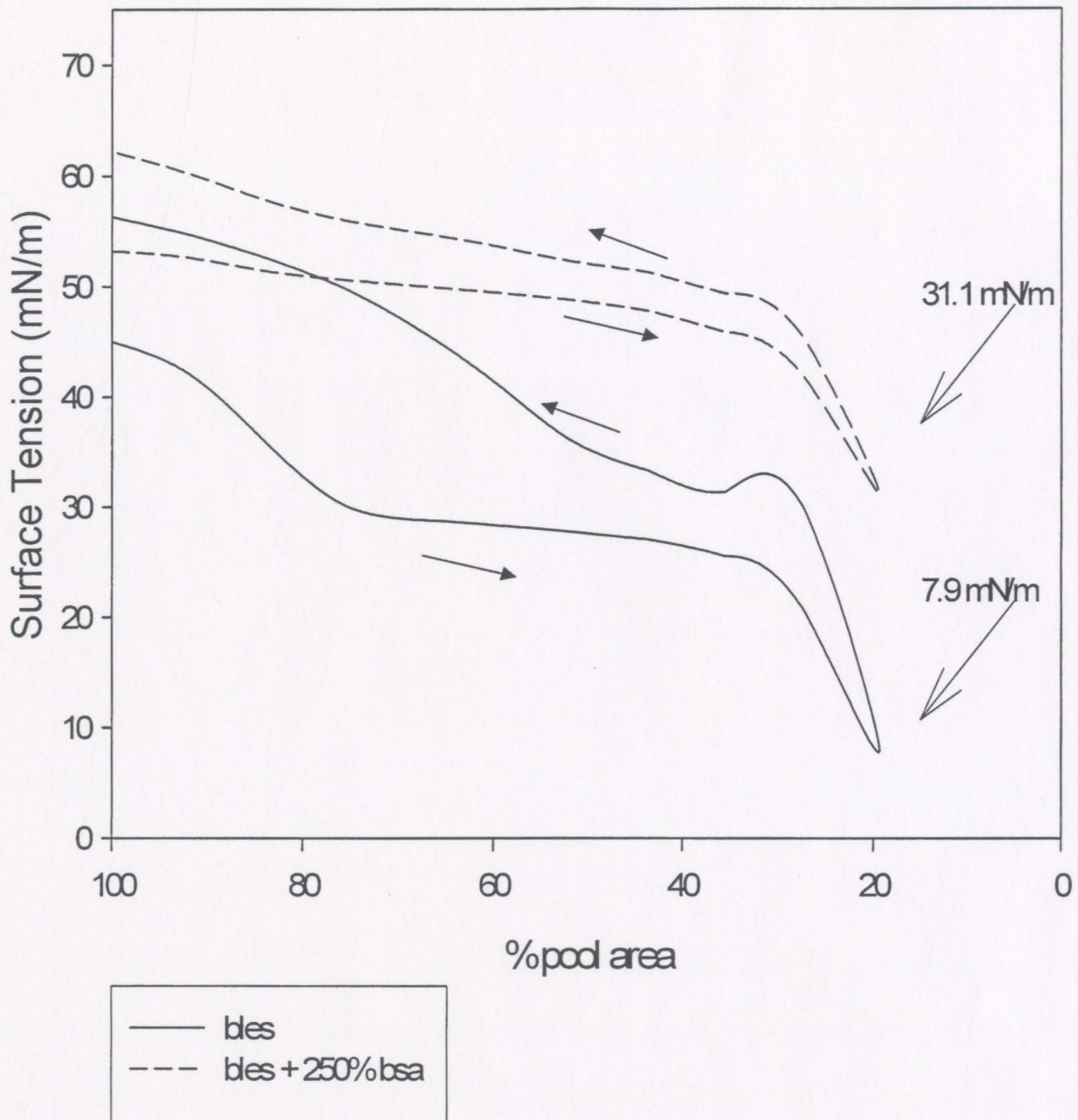
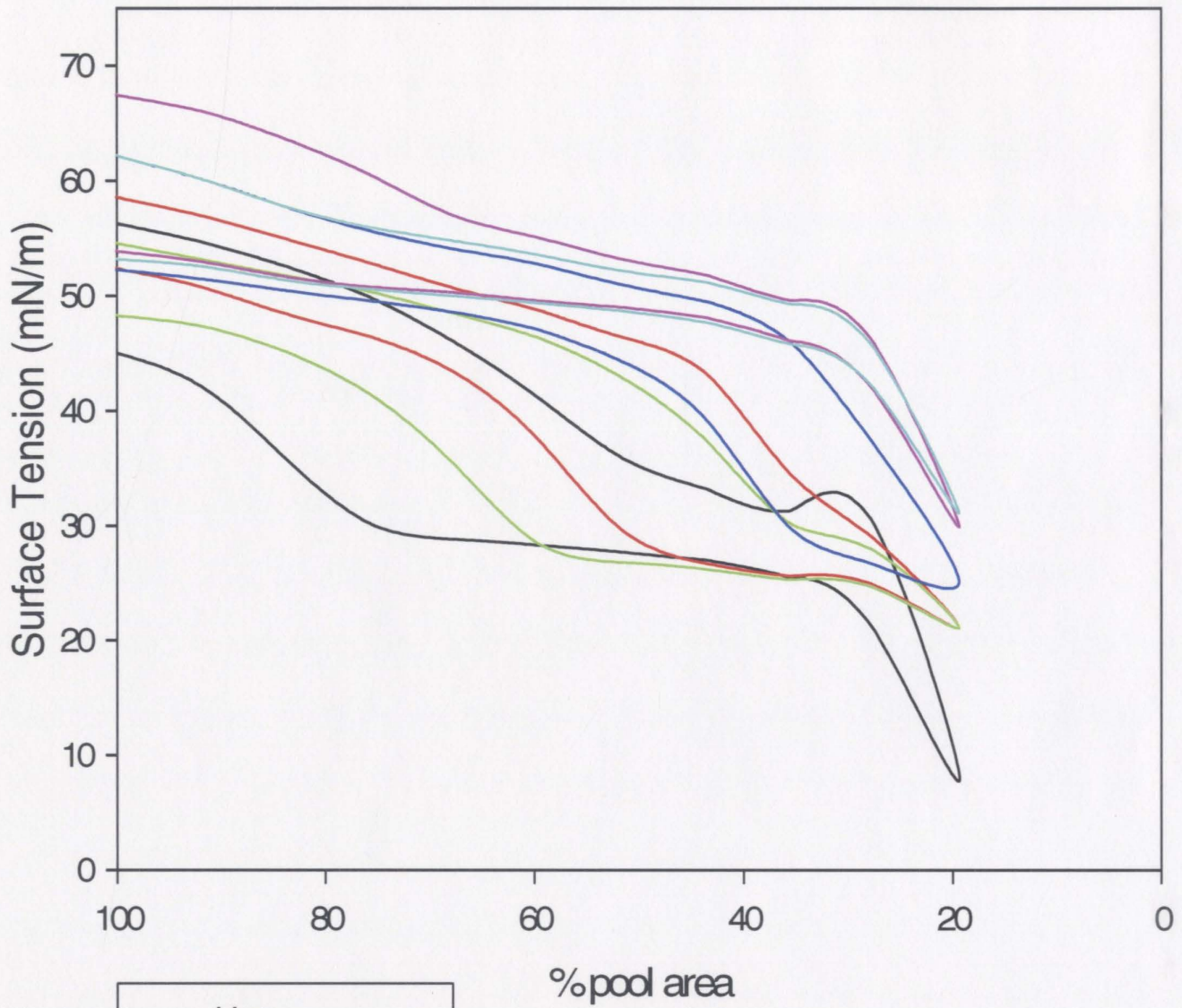
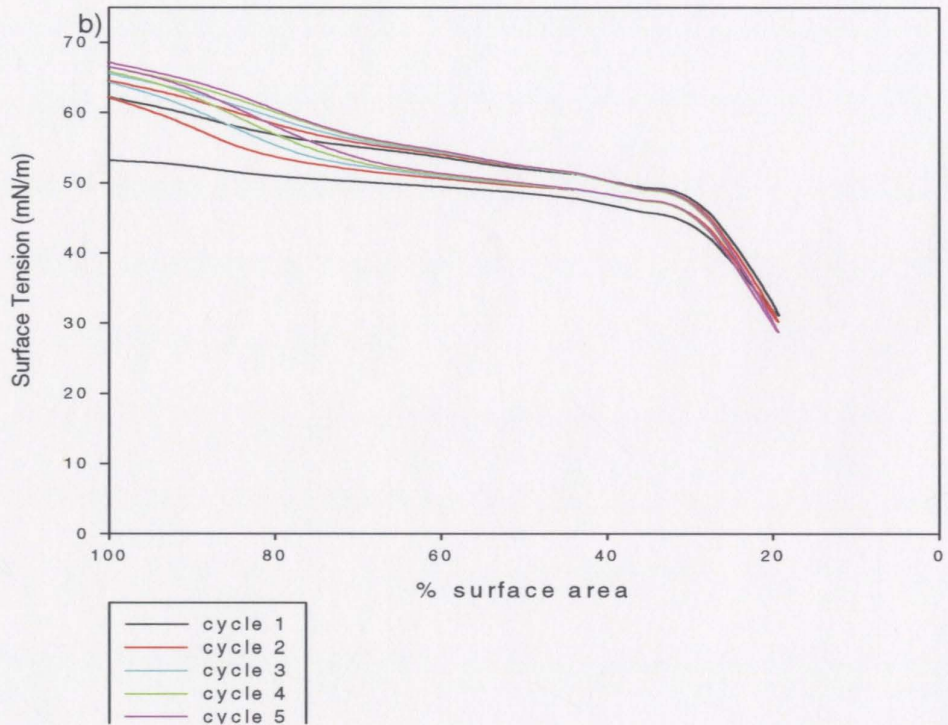
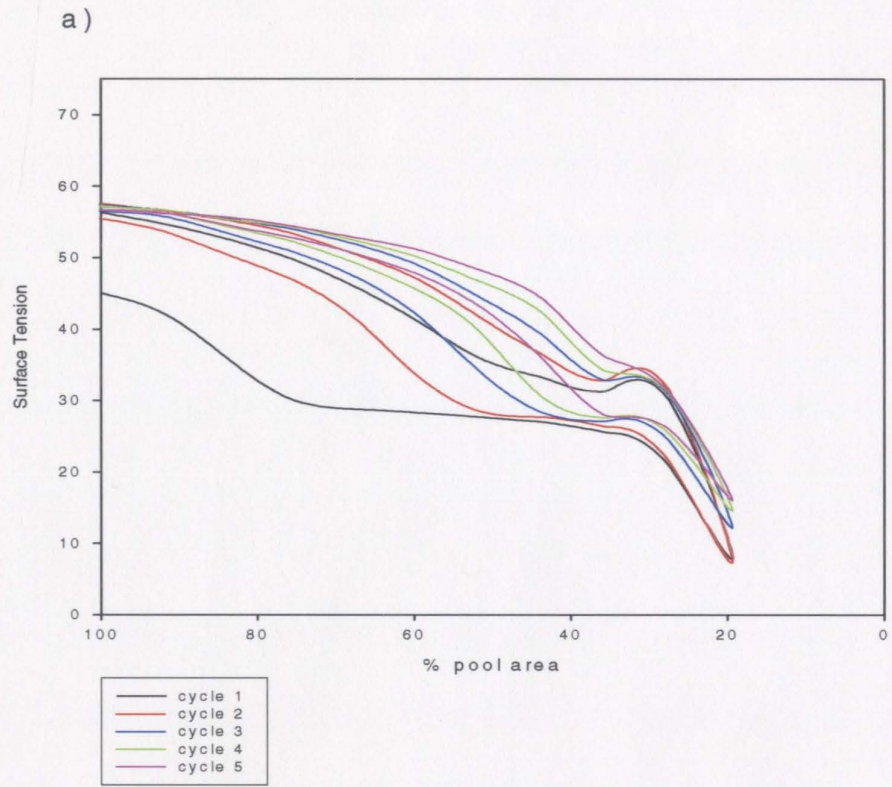


Figure 8: Surface tension vs relative pool area isotherms of the first compression-expansion cycle of solvent-spread monolayers of BLES (40 nMoles), and BLES with different concentrations of BSA (w/w) dissolved in the hypophase (12.5% - 0.02 $\mu\text{g/ml}$; 25% - 0.04 $\mu\text{g/ml}$; 50% - 0.08 $\mu\text{g/ml}$; 100% - 0.16 $\mu\text{g/ml}$; 250% - 0.41 $\mu\text{g/ml}$). The BLES: BSA stoichiometry is calculated assuming all the dissolved protein in a 200ml subphase interacts with the 40nM of lipid in the film.



Multiple dynamic cycles were also carried out, for BLES and BLES + BSA films. Five cycles were run continually with no stop in between cycles. **Figure 9** compares BLES **(a)** with BLES + 250% BSA (w/w) **(b)** films. In **Fig. 9(a)**, the first cycle of BLES films shows the decrease to the minimum γ , and the subsequent cycles show a decrease in the drop. This suggests that subsequent compressions possibly do not allow the materials to be re-adsorbed back in the films, to produce such low γ . As a result, the minimum γ shown in the first cycle was not observed in subsequent cycles. However in **Fig. 9 (b)** all cycles show that the minimum γ was reached (although γ was not as low as those in BLES alone), and the cycles exhibited very low hysteresis. By cycle 5, almost no difference between compression and expansion was noticed. As suggested by **Fig. 6** and **Fig. 9**, we can thus conclude that the solvent spread or adsorbed films of BLES with BSA are similar. This would indicate that similar BLES lipid- BSA interactions occur whether the protein approaches the monolayers from the subphase (**Fig. 9**), or whether the protein interacts with the BLES bilayer in dispersions (**Fig. 6**) which forms the adsorbed monolayers. Previous studies have suggested that, at least in the case of porcine and rat surfactant lipid extracts, solvent spread or adsorbed films are equivalent at equal γ (Nag *et al.*, 1998; Panda *et al.*, 2004).

Figure 9: Surface tension vs relative pool area graph of multiple cycles of solvent-spread monolayers of (a) BLES, and (b) BLES + 250% BSA (w/w).



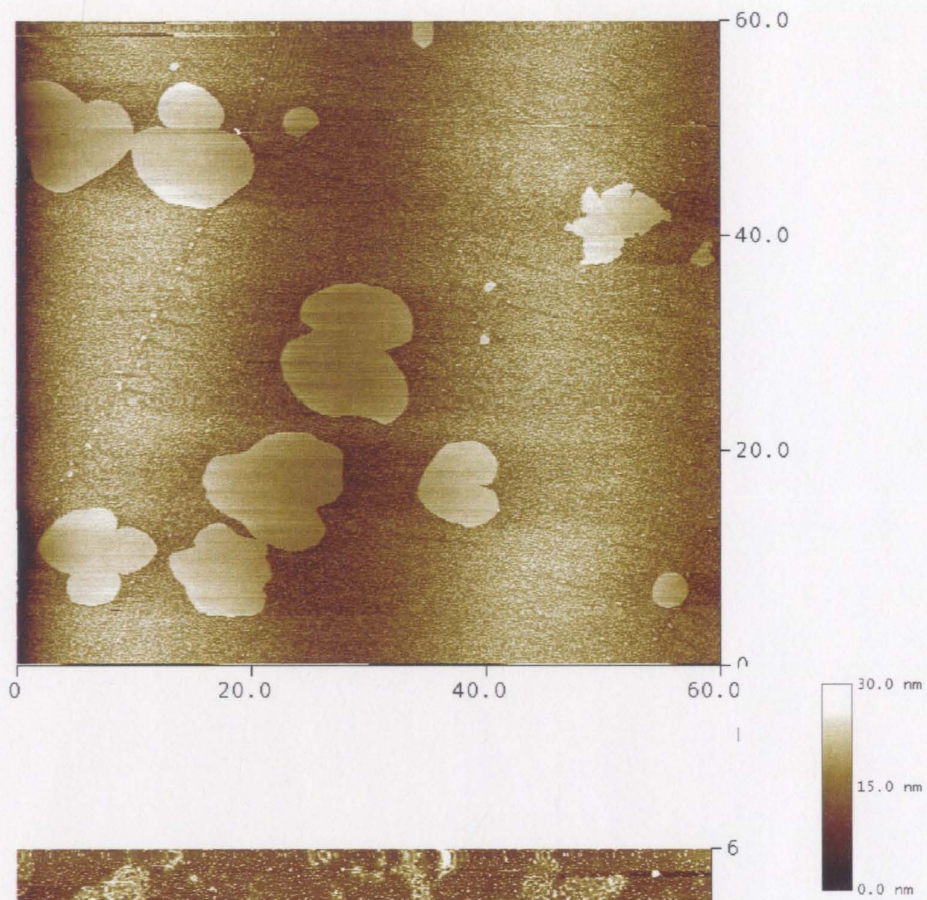
3.3 AFM Experiments

AFM experiments were carried out on BLES/BSA films adsorbed from dispersions, and the films deposited on mica. Films were adsorbed until the suggested γ (as noted in the AFM figures) were reached, and then compressed at 0.04 nm²/molecule/min. Deposits onto freshly cleaved mica were obtained for AFM measurements at the desired γ , using a vertical upstroke (pulling the mica sheet out of the water with film, using the Blodgett deposit method). **Figure 10** shows AFM images of **(a)** a deposit of BLES films taken at 40 mN/m, and **(b)** a deposit of BLES + BSA (1:1) films taken at the same γ . With BLES alone, clearly distinct condensed domains (bright regions) were visible, with a higher height than the surrounding fluid phase of the film. The height of the condensed domains appeared to be $\sim 0.7 - 0.9$ nm higher compared to the surrounding fluid phase of the film. With BSA added in such BLES films, the appearance of gel domains was less clear. The film appeared disrupted, with certain small areas with domains, and became very heterogeneous in appearance in other areas. The condensed domains were less distinct than those observed in **Fig. 10 (a)** of BLES alone. This suggests that the ordered or condensed (gel-like) domains of BLES are disrupted by BSA. Other microstructures and domains with heterogeneous topography and fluid like properties also appear.

Fig. 11 (a) shows a line section through the AFM image to show the heights of specific domains compared to the surrounding fluid phase. **Fig. 11 (b)** shows a molecular model of the lipids of BLES when they undergo a phase transition to condensed domains and how this can be imaged using AFM. Note the condensed lipids are compacted

Figure 10: AFM images of (a) deposit of BLES films on mica taken at a γ of 40mN m^{-1} , and (b) one of BLES + BSA (100% w/w) film taken at the same γ . The adsorbed films were compressed at a speed of $0.04\text{ nm}^2/\text{molecule}/\text{min}$ and stopped at desired γ for deposit on mica sheets submerged in the subphase. Image areas are $60\text{ }\mu\text{m}^2 \times 60\text{ }\mu\text{m}^2 \times 30\text{ nm}$ (colour coded bar shown). The white areas of the images are 1-2 nm higher than the surrounding darker areas.

a)



b)

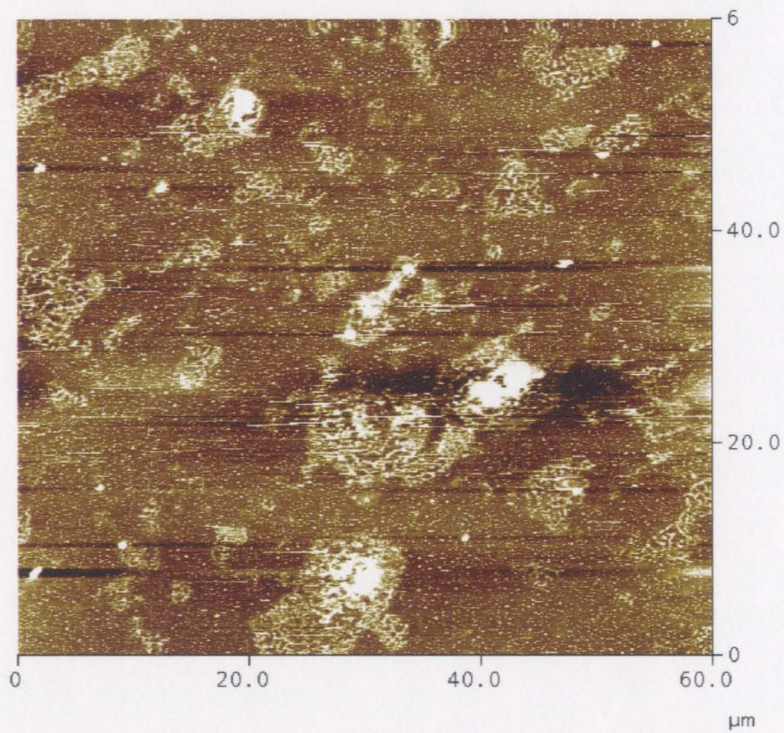
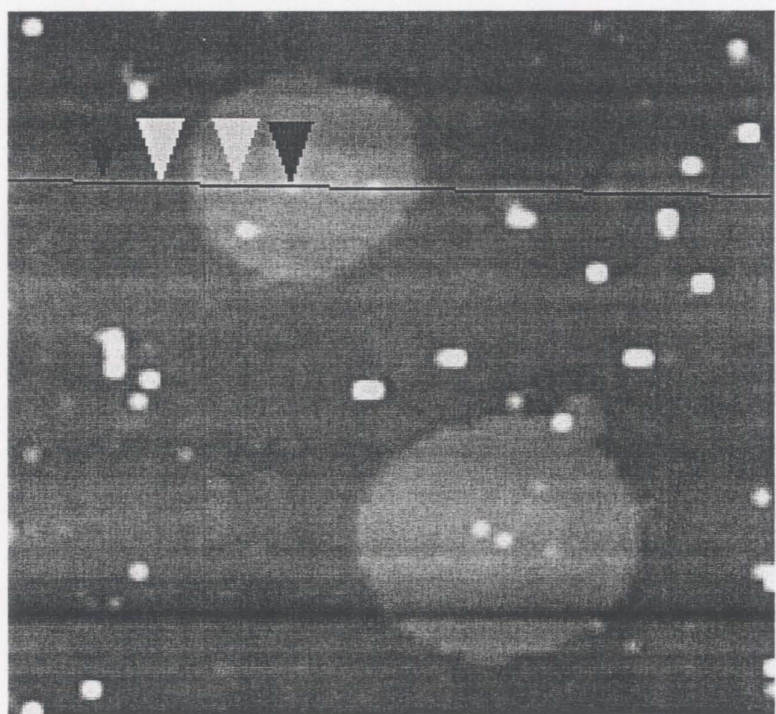
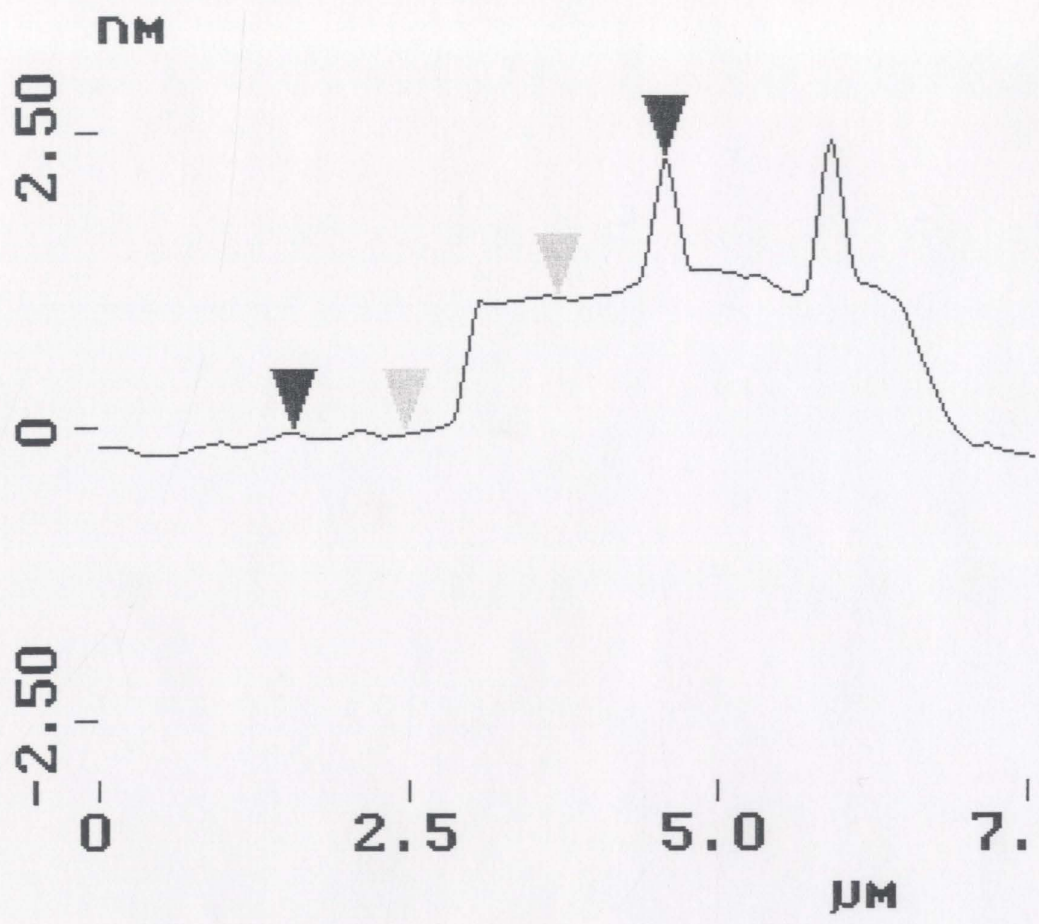
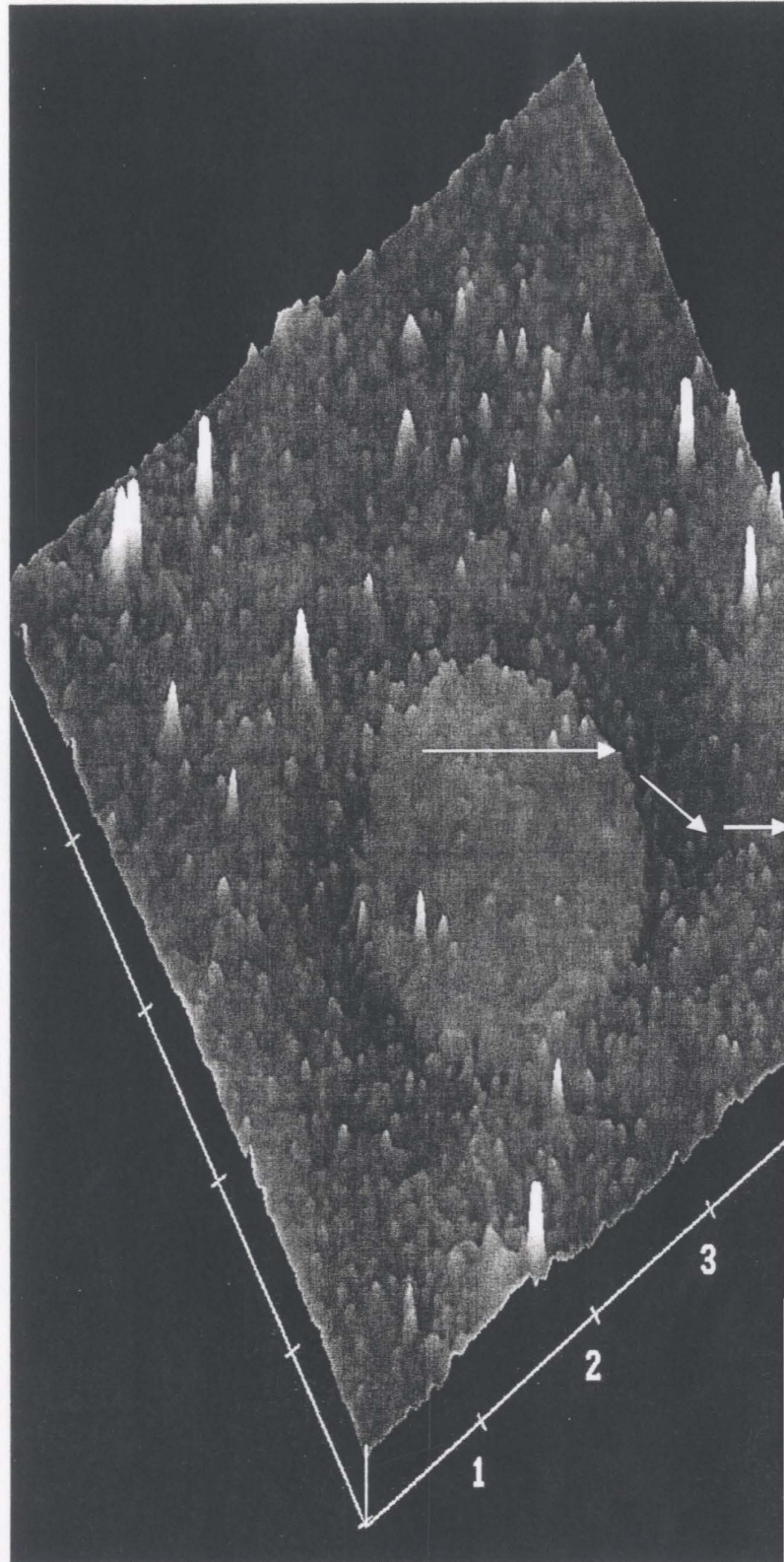
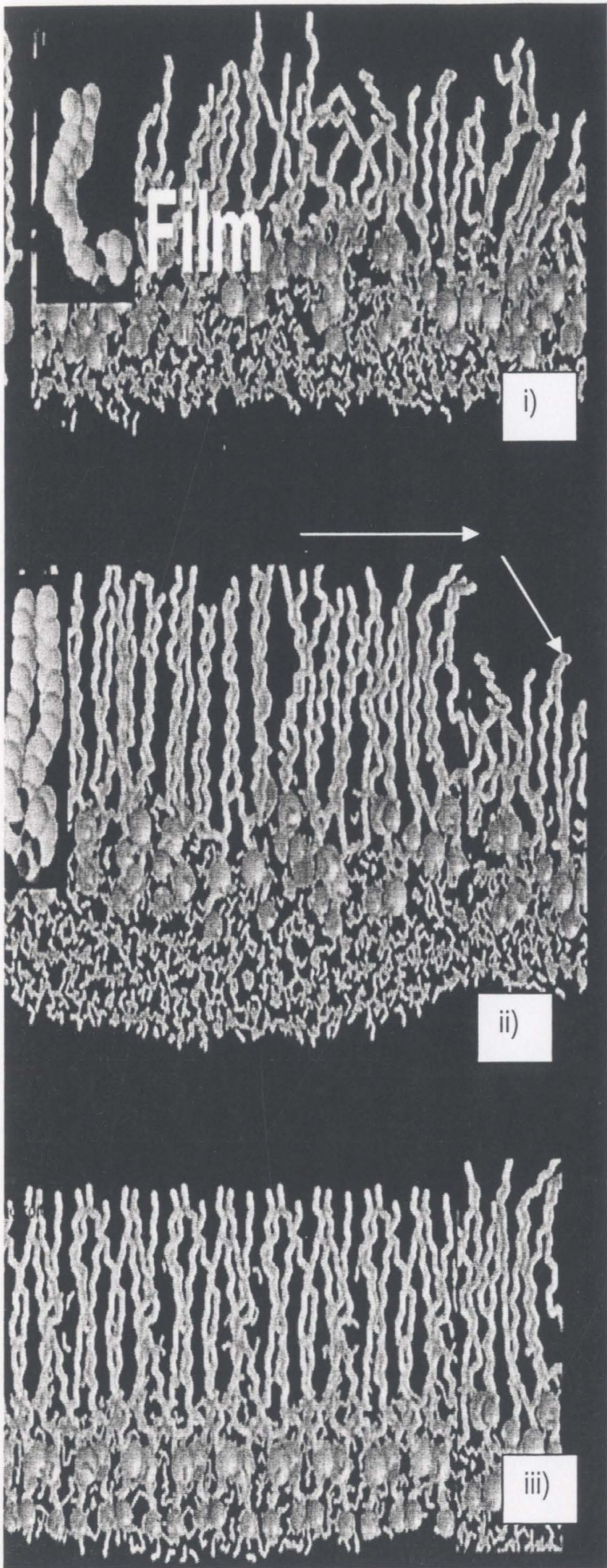


Figure 11: Line section through an AFM image from a BLES deposited film is shown in (a). The white areas correspond to the highest peaks, and the darker areas correspond to the lower regions. A molecular model showing the compacted BLES lipids when they are in condensed domains is shown in (b). The line section (a) suggests there is ~ 0.7 - 1 nm difference between the condensed domains and the surrounding fluid phase, as shown by the light grey arrows. The centers of the domains have spotted (white dots) structures which are much higher. These may be other multilayer structures (2.5 nm) or artifacts of imaging. The tilts of the phospholipids chains in the fluid (i), condensed (ii), and solid (iii) phases as shown in (b).



a)



b)

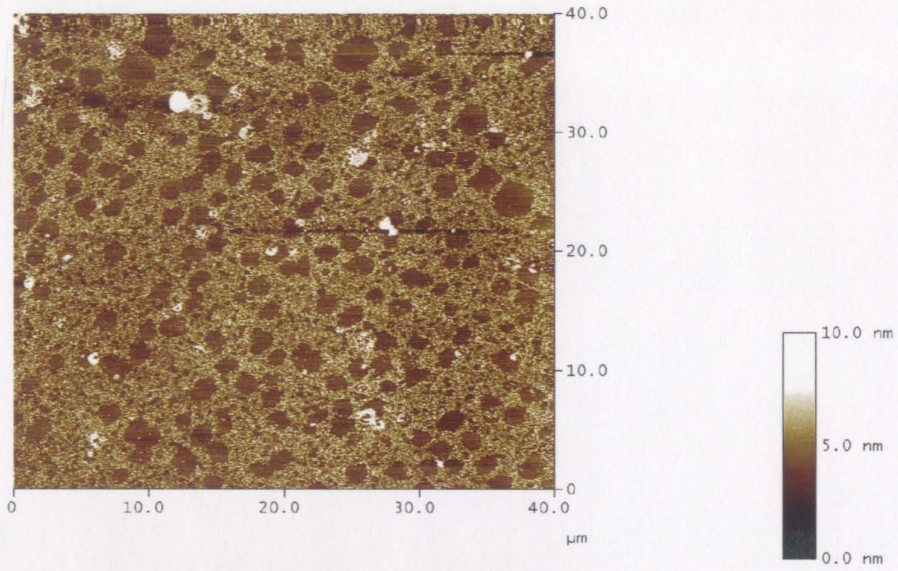
(tightly-packed), and appear higher than the fluid lipids, due to the ordering of the hydrocarbon chains in such domains, and also tilted more perpendicular to the air –water interface than the surrounding fluid phase (Nag *et al.*, 2004a; reviewed by Kaganer *et al.*, 1999).

Figure 12 shows AFM images of BLES films with different concentrations of BSA in the subphase, deposited at 30 mN/m. With BSA added in a concentration of 100% w/w **(a)**, the film appeared heterogeneous, suggesting slight disruption, and in 500% w/w **(b)**, the appearance of domains was much less, in fact they were hardly visible at all. And finally, with BSA added in 2000% w/w, the film could only be deposited at a γ of 50 mN/m **(c)**. These films could not reach low γ below 45mN/m, therefore only a deposit at γ of 50 mN/m was taken. This film appeared to consist mostly of sheets or plates of material. Thus in the images, there is no clear way to distinguish between lipid or protein domains. The AFM images of BLES (Harbottle *et al.*, 2003; Nag *et al.*, 2004b) and some of the BLES + BSA films are close approximations to those observed previously in normal and dysfunctional rat LS respectively (Panda *et al.*, 2004).

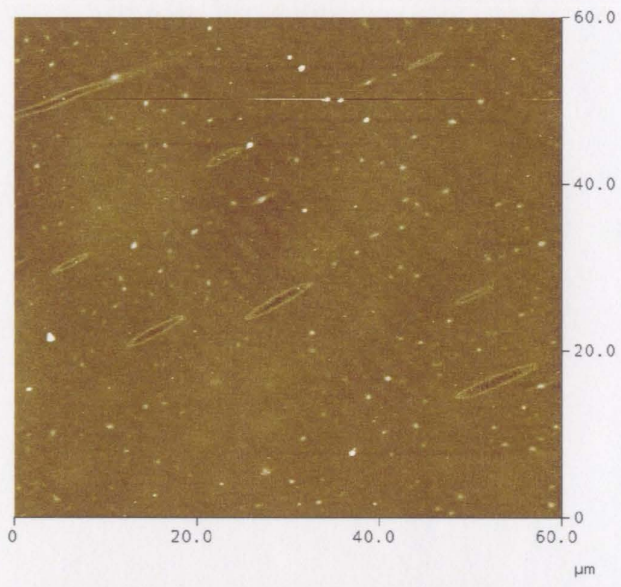
Figure 13 shows the 3-Dimensional view of the AFM images of **(a)** BLES, **(b)** BLES + BSA (100% w/w), and **(c)** BLES + BSA (250% w/w) films deposited at a γ of 30 mN/m. These images suggest a clearer view of the different types of domains appearing in each sample, and their height profile. It appeared that either the domains in **(b)** and **(c)** (with BSA) were lower in height than the surrounding fluid phase, or the fluid phase had structures which were 2-3 times higher (~20 nm) than the condensed phase. This is possible due to BSA, being concentrated in the fluid phase.

Figure 12: AFM images of BLES/BSA films of (a) BLES + BSA (100% w/w), (b) BLES + BSA (500% w/w), and (c) BLES + BSA (2000% w/w) taken at a γ of 50 mN/m. The film in (c) could not be compressed to a lower γ than 40-50 mN/m (see text). Image areas are $40\mu\text{m} \times 40\mu\text{m} \times 10\text{nm}$. White areas are 1-2 nm above the surrounding darker areas, and dark brown areas are 1-2 nm below the surrounding areas.

a)



b)



c)

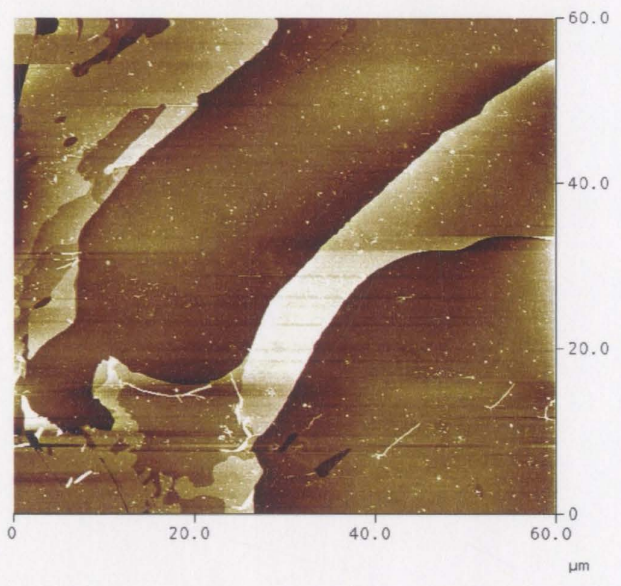
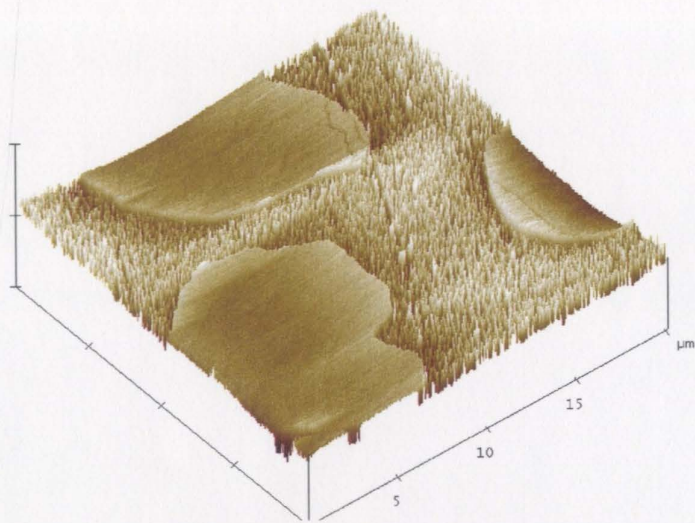
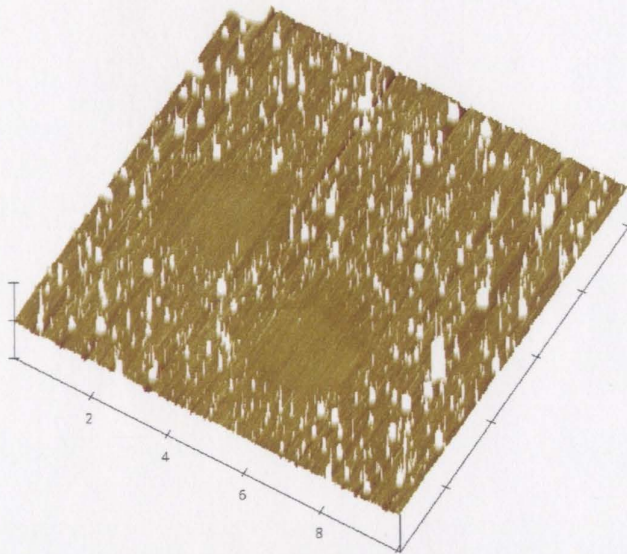


Figure 13: Three dimensional view of AFM images of (a) deposit of BLES (b) BLES + BSA (100% w/w), and (c) BLES + BSA (250% w/w) taken at a γ of 30 mN/m. Image areas are about $10\ \mu\text{m} \times 10\ \mu\text{m} \times 20\text{nm}$. Either the condensed domains in (b) and (c) (with BSA) are lower in height than the surrounding fluid phase, or the fluid phase has structures which are 2-3 times higher ($\sim 20\ \text{nm}$) than the condensed phase. This is possible due to BSA penetrating the fluid phase, or structures formed in the fluid phase, which are higher than the condensed regions. The white spots are individually too large ($2\text{-}3\ \mu\text{m}$) to be single albumin, but might be protein aggregates.

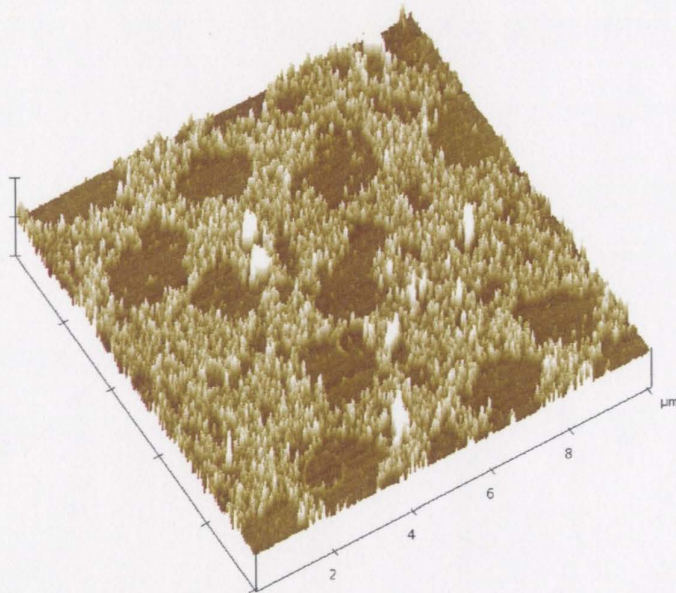
a)



b)



c)



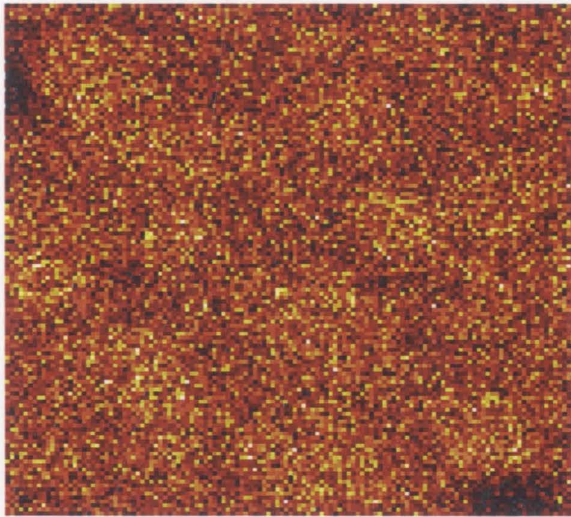
These AFM studies suggest that not only does BSA in BLES dispersions adsorb into the surface monolayers, they probably occupy the fluid phase and are enriched in this phase. BSA shifts the equilibrium drawing lipids from condensed phases to fluid phases and thereby the condensed domains disappear at the highest BSA concentration (at 2000% w/w). This suggests a complete disruption of lipid packing. The sheet like structures in **Fig. 12(d)** may suggest that films with a high amount of BSA collapse into some multilayered forms.

3.4 TOF-SIMS

Figure 14 shows Time of Flight-Secondary Ion Mass Spectrometry (TOF-SIMS) positive ion images of BLES **(a)**, and BLES + 10% BSA deposited films **(b)**. As observed in AFM, the domains of BLES are affected by BSA. With AFM, although new domains appear at high BSA concentrations it is not clear what these domains are made of or the localization of the protein in BLES. Previous studies on pure BLES using TOF-SIMS films have suggested that the domains of BLES are made of mainly DPPC and DPPG (Harbottle *et al.*, 2003). In **Fig. 14 (a)(i)** and **(b)(i)** the DPPC peak (at mass 734) image characteristic of BLES films is shown, and in **Fig. 14 (a)(ii)** and **(b)(ii)** the NH_4^+ peak image characteristic of proteins (at the amino fragments) (at mass 18) is shown. The light patches are where the specified molecular fragments appear, whereas the dark patches show the lower yield of the fragment. In **(a)** it was evident that DPPC was present in the BLES mixture through out the films, although some seemed to be

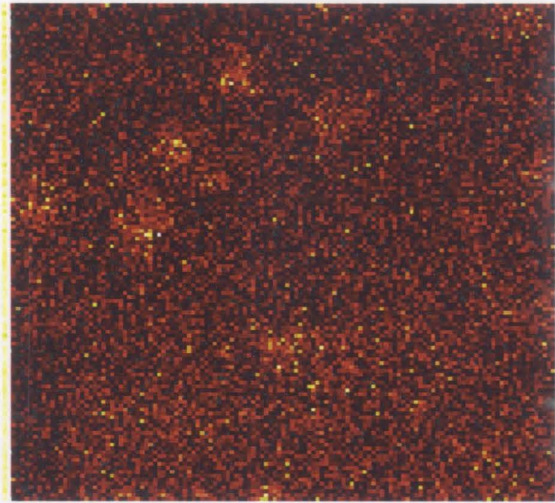
Figure 14: Time of Flight- Secondary Ion Mass Spectrometry (TOF-SIMS) positive ion images of BLES films (a), and BLES + 10% BSA films (b) deposited at a γ of 40 mN/m. The images (a)(i) and (b)(i) show the 734 peak which corresponds to the DPPC molecule of BLES. The images (a)(ii) and (b)(ii) show NH_4^+ , a characteristic peak of proteins.

a) BLES



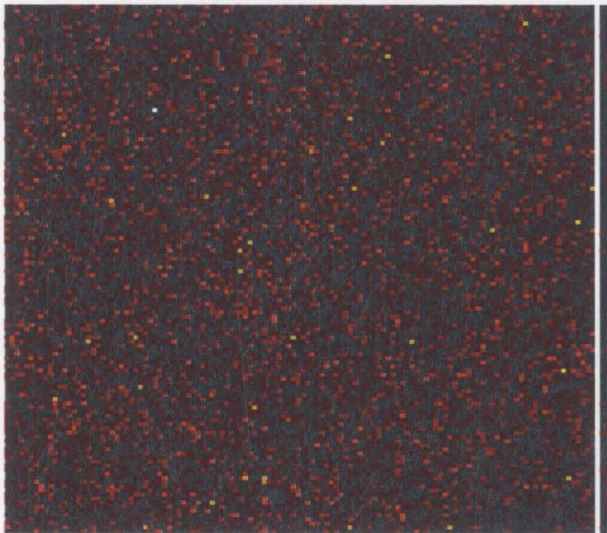
i)

b) BLES+BSA

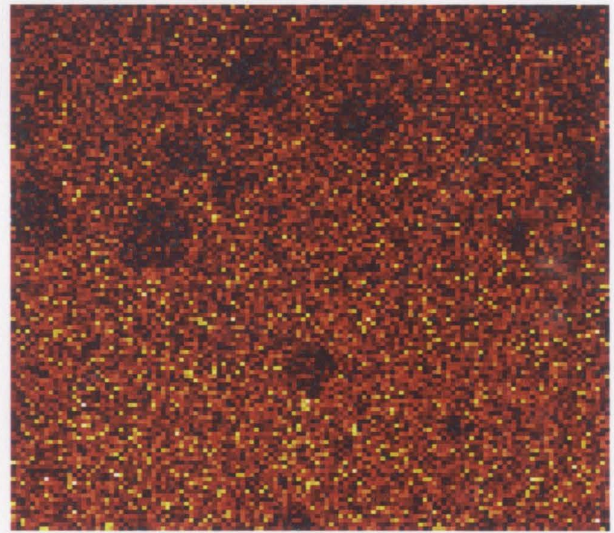


i)

DPPC (734)



ii)



ii)

NH4+/BSA (19)

10 um

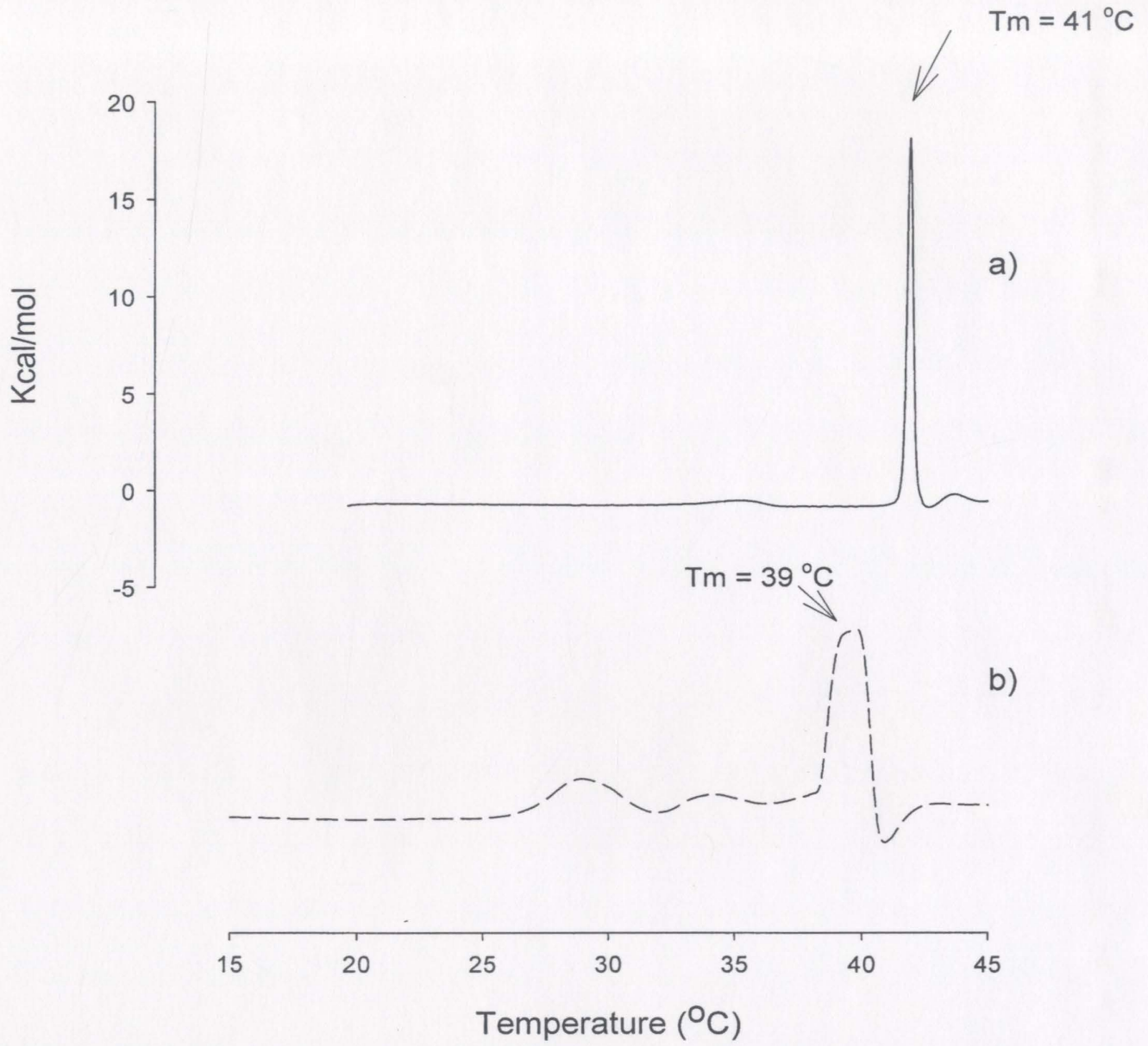
concentrated in domains **(i)**, whereas the NH_4^+ peak characteristic of protein was not **(ii)**. In the BLES + BSA film **(b)** we could observe distinct peaks of the master ion DPPC (M.W. = 734) **(i)** and BSA (NH_4^+) **(ii)**. By comparing **(b)(i)** and **(b)(ii)** it is evident that DPPC condensed domains in BLES + BSA films were devoid of BSA, which was only present in the surrounding fluid phase. The black regions in **(b)(i)** suggest the absence of the protein (BSA) in the condensed phase, and presence of DPPC in this phase. This was deduced from comparing these images with previous studies of BLES, where no distinct peaks of (NH_4^+) were observed, although SP-B and SP-C are present in BLES. However these hydrophobic proteins either do not generate major signals (2% w/w of lipids in BLES) or they possibly do not fragment as easily as the water soluble BSA.

3.5 DSC Experiments

The DSC thermal melting profiles of **(a)** DPPC, and **(b)** DPPC + 100% BSA (w/w) reconstituted dispersions are shown in **Figure 15**. The heating rate for these scans was 60°C/h. Scans were calibrated to kcal/mole. DPPC alone showed a midpoint of phase transition temperature (T_m) at 41°C, where as when BSA was added, there was a decrease of the midpoint of transition temperature to 39°C. There was also a broadening of the transition peak, suggesting that BSA is affecting the phase transition of DPPC lipids from gel to liquid crystalline phase, or the gel phase is easier to melt at a lower temperature. As well, BSA was found to alter the small pre-transition of the melting profile quite dramatically at around 35°C (the small peak at the 30-35°C range).

However, no such transition occurs in the BSA profile, thus, it is not a protein transition.

Figure 15: DSC melting profiles of (a) DPPC (2mg/ml) dispersions (multi-lamellar vesicles), and (b) DPPC + 100% BSA (10 mgs/ml) (w/w) dispersions. Scan rate was 60°C/h. Scans were calibrated to kcal/mole of phospholipid, and temperature of the midpoint of transition is noted on the graph. All DSC experiments were done 3 times, but only one data set is shown for clarity. Scan 1 is shown for both graphs however scan 2 and 3 are the same as in 1. The transitions from scan to scan (3 heating and cooling cycles) were reversible.



This suggests that the protein somehow alters the ripple phase formation or the curvature of the vesicles at this temperature.

Figure 16 shows DSC scans for **(a)** BLES dispersions and **(b)** BSA solutions, at a scan rate of 60°C/h. For BLES, the midpoint of transition temperature was 26°C. For BSA, the peak represented the denaturation temperature of the protein, which was at 65°C. This is close to previous studies done with human serum albumin, where the denaturation occurred at 61°C (Watanabe *et al.*, 2001). The curves for DPPC and BLES were both reproducible in three heating scans. This suggested that the transitions in the lipids were reversible. However, the transition (denaturation) of BSA was not reversible, and only 1 scan was performed, although multiple times with different samples.

Figure 17 shows DSC scans for BLES with increasing concentrations of BSA added to the vesicles. There appeared to be some disruption in the phase transition of the BLES lipids. As well, there appeared to be a slight broadening of the transition peak, with increasing concentrations of BSA. This suggests that the protein interacted with the bilayer, and lengthened the phase transition process of some of the gel lipids to the fluid phase. BSA does not interfere with the BLES DSC profiles since the peaks are about 40 °C apart, in the mixed systems.

Figure 18 (a) shows a comparison of two different addition methods for BSA, **(ii)** one where BSA is added to the preformed BLES dispersion of vesicles, and **(iii)** where BSA is present during the formation or reconstitution of dried BLES lipids to form the vesicles. In **(iii)** the BLES was extracted from the aqueous dispersions into C:M 3:1, and

Figure 16: DSC melting profiles of (a) BLES (2mg/ml), and (b) BSA (20mg/ml). No observable transition could be noted for BSA at lower concentration. Normalized scan 1 is shown for both graphs. Scan rate was 60°C/h. The average temperature of the midpoint of transition is noted on the graph, for BLES (26°C), and the denaturation temperature for BSA (65°C). The scan for BSA could only be performed once, and the protein could not be re-natured upon cooling. The second and third scans of BSA were similar to a flat baseline. The DSC could not operate above 78°C and therefore the curve for BSA is incomplete. Multiple scans with different samples, however, were repeatable, and for BSA denaturation, the first scan was repeatable.

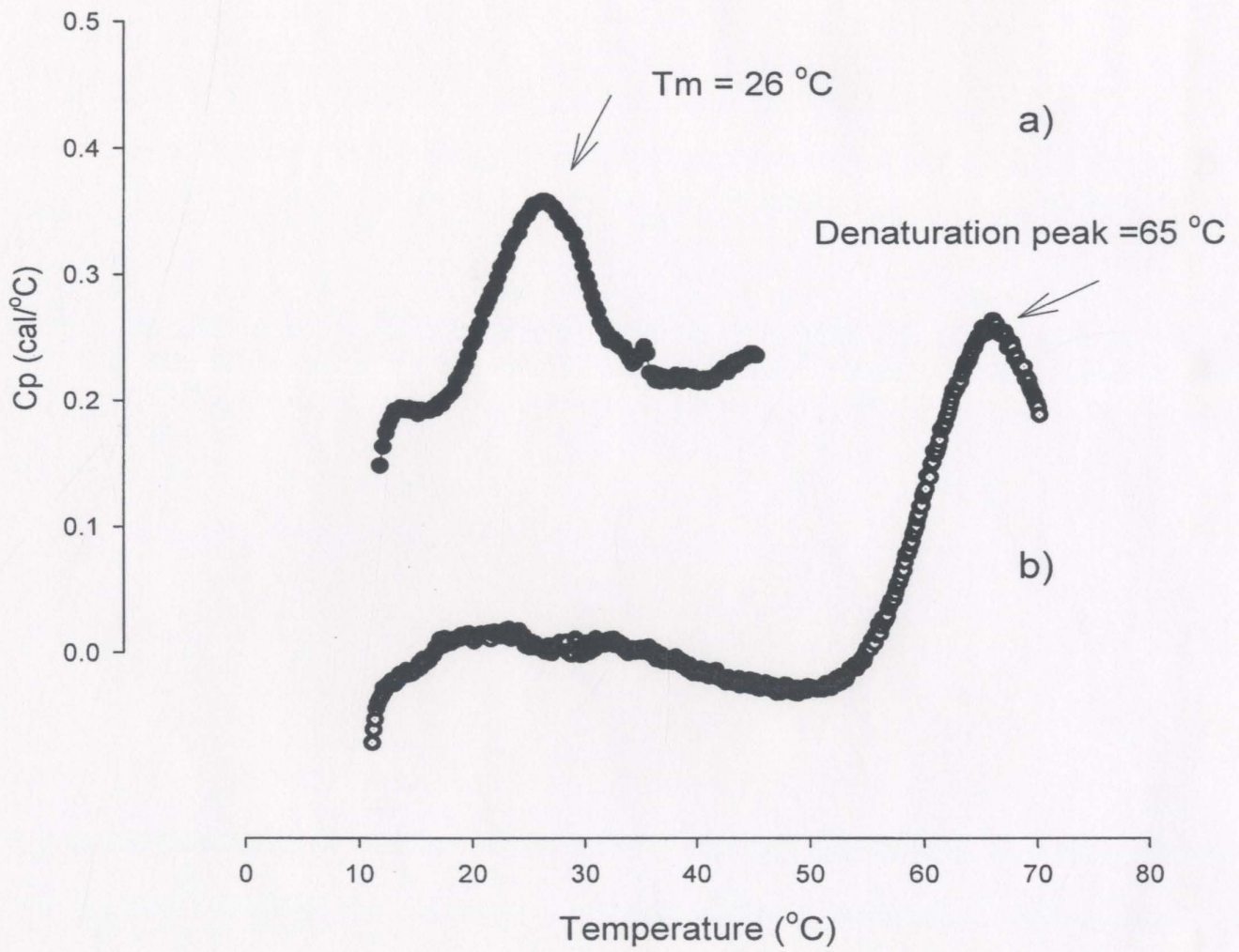


Figure 17: DSC melting profiles of (a) BLES (2mgs/ml), (b) BLES + 25% BSA (w/w) (0.5 mgs/ml), (c) BLES + 100% BSA (w/w) (2mgs/ml), and (d) BLES + 250% BSA (w/w) (5mgs/ml) added directly to the vesicles dispersions and incubated for 1 hour prior to DSC. Scan rate was 60°C/h, and scans were normalized to kcal/mole of BLES phospholipids by baseline corrections. Three separate sets of experiments were performed for these BLES/BSA mixtures with 3 individual scans per experiment, and scan 2 is shown for clarity. The midpoint of the diffuse transition was found to shift by $\pm 1^\circ\text{C}$ in the mixtures with BSA, and slight broadening of the transition was observed. Scan 2 and 3 were similar and reversible, for all samples.

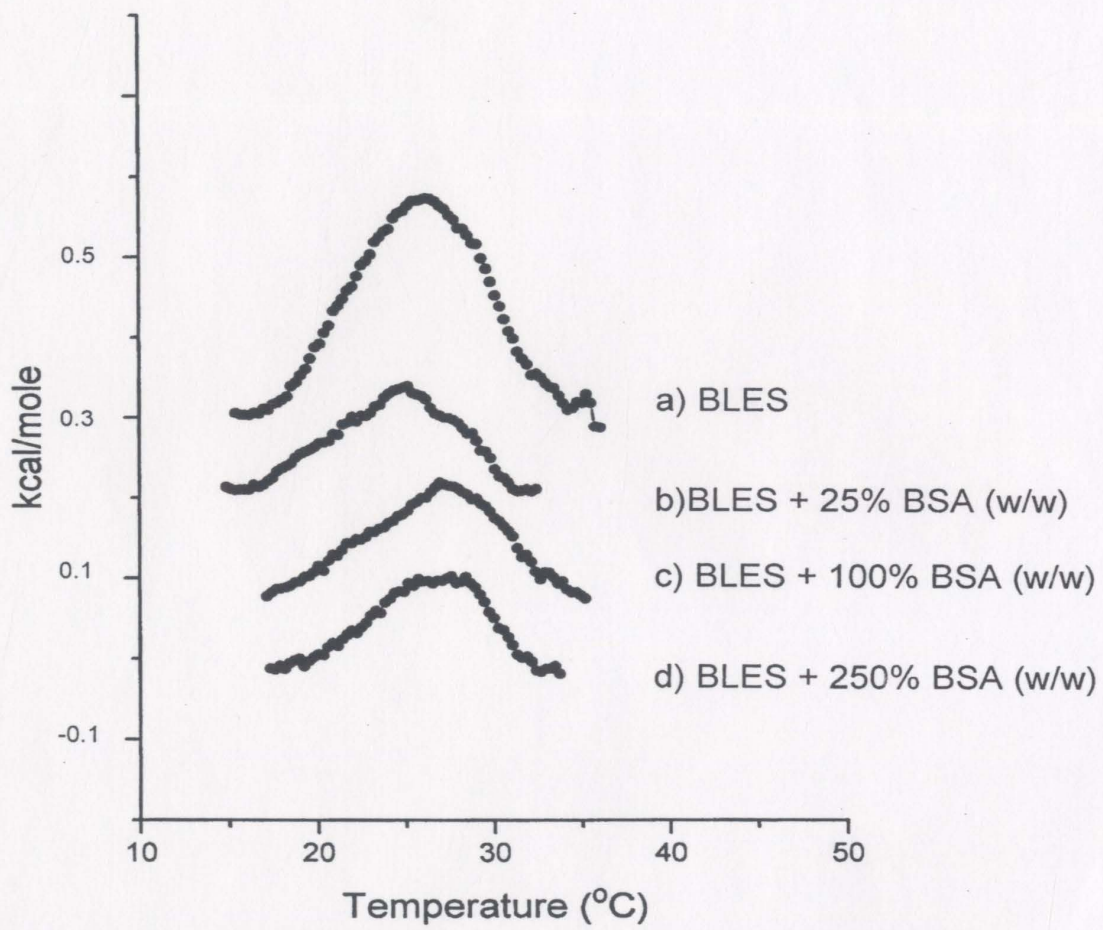
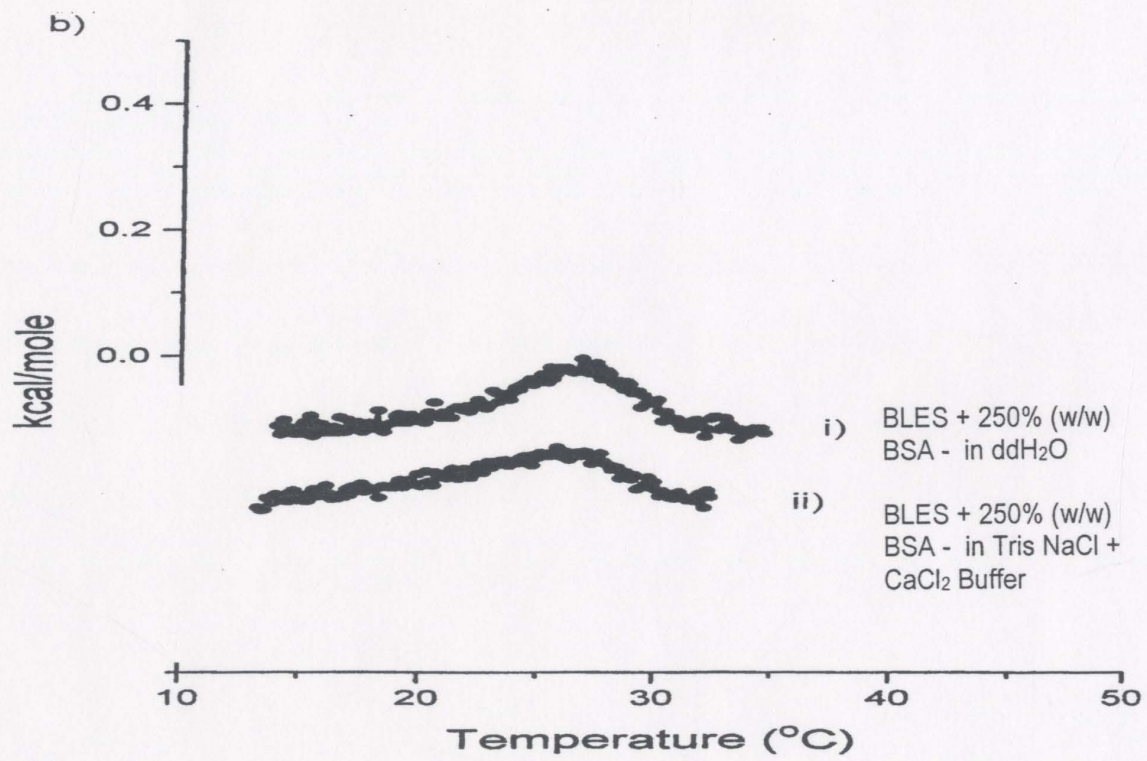
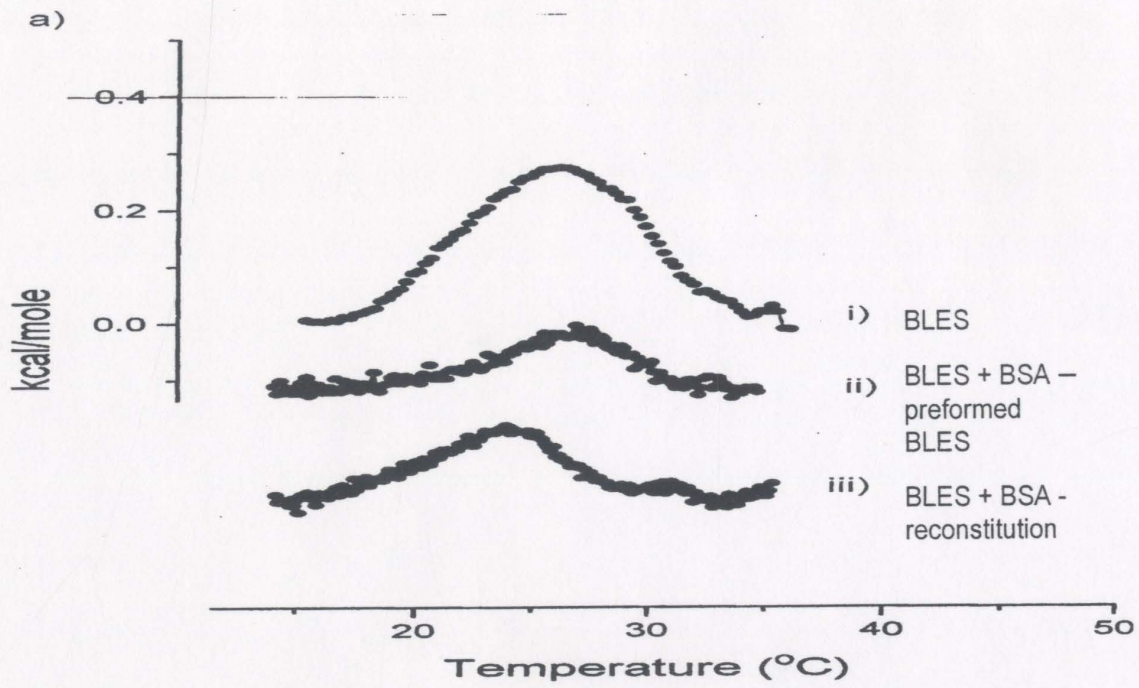


Figure 18: In (a), DSC scans of (i) BLES (2mgs/ml), (ii) BLES + 250% BSA (w/w) (5mgs/ml) added to the preformed vesicles, and (iii) BLES vesicles formed by reconstitution in the presence of 250% (w/w) BSA. In (b), DSC scans of (i) BLES + 250% BSA (w/w) diluted in ddH₂O, and (ii) BLES + 250% BSA (w/w) added to Tris HCl/NaCl Buffer with 2mM CaCl₂. Scan rate was 60 °C/h. Scans were normalized to kcal/mole of BLES phospholipid. Scan 2 is shown for all graphs.



dried under a stream of nitrogen. Dissolved BSA was then added to the dried BLES and the vesicles were reconstituted in ddH₂O by heating to 45°C and vortexing. There is a difference in the graphs, with the vesicle formation in the presence of BSA (reconstitution) causing a decrease in the midpoint transition temperature. It appears that in the reconstituted vesicles, the protein seems to interact by decreasing the thermal transition temperature more significantly than in those where they were added to the preformed vesicles in the dispersions. It is possible that all the bilayers of the multilamellar vesicles are affected by the protein dissolved between the layers in this reconstituted system, and thereby a lower transition midpoint for this reconstituted BLES/BSA system is evident, compared to the one where BSA was added to the preformed vesicle (Fig. 17).

Figure 18 (b) shows a comparison of the effect of ions or change of the buffer that the BLES/BSA dispersions are diluted in. In **(i)** the dispersion was diluted in ddH₂O, and in **(ii)** the dispersion was diluted in a Tris HCl/NaCl/CaCl₂ (2mM) buffer (preparation shown in Materials and Methods). There was a similar trend observed in both mixtures, in that, the protein decreased the thermal transition temperature slightly. This suggested that, at least in the experiments performed for BLES + BSA, no significant changes were observed with either ddH₂O or buffer. Therefore, this suggests that as long as the pH of the systems is near 7, ionic conditions do not alter (DSC measurable) the gel to liquid crystalline transitions in these lipid-protein dispersions.

3.6 Transmission Electron Microscopy

Figure 19 shows TEMs of BLES dispersion (**a**) and BLES dispersion plus 250% BSA (w/w) added to the dispersion (**b**). With BLES alone, the dispersions appeared to be multi-lamellar and the vesicles appeared tightly packed and more spherical. However, when 250% BSA was added, the vesicles had appearances in some cases that seemed to show more loosely packed lamellae. Further image analysis is required to confirm such appearances, as only 2-3 samples of this mixture were analyzed and only one representative image is shown.

3.7 FTIR Experiments

Figure 20 shows a cartoon diagram of the DPPC molecule with the major bond vibrations that can be observed using FTIR.

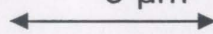
Initially, complete spectral scans were done for DPPC, BLES, and BSA (**Figure 21**) in transmittance modes. By looking at the full spectra, there seemed to be very little difference between the samples, due to extremely weak signals. Prominent peaks such as H₂O and CO₂ appeared in the full spectra, and submerged the weak bands of CH₂, Amide I, and Amide II. The C=O peaks are close to those of CO₂ and thus couldn't be further analyzed. Since it was very difficult to distinguish between the different samples, scans were performed focusing only on the specific range of wavenumbers of the areas of interest, where the stretching modes of certain bonds of the phospholipids molecule, such as the PO₂⁻, C=O and CH₂ appeared (Mautone *et al.*, 1987).

Figure 19: TEMs of (a) BLES (2mgs/ml) vesicles and (b) BLES + 250% BSA (w/w) (5 mg/ml) where BSA was added to the preformed BLES dispersions. Samples were prepared and embedded according to materials and methods (Section 2.4.5), and they were positively stained with uranyl acetate and lead citrate. Black lines in the images are about 4-5 nm thick suggesting that they are lipid bilayers. Scale bar applies to both images.

a)



6 μm



b)

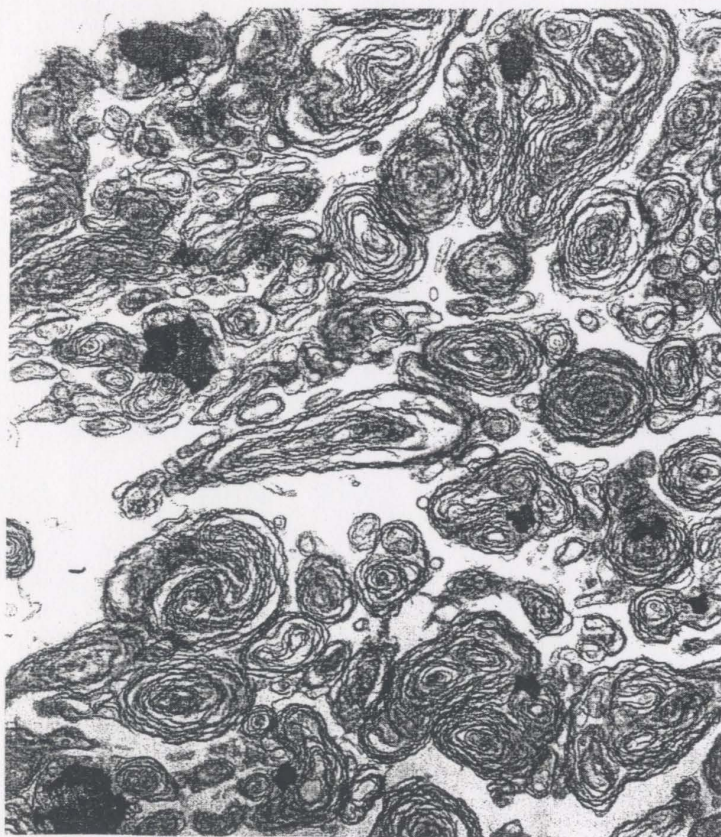


Figure 20: Diagram of the DPPC phospholipid molecule, showing the vibrational bands observed by FTIR. These bond stretches have been observed by others (Mendelsohn and Mantsch, 1986) using specific deuterated lipids at exact bond positions. However, the CH_2 and CH_3 stretching modes are an average from the chains as well as the headgroup region, and cannot be clearly distinguished without specific deuteration of the groups in the lipids.

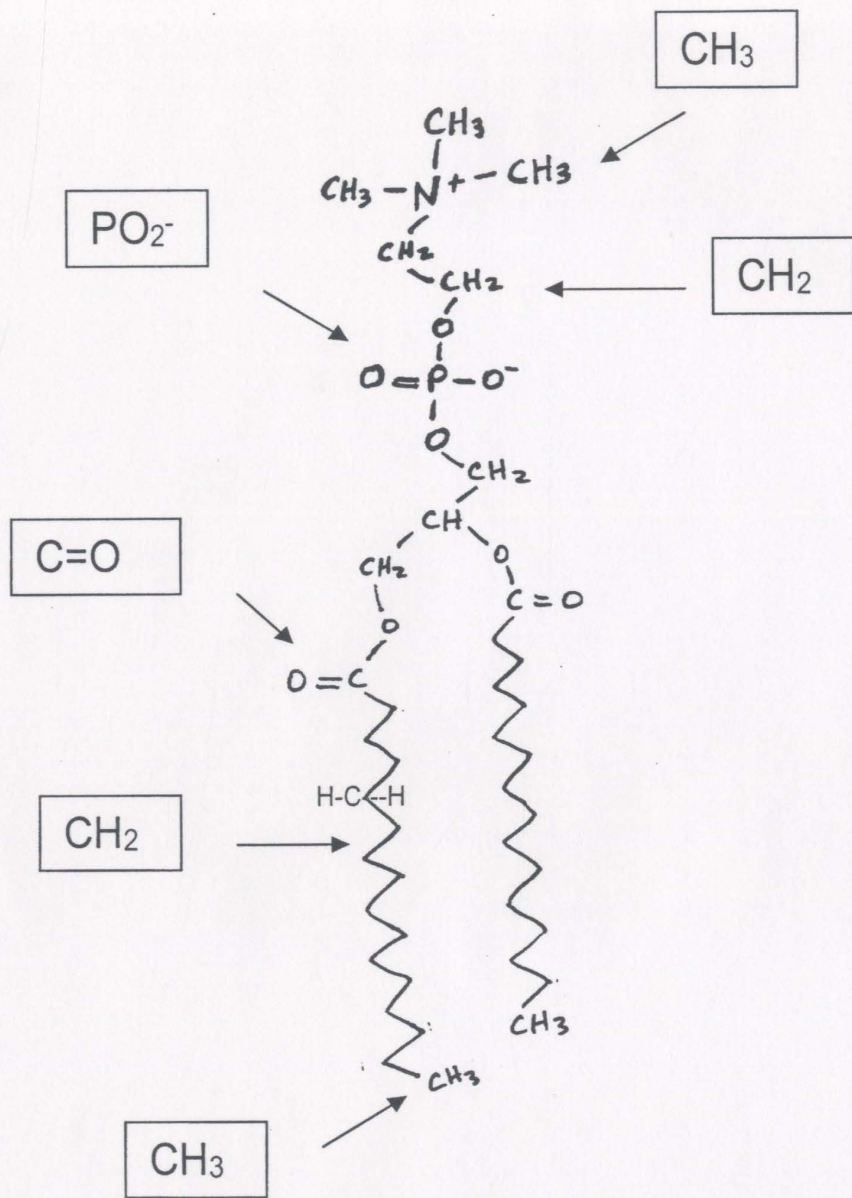
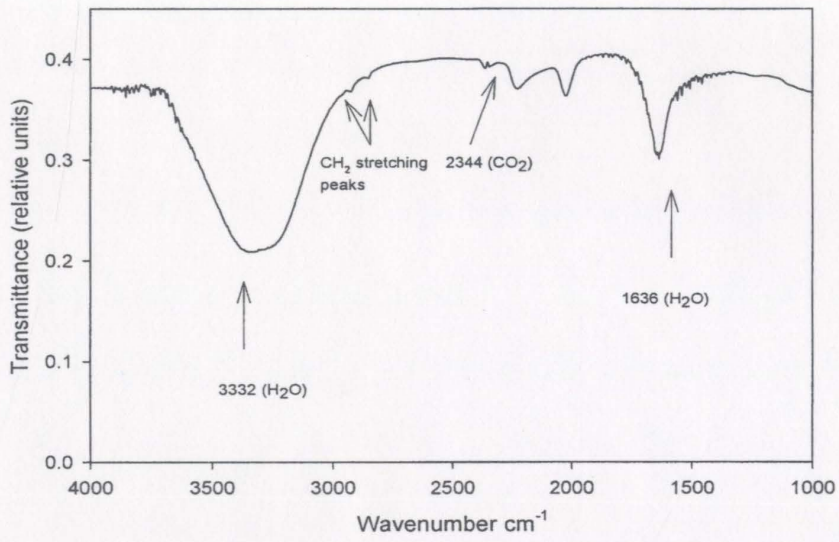
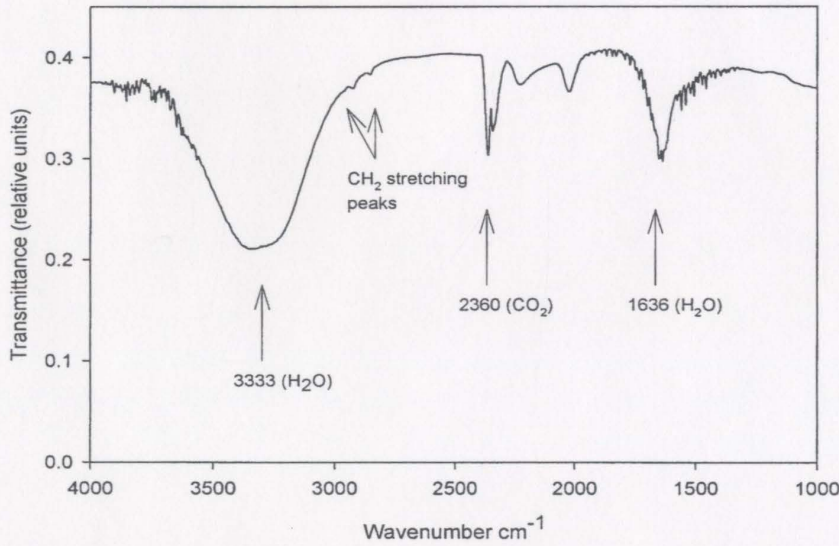


Figure 21: Complete FTIR spectra of dispersions of (a) 27mg/ml DPPC, (b) 27mg/ml BLES, and (c) 27mg/ml BSA. The spectra are all obtained in transmittance mode. The total number of scans carried out in each sample was 15. The spectra look very similar with prominent peaks such as the H₂O (at 3333 cm⁻¹), CO₂ (at 2350 ± 10 cm⁻¹), and CH₂ stretching modes (at 2850 and 2925 cm⁻¹). FTIR spectra were obtained for 3 independent samples.

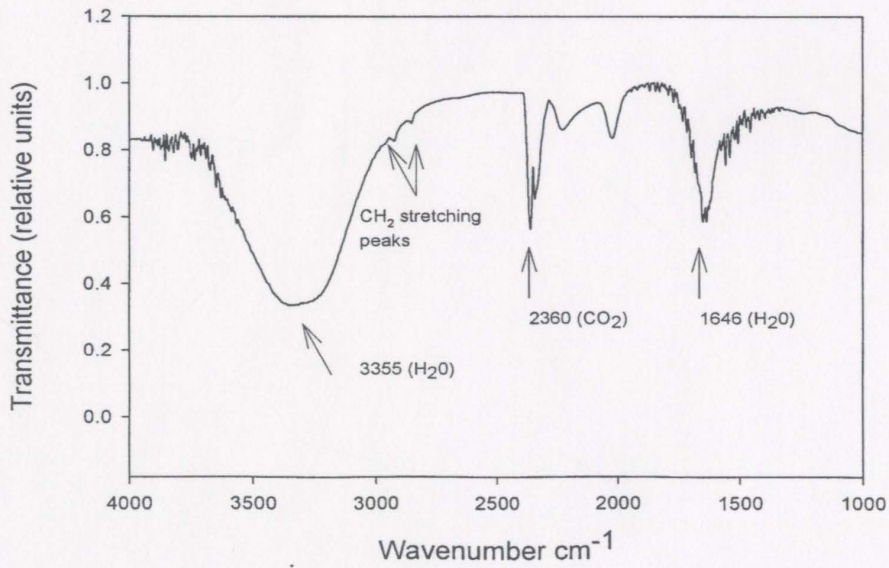
a)



b)



c)

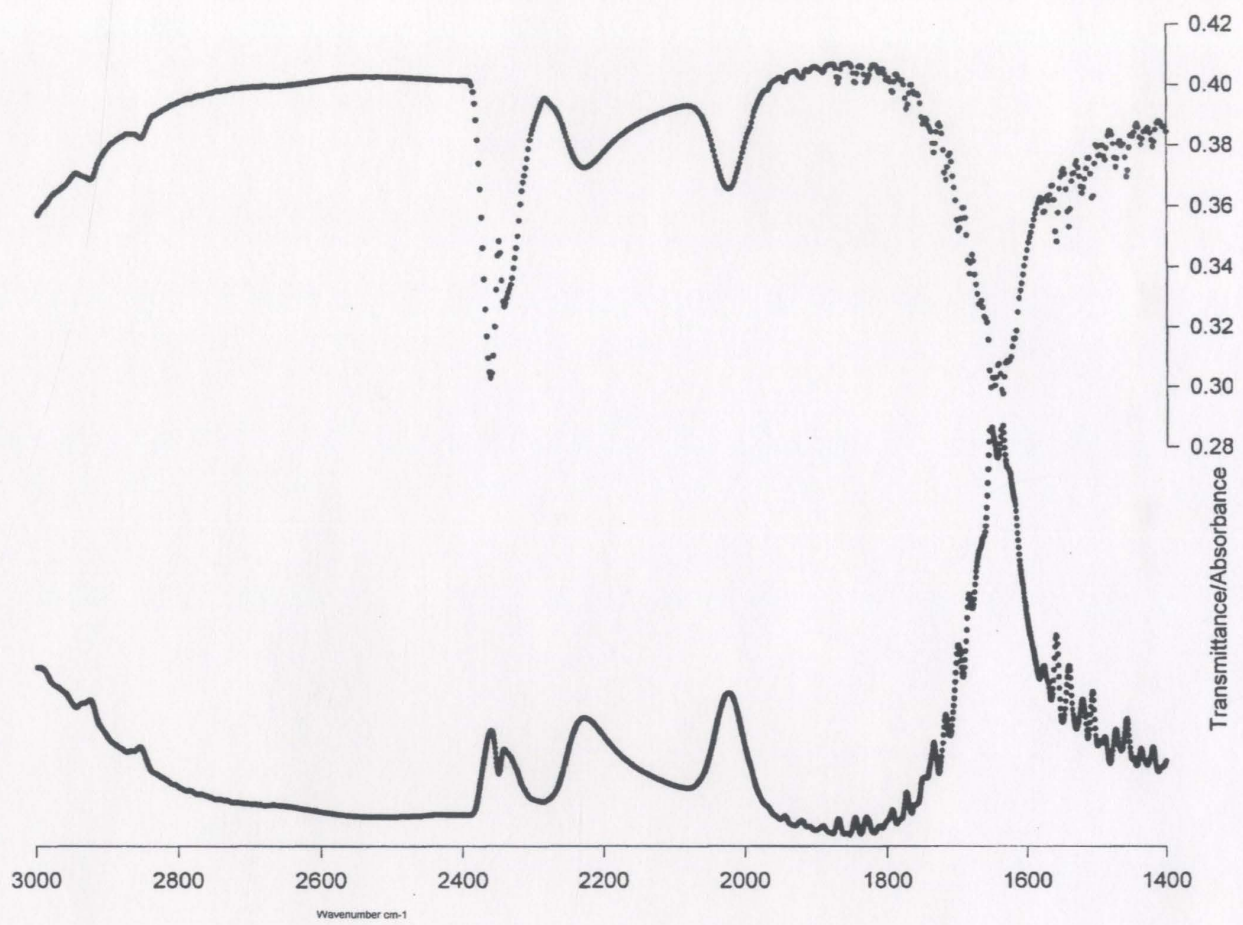


The specific range spectra were all done in absorbance mode. By comparing the transmittance and absorbance modes, there was very little difference, so all spectra were conducted using absorbance (**Figure 22**).

In **Figure 23 (a)**, the PO_2^- asymmetric stretching mode was focused on and compared with different concentrations of BSA, as this group is only present in the headgroup of the lipid molecule. With increasing concentrations of BSA, there was a broadening of the peak at 1228 cm^{-1} . This suggested that the BSA was interacting with the PO_2^- group, and that it was affecting the motions of the P-O bonds in the head group of the molecule. **Fig. 23 (b)** shows a similar pattern occurring with the C=O stretching mode. Once again, there was a change in the 1733 peak. This group is also located near the head region of the molecule, at the end of the phospholipid chain.

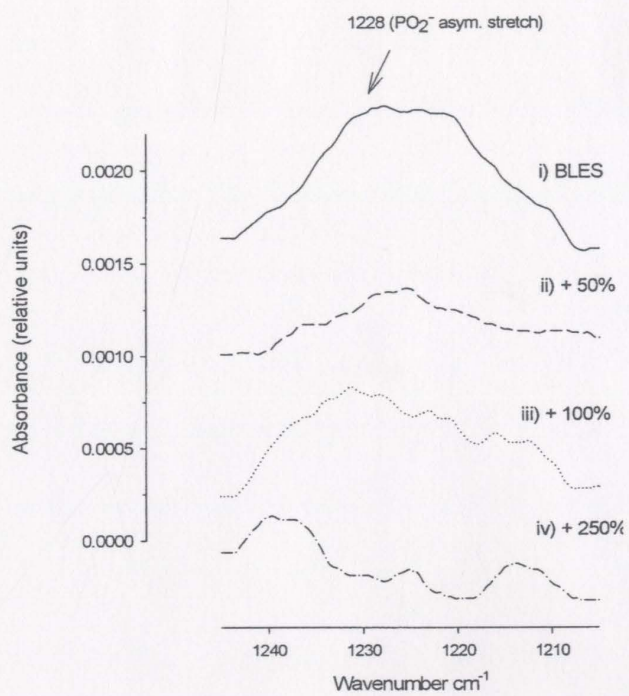
Fig. 23 (c) and (d) shows graphs focused on the CH_2 symmetric and asymmetric stretching modes of the BLES/BSA system respectively. It is not clear whether or not the signals were coming from the head group and/or tail region for CH_2 and CH_3 , since these bonds appear in both regions of the molecule, and possibly the average data was displayed. This suggests that BSA perhaps makes more room between the lipids in the head or tail region, and so the methyl groups have higher motion or vibrations. It is clear, however, that BSA affects the CH_2 stretching modes of the phospholipid molecule.

Figure 22: Spectra (3000-1400 cm^{-1}) of comparison of transmittance and absorbance modes for 27 mgs/ml BLES. Both spectra look the same with one being the reverse of the other.

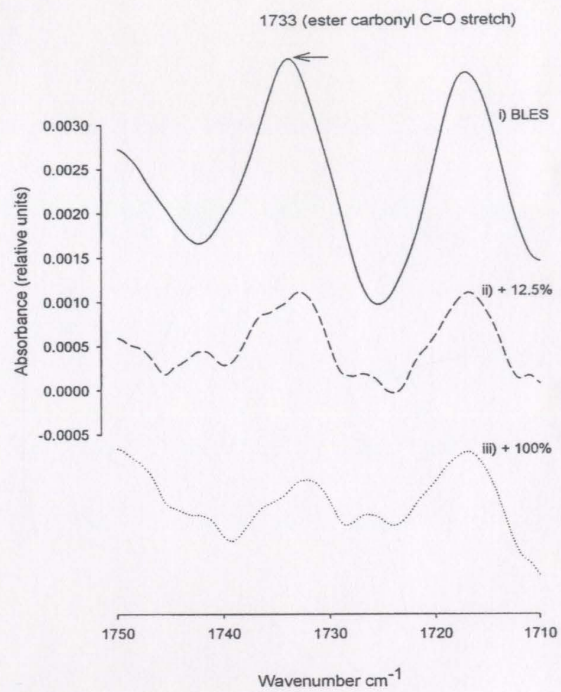


Wavenumber cm^{-1}

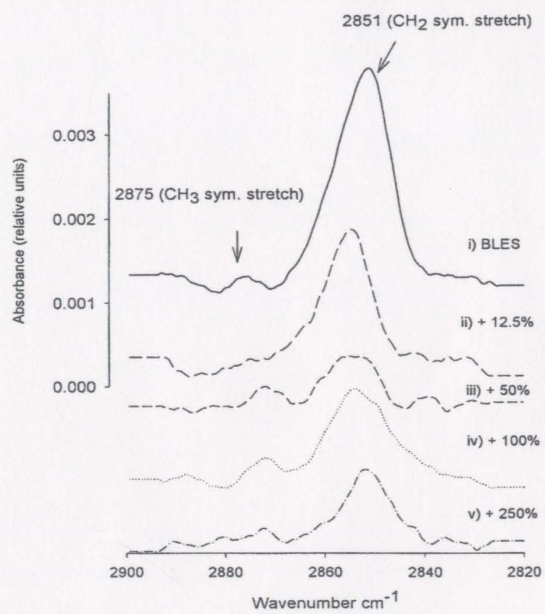
Figure 23: FTIR graphs focusing on the PO_2^- asymmetric stretching mode (a) of (i) BLES, (ii) BLES + 50% BSA (w/w), (iii) BLES + 100% BSA (w/w) and (iv) BLES + 250% BSA (w/w) dispersions in water. In (b) FTIR graphs focusing on the C=O stretching mode of (i) BLES, (ii) BLES + 12.5% BSA (w/w), and (iii) BLES + 100% BSA (w/w). In (c), FTIR graphs focusing on the CH_2 symmetric stretching mode of (i) BLES, (ii) BLES + 12.5% BSA (w/w), (iii) BLES + 50% BSA (w/w), (iv) BLES + 100% BSA (w/w), and (v) BLES + 250% BSA (w/w). In (d), FTIR graphs focusing on the CH_2 asymmetric stretching mode of the same mixtures in (c). Spectra are in absorbance mode.



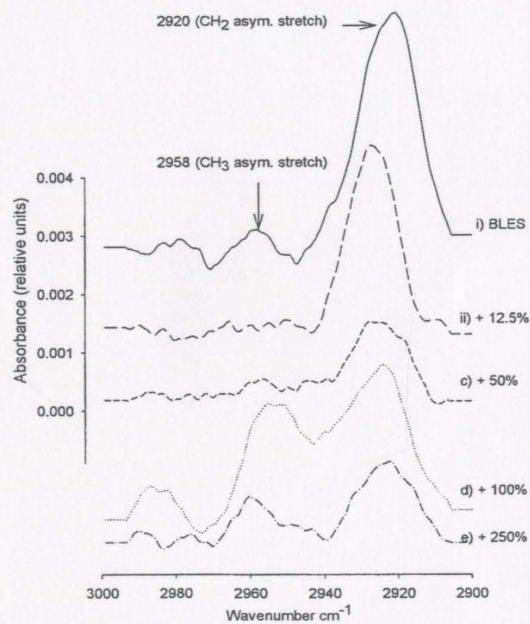
a)



b)



c)

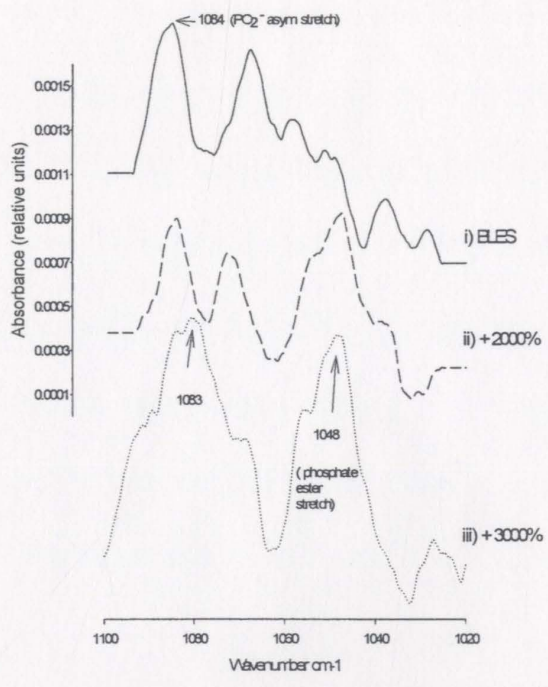


d)

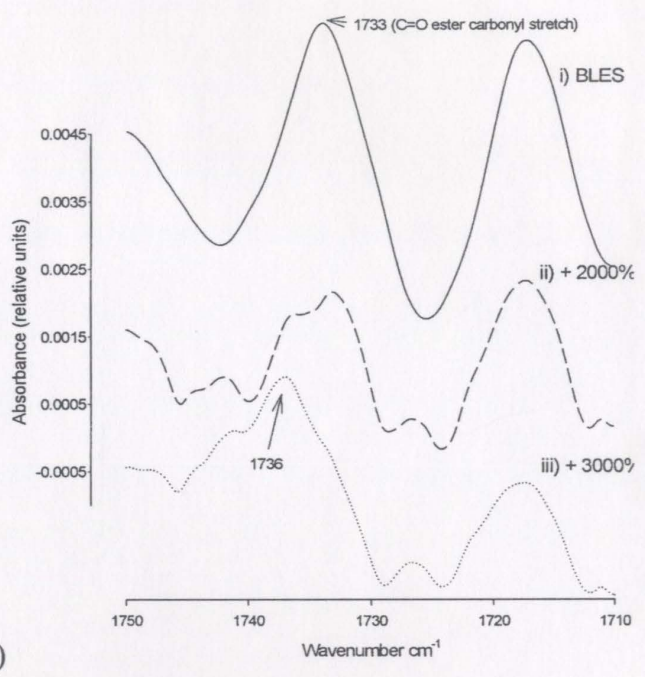
Figure 24 shows spectra for each of the stretching modes with very high concentrations of BSA added. Spectrum **(a)** focuses on the PO_2^- symmetric stretching mode. There seemed to be a shift in the PO_2^- asymmetric stretch, as well as the appearance of another peak which is the phosphate ester stretch. This once again suggests that BSA disrupted the lipid packing, by interacting with the head groups. This may have caused space between the groups, allowing less movement of the bonds, at least in the head group region. Spectrum **(b)** shows a similar trend with a shift in the $\text{C}=\text{O}$ peak, suggesting that the BSA probably approached the head group region, and some of the protein inserted slightly into the hydrophobic area of the bilayers.

Fig. 24 (c) and **(d)** show once more a reduction in the CH_2 peaks, but appearance of the CH_3 peaks (at 2871 and 2970 cm^{-1}). Once again, it is unclear if these signals are coming from the head group region alone, or from the head and tail regions combined. In any case, BSA caused a disruption of the stretching of these hydrocarbon bonds. If the signals were mainly from the CH_2 of the hydrocarbon chains, then it suggests that BSA inserted between the phosphatidylcholine molecules, and the effect was translated into the central hydrophobic core. This was substantiated by the increase in the peaks appearing for CH_3 at 2871 cm^{-1} , and suggested the possibility of increased motion of the CH_3 at the end of the fatty acyl chains.

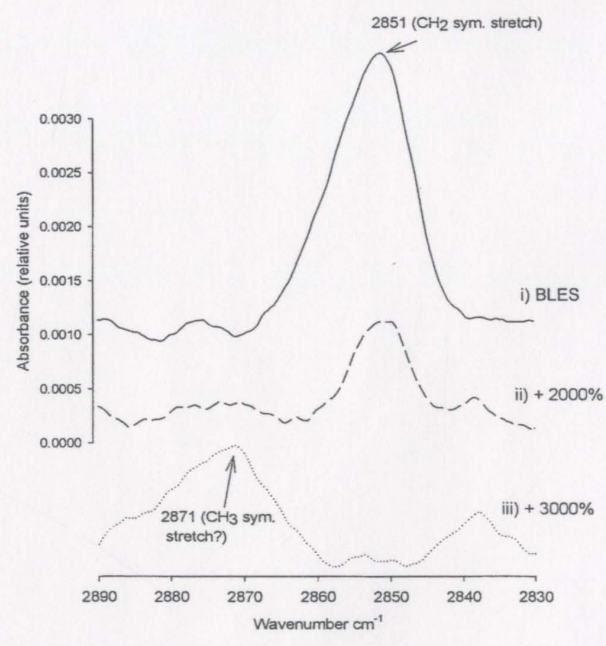
Figure 24: FTIR spectra of BLES focusing on the addition of high concentrations of BSA. In (a), the PO_2^- symmetric stretching mode of (i) BLES, (ii) BLES + 2000% BSA (w/w), and (iii) BLES + 3000% BSA (w/w). In (b), C=O stretching mode of (i) BLES, (ii) BLES + 2000% BSA (w/w), and (iii) BLES + 3000% BSA (w/w). In (c), CH_2 symmetric stretching mode of (i) BLES, (ii) BLES + 2000% BSA (w/w), and (iii) BLES + 3000% BSA (w/w). In (d), CH_2 asymmetric stretching mode of (i) BLES, (ii) BLES + 2000% BSA (w/w), and (iii) BLES + 3000% BSA (w/w). Spectra are in absorbance mode. High concentrations were studied because the spectra obtained of the lower concentrations had high variability (since the signals were very weak). However, the highest concentrations of BSA were chosen to demonstrate the laboratory assigned concentrations where BSA-induced complete inhibition of BLES occurs, as shown in previous studies and in fig. 5.



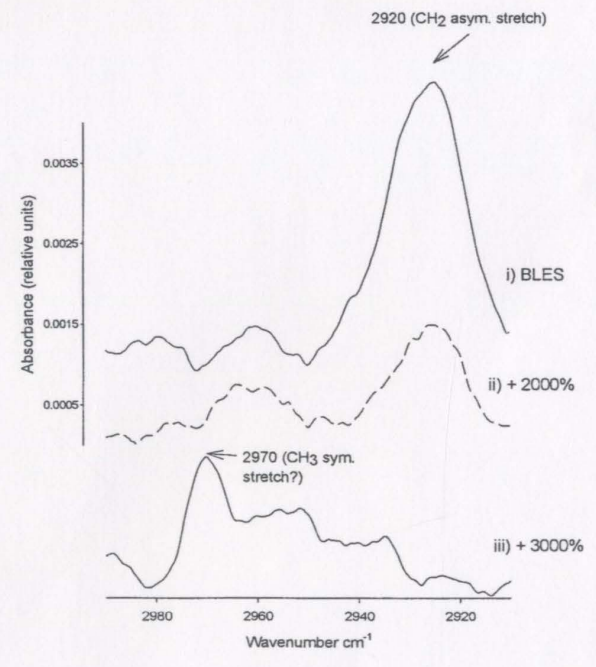
a)



b)



c)



d)

The FTIR data taken collectively suggests that at lower concentrations of BSA only minimal perturbations of the BLES bilayers are observed. However, at very high concentrations (**Fig. 24**), the PO_4^- , CH_2 , CH_3 , and C=O stretches are altered. Since the C=O and PO_4^- are distinct for the headgroup region, we can assume that BSA at least affects the packing of the phospholipids in the outermost layers of the multilamellar vesicle bilayer. Further studies using a fluid cell (where the IR beam passes through the whole sample) as well as selective labeling of lipids by deuterium at CH_3 and CH_2 regions of the headgroups are required to comprehensively understand these systems (Dluhy and Mendelsohn, 1988; Mendelsohn et al., 1984).

DISCUSSION

A number of previous studies on LS inhibition, and the possible mechanisms involved in such inhibitions *in vitro* have been performed by others (Enhorning, 1977; reviewed by Griese, 1999; Holm *et al.*, 1988; reviewed by Holm, 1992; Holm *et al.*, 1999; Keough *et al.*, 1989; Panda *et al.*, 2004). Also, some of these studies have looked at the effects of physiological changes in the lung, such as ions, pH, and temperature fluxes, as well as serum protein transport on the function and inhibition of LS (Holm, 1992). Many serum proteins have been studied such as albumin, fibrinogen, C-reactive protein, and globulin, among others, and all have been shown to inhibit LS function, by preventing the reduction of γ (mN/m) in the lipid-protein films to near 0 mN/m (Amirkhanian and Taeusch, 1993; Casals *et al.*, 1998; Fuchimukai *et al.*, 1987; Holm, 1992; Holm *et al.*, 1988; Keough *et al.*, 1989; Liu and Chang, 2002; Panda *et al.*, 2004). These studies have shown that LS-protein films could reduce γ only to 25-30 mN/m in the presence of serum protein, and adsorption to the equilibrium γ values of 20mN/m is also inhibited. However the concentrations of proteins tested have been quite variant and in most cases non-physiological or non-pathological, and various different surfactant preparations have been used.

In a recent study, Panda *et al.* (2004) had examined LS from normal, ventilated, and injured ventilated lungs of rats, and had noticed a 3 fold increase in the amounts of serum protein associated with surfactant in the injured ventilated lungs compared with normal lungs. The soluble proteins were approximately 280 $\mu\text{g/lung pair}$ in normal lungs

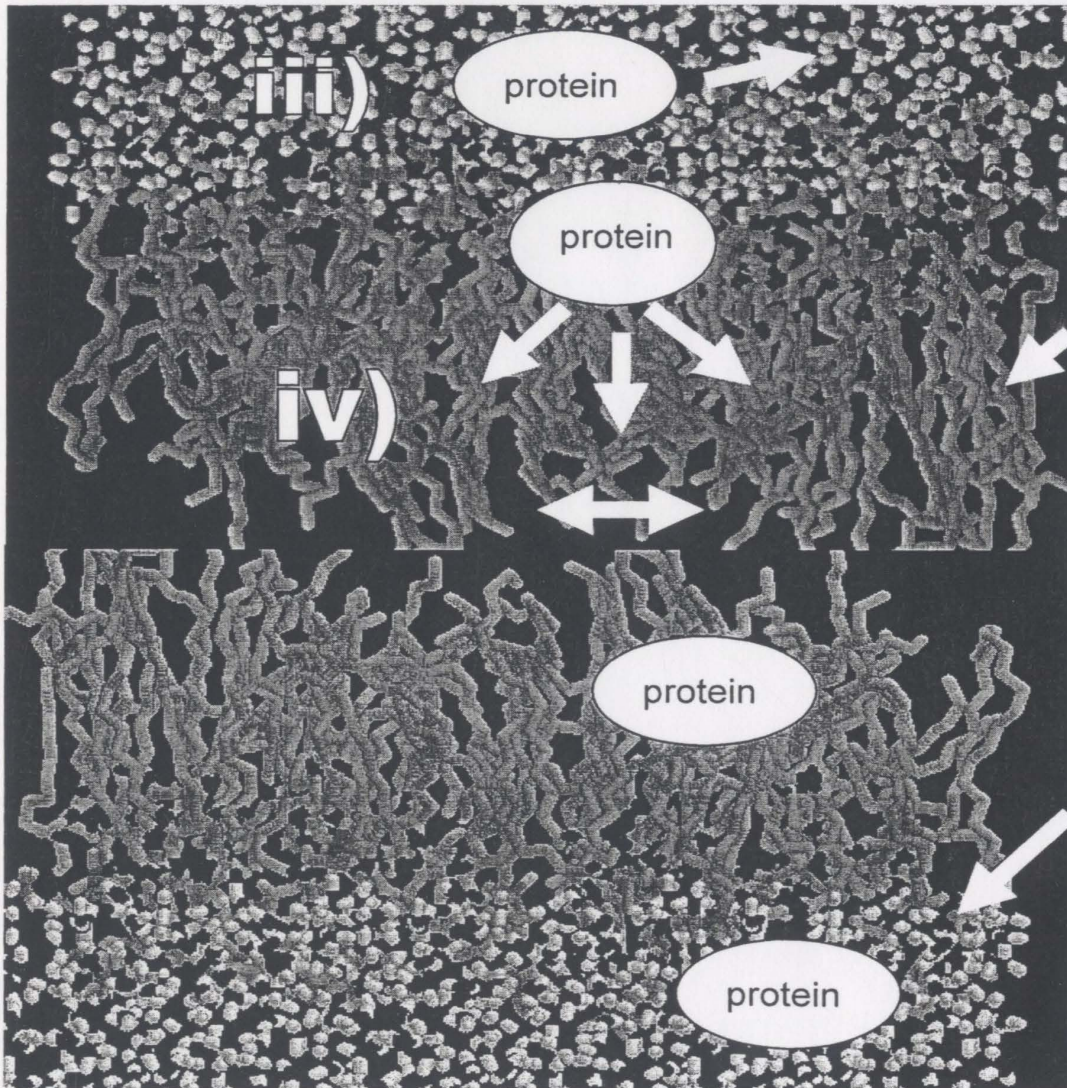
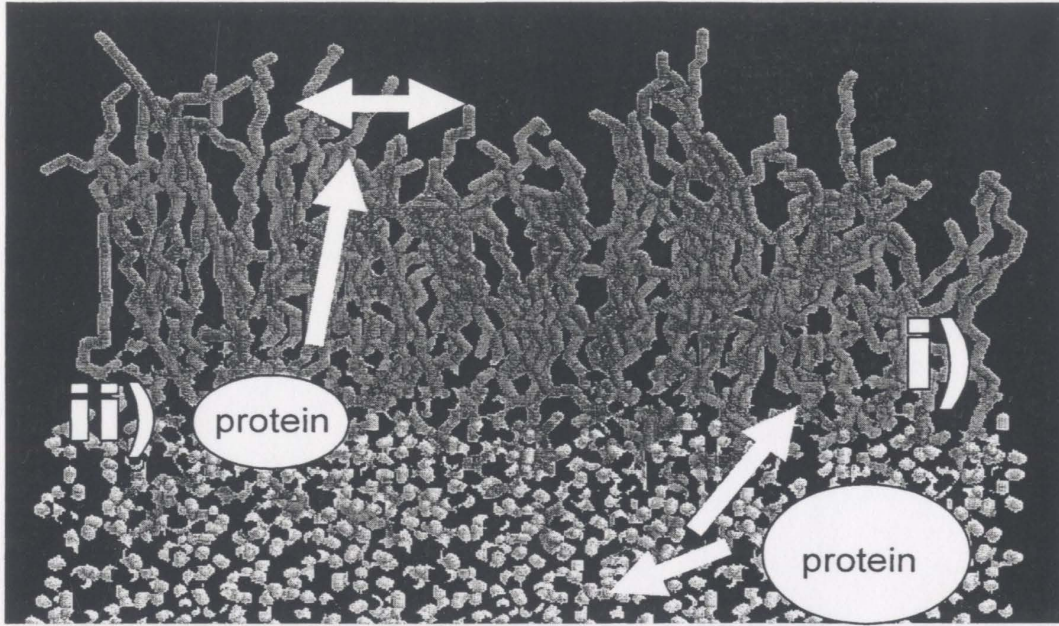
versus 830 $\mu\text{g}/\text{lung}$ pair in injured lungs, whereas the phospholipid levels were similar, in both. This means that the lipid:protein mass ratio of 4:1 in normal lungs had decreased to 1:1 in injured ventilated lungs, showing a possibility of a much greater lipid- serum protein interaction in lung disease. However, most previous studies had not examined such small ratios when testing inhibition in the laboratory. Studies on albumin and on other serum proteins have been done using extremely high concentrations of protein, such as 500 % w/w of surfactant lipids (Enhorning *et al.*, 2000), and others with 1:10, 1:15, and 1:20 lipid:protein ratios (Holm, 1992; Notter, 2000; Otsubo and Takei, 2002). These have shown LS inhibition in varying degrees. Some studies have tested lower concentrations, similar to the physiological concentrations (Amirkhanian and Taeusch, 1993; Casals *et al.*, 1998; Liu and Chang, 2002). However they utilized fibrinogen and C-reactive protein which have a much greater inhibitory effect than albumin and thus require very low concentrations (Enhorning *et al.*, 2000, Nag *et al.*, 2004c). Also in one such study it was suggested that there may be specific protein-ligand interactions such as C-reactive protein (CRP) with PC headgroups (Nag *et al.*, 2004c). However all these studies are difficult to compare considering the varying amounts of proteins used, composition of surfactant, and only a single type of surface tension measurement was performed (reviewed by Holm, 1992). As well, these studies used different types of model lipid- protein (SP-B/C) surfactants and very different surface-activity techniques such as the capillary surfactometer, which measures air flow (Enhorning *et al.*, 2000). Our study attempted to determine the interaction of LS with albumin at physiological

concentrations as well as at the higher concentrations used by others, in a monolayer and bilayer system of a defined extracted bovine lung surfactant (BLES).

Different but complementary techniques were used in this study, such as Langmuir-Blodgett dynamic compression-expansion, adsorption, TOF-SIMS, and AFM to study the interaction of albumin with BLES monolayers, and DSC, FTIR and TEM with BLES bilayers at very low and high concentrations of BSA. Through these complementary studies, we were able to observe the biophysical properties of LS which suggest possible molecular mechanisms of the different ways that albumin may interact with bovine LS monolayers or bilayers. In this study, interactions were examined with only the lipid components of bovine surfactant, however, the presence of SP-B/SP-C (Fig. 4) may also have mediated such interactions. **Figure 25** shows molecular dynamics (computer) simulation images of a DPPC monolayer and a bilayer, and the possible areas that albumin can interact with these model membranes, as used in our study.

Although the present study focuses on various monolayer as well as bilayer systems, the discussion is mainly based on information obtained from individual techniques. This is due to information or results obtained by a specific method allowing for testing a subsequent method. For example, imaging monolayer domain formation (as in AFM) was first performed, and then TOF-SIMS suggested the composition of the domains. Electron microscopy suggested albumin did not disrupt bilayer structures overall, and thus DSC was performed. Most of the samples were tested simultaneously using the multiple methods.

Figure 25: Molecular model of a BLES monolayer (a) and bilayer (b) with BSA. The model was constructed using 40 DPPC molecules using Molecular Dynamic simulations. These were a generous gift of Derrick Lee and Dr. V. Booth from the Computer and Visualization Center in the department of Physics (Unpublished Data). Arrows show the possible areas that BSA (protein) might affect the BLES lipids. In monolayers, it might penetrate near the headgroup region (i) which could translate into extra movement of the hydrocarbon chains. The protein may also perturb or have a disordering effect deep into the bilayer interior (ii), causing an increased movement of the chains. In bilayers, the protein might also affect the head group regions of the bilayers (iii), it may not penetrate deep into the bilayer (iv), however it could affect the movement of the phospholipid chains (X). It may also have a greater effect when located in between the bilayers of multilamellar vesicles in reconstituted vesicles (Y) (as in Fig. 18).



Normal System

(X)

(Y)

Reconstituted System

4.1 Mass Spectrometry

ESI-MS and MALDI-MS enabled us to accurately determine the different phospholipid, and protein components of BLES.

With ESI run in the positive mode, the major phospholipid found was DPPC (at m/z 734) and the next major one was POPC (at m/z 760). In the negative mode, we found POPG to be the most prominent (at m/z 747) and DPPG to be the next prominent phospholipid (at m/z 721). The positive mode was acquired by using the solvents suggested by Harbottle *et al.* (2003). Similar compositions have been shown previously with BLES (Harbottle *et al.*, 2003) and bronchoalveolar lavage fluid in humans (Postle, 2000; Postle *et al.*, 1999). In these studies it was found that ions such as Na^+ and K^+ interact strongly with the lipids and conjugate ions $[\text{M} + 23 (\text{Na}^+)]$ are normally detected. However, we found that by adding NH_4OH , the conjugate metal ions could be removed and only parent or native ions were detected. The ESI-MS result suggests that the lipid composition of BLES is very close to those of humans (Postle, 2000; Postle *et al.*, 1999) and some other mammalian species (Paananen *et al.*, 2002; Postle *et al.*, 2001). The abundance of each phospholipid may vary slightly compared to the other studies, but that may be due to different animal sources of LS extracts. For example, Paananen *et al.* (2002) studied the phospholipid molecular species composition of eustachian tube lavage fluid, and Postle *et al.*, (1999) studied the phospholipids' molecular species composition of bronchoalveolar lavage of humans. The distribution of at least DPPC and POPC, however, was very similar to those in BLES, in both of these studies.

MALDI-TOF MS on BLES was done to compare the amount of SP-B and SP-C present in bovine LS. To the best of our knowledge, this is the first time the hydrophobic protein ratios have been directly measured in an LS system with the lipids. The ion observed at m/z 4041 was assigned to SP-C, and the ions observed at m/z 8676 and m/z 17320 were assigned to the SP-B monomer and dimer respectively. It was determined that there was approximately 2-3 times as much SP-C in BLES than SP-B. Previously, MALDI-MS had been applied to isolated SP-B and SP-C. Nag *et al.*, (1997b) used MALDI on fluorescently labelled porcine SP-B and SP-C to determine if the proteins were intact and fluorescently labelled. They found the characteristic ion for the unlabelled porcine SP-C at m/z 4186 and that for the porcine SP-B at m/z 8710. The difference in molecular weights of SP-C in this study with those in BLES is possibly due to the SP-C having slightly different amino acid composition. Bovine SP-C is found to have a molecular weight of approximately 150 Da less than porcine SP-C (Johansson, 1998). As well, Gustafsson *et al.* (2001) did studies using MALDI on isolated SP-C using the solvent mixture that was mentioned in the materials and methods section of this study. They found the characteristic ion for non-palmitoylated SP-C at m/z 3738. The difference in the M.W. of SP-C in the mentioned study and the molecular weight of SP-C in BLES determined in our study suggests that SP-C in BLES is intact and contains the two palmitoyl chains.

4.2 Surface Balance (Monolayer) Studies

The surface balance was used to study the interaction of albumin with BLES monolayers as well as the mixed bilayer dispersion used to adsorb such monolayers. In adsorption experiments the monolayers were studied by injecting BLES/BSA mixed dispersions underneath the clean surface of the ddH₂O subphase. Results suggested that BLES/BSA mixed dispersions did not lower γ to the same degree as that obtained with BLES dispersions alone. As well, with increasing concentrations of BSA (12.5-250% w/w) added to BLES, the γ decreased by about 20-10 mN/m in the first 90 seconds compared to the rapid decrease in γ of 40mN/m obtained for BLES alone. This suggests that albumin inhibits surface adsorption of BLES lipids to the air water interface. This occurs possibly by albumin competing with the lipids for the surface and, therefore, preventing some of the lipids from reaching the surface at once or delaying a tightly packed monolayer formation. With increasing concentrations of albumin added to BLES, possibly more albumin competes for the surface, therefore preventing more of the BLES lipids from adsorbing to the surface. After the initial 90 seconds, the protein and lipids must have settled on the surface, causing very little change in γ after that point. A similar trend was observed in previous studies with various serum proteins (Fuchimukai *et al.*, 1987; Holm *et al.*, 1985; Holm *et al.*, 1987; Holm *et al.*, 1988; Keough *et al.*, 1989; McEachren and Keough, 1995; Wang and Notter, 1998). In a number of these studies inhibition of adsorption was somewhat similar to those observed here. An equilibrium surface tension ($\gamma \sim 25\text{mN/m}$) was never reached under any of the conditions of this protocol. Wang and Notter (1998) and Holm *et al.* (1988) studied calf lung surfactant

extract (CLSE) obtained from excised lungs. CLSE differs in composition from BLES in that it contains all the neutral lipid components of natural LS, whereas BLES has the neutral lipids removed, however equilibrium adsorption was the same as ours. Additionally, McEachren and Keough (1995) used porcine pulmonary surfactant, which also has a different composition than BLES, but the inhibition of CRP was similar as with our high concentration of albumin. Furthermore, studies were done on other plasma proteins in addition to albumin, which are known to exhibit different inhibitory effects (Fuchimukai *et al.*, 1987). Although different techniques such as the pulsating bubble surfactometer, and adsorption apparatus were used in these studies, there seemed to be a general trend since adsorption was inhibited in all these studies similar to the results reported here.

In compression-expansion experiments, BSA was dissolved in the ddH₂O subphase, and a BLES film was spread on the surface of the air-water interface. Compression-expansion cycles were done with different concentrations of BSA in the subphase, and γ -A isotherms were obtained (Fig. 8). With increasing concentrations of BSA in the mixtures, the ability to reach minimum γ of the BLES film was decreased, suggesting that albumin must have entered the film and interfered with further lipid adsorption. As well, with the adsorbed mixed BLES/BSA dispersions, the ability of BLES dispersions to reach minimum γ was similar (Fig. 6). In addition, the transition plateau of the isotherm was prolonged when BSA was added, suggesting that the protein remained in the monolayers and strongly associated with the lipids at low γ and could not be easily squeezed out. This also suggests that the phase transition that usually occurs

from an expanded to condensed phase in films upon compression of pure LS films was altered by BSA (Nag *et al.*, 1998). This correlates with our study using TOF-SIMS and AFM, in which we found the protein to be present in the fluid phase and possibly forming protein-BLES phospholipids complexes, which do not tend to be easily squeezed-out even after multiple cycling.

Differences in the degree of γ reduction of LS films are due to differences in the types of model surfactant film used, the type of instrument, the speeds of compression, as well as the procedure of incorporating the serum protein into the subphase. For example, Holm *et al.* (1999) studied calf lung surfactant extract (CLSE) using a pulsating bubble apparatus. CLSE may have a slightly different γ lowering ability due to the different compositions of lipids and proteins in the extract. It is highly possible that small differences in composition, such as presence of cholesterol in CLSE, may cause the films to interact differently with BSA. As well, the pulsating bubble apparatus may produce different results than a Langmuir surface balance due to leakage of the films, and creeping of lipids in and around the barrier. In addition, Warriner *et al.* (2002) incorporated albumin into the subphase of a preformed replacement LS film, by injecting BSA beneath the preformed film. This difference in method may have also contributed to the differences in our results with theirs (as far as the minimum γ reached) which was somewhat different than those observed here.

4.3 AFM and TOF-SIMS

AFM has become a very powerful tool for imaging biological structures non-invasively, and many studies have been performed on model membranes (Chi *et al.*, 1994; Engel and Müller, 2000; reviewed by Hansma *et al.*, 1997; Janshoff, 2001). It is very advantageous in that it can provide three dimensional information regarding materials at a molecular level, without staining or embedding of samples. Studies have been performed on model lung surfactant using AFM (Baro *et al.*, 1985; Flanders and Dunn, 2002; Nag *et al.*, 1999; Nag *et al.*, 2002b; von Nahmen *et al.*, 1997; Panaiotov *et al.*, 1996), however, at present, none have studied the interaction of plasma proteins with LS directly. This study obtained AFM images of BLES, and BLES films spread on a subphase with various concentrations of BSA. BLES films alone, compressed to a low γ , showed high, and well defined condensed domains. However, when BSA was added to the subphase before the BLES films were solvent-spread, the BLES lipid domains became less defined and more numerous. These films also appeared very heterogeneous. In the image of BLES:BSA 1:20 mixture [Fig. 12(c)], large areas without domains were visible with folded sheets. In the image of the BLES:BSA 1:5 mixture deposited at 30mN/m [Fig. 12(b)] the film appeared almost completely homogeneous, and lipid domains were not visible. This might mean that at that concentration of BSA, most of the condensed (tightly packed) domains of BLES were abolished, and the lipids were all fluid at that γ (30 mN/m). This would suggest that BSA does not allow phase separation of DPPC in BLES films.

Panda *et al.* (2004) noted well defined liquid condensed domains in the LS films of normal rat lungs, whereas there were smaller, intermediate height, possibly fluid domains in LS films of injured ventilated rat lungs. Another observation in our study was that in the mixture of BLES: BSA 1:20 films, the γ went down to only 50 mN/m upon cycling. Panda *et al.* (2004) noted similar results with the injured ventilated LS films and postulated that the surfactant failed to attain low γ because it did not spread at a rate high enough to keep up with the compression-expansion cycle during expansion. In any case, it is evident with AFM studies that albumin affects the formation of well defined domains of BLES, and also reduces the γ lowering ability of BLES films. As well, the large amorphous regions found in BLES + BSA show that the proteins may have penetrated such films and were capable of forming domains themselves (Nag *et al.*, 2004b).

Furthermore, the AFM results correlate well with the surface balance studies. The diminished formation of well defined domains shows that the phase transition of the lipids from liquid to condensed (gel-like) phase is diminished. Once again, the structure-function studies show that the disruption of BSA on lipid packing occurred, and can be correlated.

TOF-SIMS was applied to deposited BLES/BSA films to observe the localization of BSA in BLES films. As mentioned before, previous studies on pure BLES films using TOF-SIMS have suggested that the condensed domains of BLES are made of mainly DPPC and DPPG (Harbottle *et al.*, 2003). In our results, it appeared that BSA was absent in the condensed phase and present in the fluid phase of these films, whereas DPPC was present more in the condensed phase. These results correlate with the results obtained

from AFM, in that BSA seemed to interact with the BLES lipids in the fluid phase, and prevent them from forming more condensed domains, at a low γ . Previous studies have looked at the localization of surfactant lipids and proteins (such as SP-C) in films using TOF-SIMS (Bourdos *et al.*, 2000; Galla *et al.*, 1998; Harbottle *et al.*, 2003). Results examining the surfactant lipids were similar, in that DPPC lipids formed the condensed domains upon compression of the film suggesting that phospholipids could phase segregate out of the fluid phase at low γ . However when a soluble protein (BSA) was present in the films, the phase segregation process was not only altered but, specifically, the protein concentrated the fluid phase, causing this alteration.

The TOF-SIMS technique is limited to the rate of desorption of material from structures such as our BLES films, during sputtering by a primary ion beam (Bourdos *et al.*, 2000). The signal from BSA for the NH_4^+ ion was weak, due to the fact that either BSA did not completely fragment, or the protein did not desorb completely from the films to produce the signal. It also leads to another interesting possibility that the lipid-BSA complexes formed in the fluid phase (bright spots in AFM images) were difficult to fragment and/or also desorb from the films. In that case, the BSA-BLES (fluid lipid) interactions were possibly stronger than those of the protein with the condensed phase.

4.4 Differential Scanning Calorimetry

Previous studies have been done with DSC on surfactant dispersions (Hosokawa, 2003; Keough and Taeusch, 1986; Mautone *et al.*, 1987; McMurchie *et al.*, 1983; Shiffer *et al.*, 1993) as well as on pure albumin (Giancola *et al.*, 1997). This study looked at the

effect of addition of albumin to BLES on the thermotropic chain melting properties of BLES bilayers. With addition of albumin to both DPPC and BLES bilayer dispersions, there was a slight decrease in midpoint temperature, as well as a broadening of the transition peaks. This suggests that albumin disrupted the outer lipid bilayer of the multi-lamellar vesicles [Fig. 25 (b)], and affected the ability of the lipids to undergo a phase transition to the fluid phase. This is evident from the peaks shifting to a slightly lower transition temperature. Since BSA disrupted the packing, the gel regions also became more fluid, and the phase transition temperature was lowered. This suggests that when BSA interacts with the bilayer, it increases the fluidity of the lipids, thereby impeding the lipids from forming a tightly packed gel phase. This in turn causes the heterogeneity of the transition, as well as the shift in temperature to lower values.

Our DSC results strongly correlate with the studies on monolayers. It seems that in both monolayers and bilayers of BLES a similar interaction is occurring with BSA and BLES, in that BSA disrupts the lipid packing and the phase transition between fluid to gel phase. This is only possible (as seen in our TOF-SIMS results) if the protein interacts strongly with the lipids in the fluid phase. Once this occurs (whether in monolayers or bilayers) it is difficult to remove the protein's effect by changing the packing parameters either by thermal cycling in DSC or surface pressure cycling in monolayers. It is, however, puzzling that a water soluble protein would normally penetrate the bilayer hydrophobic core. However, since BSA has a number of hydrophobic pockets and its main function in plasma is to transport fatty acids after binding to them, significant hydrophobic interactions between BLES bilayers and BSA cannot be ruled out.

However, the possibility that BSA may actually disrupt packing at the head group of the phospholipids, and that such effects cause a more loose packing of the chains, seems like a more feasible explanation.

Experiments were also carried out to determine the difference in the effect of BSA, when BSA is on the outside of the first bilayer, or when it is inserted into the water layer of multiple bilayers of the multilamellar vesicles (MLV). When BSA was reconstituted into the MLV, there was a decremental shift in midpoint transition temperature by about 3 °C since, possibly, more bilayers were affected in the dispersions in the reconstitution experiment (Fig. 18). As well, using buffer instead of ddH₂O caused a slight increase in the area under the curve. It is possible that more BSA was present between the multiple lamellae of these reconstituted vesicles. As BLES contains a host of lipids which are charged, ionic repulsions between the lipid head groups and the negatively charged protein is also possible as seen in the FTIR stretching changes of the phosphate bonds. This may explain the elongation of the vesicles observed in the TEM [Fig. 19 (b)].

Studies observing the interaction of phospholipids and extrinsic (water-soluble) proteins using DSC have been carried out by others (Chapman *et al.*, 1974; Galántai and Bárdos-Nagy, 2000; Gomez-Fernandez *et al.*, 1979; reviewed by Bach, 1983). Similar trends to our results have been observed. For example, Galántai and Bárdos-Nagy, (2000) observed an increase of the pre-transition temperature of DMPC and DMPG liposomes when human serum albumin was added. As well, Chapman *et al.* (1974) observed a decrease in melting temperature of DPPC dispersions when cytochrome C

was added. In these studies, the lipid-protein ratios were much higher than those used in our study. Therefore, these results cannot be accurately compared to our results, since the mixtures tested were functionally and compositionally very different from LS/BSA, and studied as models of biological membranes (Chapman *et al.*, 1974; Bach, 1983).

4.5 Transmission Electron Microscopy

TEM was done to determine the effect of BSA on the BLES bilayer vesicles visually. In the TEM with BLES alone, the vesicles appeared concentric and tightly packed. However, when BSA was added, the vesicles appeared elongated and less tightly packed. This suggests that BSA may incorporate between the BLES lipid bilayers, and, possibly, may affect the packing of lamellae in the MLV. By doing so, it is suggested that BSA disrupts the inter-bilayer packing, and loosely packed liposomal structures are thus observed. However, major TEM analysis with various concentrations of BSA added to BLES are required to get a quantitative handle on these structures.

There have been previous studies done on EMs of BLES, but none, to our knowledge, have looked at the effect of plasma proteins on BLES using this technique (Nag *et al.*, 2004a). In the lung during disease and dysfunction, such structures as defined MLV and TM are absent. It seems our study suggests that the plasma proteins may disrupt the organization of LS bilayers, or possibly the secretory form of LB *in vivo* (Fig. 19). This in turn may not allow such vesicles to undergo a transformation to TM, or the most surface active form, as suggested by others (Nag *et al.*, 2002a; Larsson *et al.*, 2003).

As seen in the DSC results (Section 3.5), the effects of protein on the outer most bilayer of the MLV as well as in the reconstituted systems were not reversible. A previous study using giant MLV of BLES has shown the presence of gel domains at 37°C (Nag *et al.*, 2002a). Also, in our study we have observed such domains in monolayers. It is possible that the BSA probably interacts with BLES monolayers or bilayers at or close to the gel-fluid phase transition regime. This is possible since other studies have shown that interaction of proteins and additives with pure lipid bilayers occurs during defect formation (near the domain boundaries) and during domain nucleation in typical membrane systems (Mouritsen *et al.*, 1989). For BSA + BLES systems, as the first scan of the DSC is always different (data not shown) from the two successive scans, it is evident that the protein interaction may occur with such defects or domains during their formation at 37°C during the first scan. The AFM results clearly suggest that protein decreases the condensed domains and eventually abolishes them at least in monolayers.

4.6 Fourier Transform Infrared Spectroscopy

Infrared Spectroscopy is an emerging technique in the study of complex biochemical systems. IR has many advantages over other techniques such as fluorescence spectroscopy, as external probes are not required. It can monitor absorptions in all regions of the molecule, in contrast to fluorescence spectroscopy which monitors only the chromophores of a target molecule. As well, the time scale for measurements is fast compared to other techniques (Dluhy and Mendelsohn, 1988). Techniques that demand high sensitivity are now routinely available using FTIR

instruments, thereby decreasing the amounts of materials required for some studies (Dluhy and Mendelsohn, 1988).

This study used FTIR to determine the change in peak frequency and wavenumber of the bond stretches in the phospholipids molecule of BLES and also when BSA is added to BLES. Several vibrational modes were observed: the PO_2^- asymmetric (at 1228 cm^{-1}) and symmetric (at 1089 cm^{-1}), C=O (at 1733 cm^{-1}), and CH_2 symmetric (at 2851 cm^{-1}) and asymmetric (at 2920 cm^{-1}) stretching modes (Fig. 23-24). During our study, we observed that some peaks were shifted, whereas others were broadened. A shift to a higher wavenumber indicated an increased fluidity in the sample. For example, the PO_2^- asymmetric peak (Fig. 23) seemed to move to a higher wavenumber (1228 cm^{-1} up to 1240 cm^{-1}) with BSA. This would suggest that the protein induced some sort of fluidity, since others have shown that a shift to higher wavenumbers for lipid means more fluidity (Dluhy and Mendelsohn, 1988). Slight broadening of the C=O peak was observed, which may be related to hydration of the system as suggested by others (Lis *et al.*, 1976). Lis *et al.* has shown a broadening of specific peaks in DMPC membranes to be related to an increase of hydration of the system. CH_2 and CH_3 peaks were not altered dramatically however were slightly broadened.

The FTIR of pure protein did not show any C=O and PO_2^- peaks, and therefore, is assumed not to directly contribute to the lipid peaks of BLES. The CH_2 peaks were present in all samples, however, these protein peaks did not add to the BLES system since they were reduced in amounts.

With increasing concentrations of BSA, the main peaks of BLES in the headgroup (PO_4^- , $\text{C}=\text{O}$) were suppressed, and shifted slightly to different wavenumbers. At extremely high concentrations of BSA, the CH_2 peaks were also sometimes absent and new peaks appeared for the CH_3 groups (Fig. 24). The effect of BSA on the phosphate stretching vibrations suggests that the negatively charged protein may also be interacting with the head group region through charge-charge repulsions. This columbic repulsion possibly occurs as BSA at pH 7 is highly negative (-17 charge per protein) and this may have repulsive effects with the negatively charged phospholipids such as PG in BLES. The CH_2 stretching modes may not be informative because we are not sure whether the C-H stretching vibrations are observed from the hydrophobic chains, or from the head group, as both contain CH_2 and CH_3 groups. Further studies are required using deuterated phospholipids in BLES using FTIR. However, introduction of probes has its limitations, and other strategies of concentrating BLES and using liquid cells may have to be adopted.

Many of the FTIR signals seen were weak, due to the water absorption and CO_2 absorption bands (since the samples were not degassed, and were in contact with air) in the full spectra. Therefore, it was difficult to see the changes in each of the stretching modes in the complete spectra, at low concentrations of BSA.

Previous studies have looked at the stretching modes of the bonds in the phospholipid molecules of similar surfactants and membrane lipid systems (Arrondo and Goñi, 1998; Chia and Mendelsohn, 1996; Dluhy *et al.*, 1989; Mautone *et al.*, 1987; Mendelsohn *et al.*, 1984; Mendelsohn and Mantsh, 1986; Reilly *et al.*, 1989). Dluhy *et*

al., (1989) examined the stretching modes of intact pulmonary surfactant isolated from bovine lung lavage, as a function of temperature and noticed an increase in wavenumber. At room temperature however, the wavenumber of the CH₂ stretching modes were very similar to our results varying only by one or two wavenumbers (Mautone *et al.*, 1987). The difference may be due to the fact that natural LS has cholesterol in it (and thus may be more fluid) whereas BLES does not. Reilly *et al.* (1989) used DSC and FTIR to study the interaction of SP-A reconstituted into a binary lipid mixture of acyl chain predeuterated DPPC: DPPG. They observed that high levels of SP-A induced an ordering of the phospholipids, as shown by an increase in temperature of phase transition, and also an incremental shift in wavenumber with an increase in temperature. As an attenuated system (ATR) was used by these authors, it is possible that our FTIR does not have the sensitivity to detect such changes. However, it is more likely that BSA does not have the same effect as SP-A, due to completely different structural and functional properties of the protein. In fact, few previous studies have shown SP-A to remove the inhibition of surfactant caused by plasma proteins (Casals *et al.*, 1998; Cockshutt *et al.*, 1990; Nag *et al.*, 2004c). Taking into account the disrupting effect of BSA on BLES and these other studies on SP-A, it is highly possible that SP-A actually increases the ordering of the phospholipids in surfactant. This also may be the reason why SP-A enhances the adsorption [instead of inhibiting it (as BSA)] of LS lipids by ordering them (Nag *et al.*, 2004c). This ordering (into specific structures such as TM and more compact bilayers) may be tolerated with a reasonable amount of inhibitory proteins, but is eventually destroyed after a certain concentration of protein is reached. This may be the reason TM

type structures are not observed in dysfunctional surfactant dispersions (Panda *et al.*, 2004).

Some other studies have looked at protein lipid interactions with LS lipids, as well. Mendelsohn *et al.* (1984) noted a shift in wavenumber of the CH₂ stretching modes of PS when the transmembrane protein glycophorin was added to the PS membranes. This shift was towards a higher wavenumber, suggesting disorder of the lipids induced by the protein. These results correlate with ours, in that the protein was perturbing the bilayer packing, causing disorder of the hydrophobic chains. Similar results using FTIR have been observed in studies of DMPC with gramicidin A, DPPC and ATPase, DPPC and bacteriorhodopsin (Cortijo *et al.*, 1982), and DMPC with glycophorin (Mendelsohn and Mantsch, 1986). Although these studies have observed the effects of different types of proteins with different lipids, the trend is the same as our results with BLES/BSA, with slight differences in wavenumber. Others looked at lipid-protein interactions in membranes using a similar technique such as Raman spectroscopy. Lis *et al.* (1976) have shown that fibrinogen and albumin caused the CH₂ band to broaden, indicating that both proteins caused the lipid to undergo a conformational change to a more fluid phase. As well, the CH₃ band increased to a greater extent compared to CH₂, indicating that albumin and fibrinogen may penetrate the hydrocarbon chain, or the effect is translated to such regions, as we have observed in our studies.

The FTIR results relate to the previous observations of packing of BLES monolayers, as well as the DSC results on BLES bilayers. FTIR studies showed a penetration of BSA into the bilayer membrane, affecting lipid packing and disrupting the

stretching vibrations. This is similar to the DSC results, in that BSA appears to perturb the bilayer membrane, changing the pre-transition of DPPC as well as the broadening of the gel to fluid transition. The monolayer studies using AFM and TOF-SIMS also show that the protein is present in the fluid regions of the lipids.

4.7 Summary and Conclusions

LS is essential for lung function and normal respiration. Dysfunction of LS can contribute to diseases such as ARDS, among others. During ARDS, plasma proteins are one of the major contributors to inhibition of LS surface activity. Several studies have looked at effects of different plasma proteins (at various concentrations) on LS activity, however, to our knowledge, none to date have looked at the effect of small and large concentrations of serum albumin (more physiological), with monolayers and bilayers of LS.

In this study, several experiments were done on BLES monolayers and bilayers, and propositions have been made regarding some possible molecular interaction and association of albumin with BLES. Monolayer studies showed that albumin inhibits surfactant adsorption to an air-water interface, and does not allow low γ by BLES to be reached ($>10\text{mN/m}$). As well AFM studies showed that albumin inhibits the formation of well defined domains at low γ , or a decrease in condensation of the films. TOF-SIMS studies showed that albumin remains mostly in the fluid phase of lipids. DSC studies showed that albumin broadens the phase transition, and causes a decremental shift in midpoint transition temperature therefore suggesting that the protein perturbs bilayer

packing, and slightly fluidizes such bilayers. As well, FTIR showed that the protein associates with BLES bilayers near the head group and the effects are possibly translated deep into the hydrophobic core. By using different techniques, we were able to observe similar patterns of the interaction of albumin to BLES lipids, thereby suggesting a molecular model for the interaction of a serum protein with lung surfactant model membranes.

These results have prompted us to suggest a possible mechanism for albumin inhibition of surfactant. The inhibition is possibly caused by interaction and association of the protein with surfactant lipids in the fluid phase of monolayers and bilayers. Perturbation of lipid chain packing is possible if the proteins' effect is not only in the head group region but also deep in the core of the layers (Fig. 25). These results validate the hypothesis posed in section 1.8.

4.8 Future Directions

Further studies should be done to better understand the mechanism in which albumin, or other plasma proteins affect surfactant function. Wang and Notter, (1998) suggested that supplementation with large amounts of exogenous CLSE would be effective in reversing inactivation by the mixture of blood proteins. This could be useful for a future study, by increasing the concentration of BLES and determining the effects of high concentrations of albumin on it, to determine if albumin still competes for the surface, and decreases BLES adsorption. Holm *et al.* (1999) noted that free fatty acid lysophosphatidylcholine (LPC) was found to reduce surface activity even at high

concentrations of LS where inhibition by other serum proteins was abolished. It was suggested that LPC and albumin act in different ways to inhibit the films from reaching low γ (Cockshutt and Possmayer, 1991). This may be a suggestion for future study: testing the different inhibition mechanisms of plasma proteins, and free fatty acids on BLES. In addition, experiments should be done with multiple ionic and buffered states. Further FTIR studies should be done to determine the effect of albumin on the hydrophobic tails of the phospholipid molecules, as well, the temperature dependent shift in wavenumber when a protein is added to the mixture, and the effects would be interesting to observe. In addition, experiments should be done on how albumin affects surfactant proteins SP-B and SP-C present in BLES, probably by labeling such proteins with chromophores. Some of these studies are being attempted in our laboratory, by others.

REFERENCES

- Avery, M.E., Mead, J. (1959) Surface properties in relation to atelectasis and hyaline membrane disease. *Amer. Med. Assoc. J. Dis. Child* 97(5 Part 1): 517-523.
- Ashbaugh, D.G., Bigelow, D.B., Petty, T.L., and Levine, B.E. (1967). Acute respiratory distress in adults. *Lancet*. 2(7511): 319-323.
- Amirkhanian, J.D., and Taeusch, H.W. (1993). Reversible and irreversible inactivation of preformed pulmonary surfactant surface films by changes in subphase constituents. *Biochim. Biophys. Acta*. 1165: 321-326.
- Arrondo, J.L.R., and Goñi, F.M. (1998). Infrared studies of protein-induced perturbation of lipids in lipoproteins and membranes. *Chem. Phys. Lip.* 96: 53-68.
- Baatz, J.E., Elledge, B., and Whitsett, J.A. (1990). Surfactant protein SP-B induces ordering at the surface of model membrane bilayers. *Biochemistry*. 29: 6714-6720.
- Bach, D. (1983). Chapter 1: Calorimetric studies of model and natural biomembranes. *Biomembrane Structure and Function*. Ed. Dennis Chapman. The MacMillan Press Limited, London.
- Bardos-Nagy, I., and Galantai, R. (2003). Effect of Trehalose on the nonbond associative interactions between small unilamellar vesicles, and human serum albumin and on the aging process. *Langmuir*. 19: 146-153.
- Baro, A.M., Miranda, R., Alaman, J., Garcia, N., Binnig, G., Rohrer, H., Gerber, C., and Carrascosa, J.L. (1985). Determination of surface topography of biological specimens at high resolution by scanning tunneling microscopy. *Nature*. 315(6106): 253-254.
- Bartlett, G.R. (1959). Phosphorus Assay in Column Chromatography. *J. Biol. Chem.* 234: 466-468.
- Beers, M.F., and Fisher, A.B. (1992). Surfactant protein C- A review of its unique properties and metabolism. *Amer. J. of Physiol. (Lung Cell. Mol. Physiol)*. 263: L151-L160.
- Bernard, G.R., and Brigham, K.L. (1986). Pulmonary edema: Pathophysiologic mechanisms and new approaches to therapy. *Chest*. 89(4):594-600.

- Bernard, G.R., Artigas, A., Brigham, K.L., Carlet, J., Falke, K., Hudson, L., Lamy, M., Legall, J.R., Morris, A., and Spragg, R. (1994). The American-European consensus conference on ARDS: Definitions, mechanisms, relevant outcomes, and clinical trial coordination. *Amer. J. Respir. Crit. Care Med.* 149: 818-824.
- Bligh, E., and Dyer, W. (1959). A rapid method of total lipid extraction and purification. *Can. J. Biochem. Physiol.* 37: 911-917.
- Body, D.R. (1971). The phospholipids composition of pig lung surfactant. *Lipids.* 6(9): 625-629.
- Bourdos, N., Kollmer, F., Benninghoven, A., Ross, M., Sieber, M., and Galla, H-J. (2000). Analysis of lung surfactant model systems with time-of-flight secondary ion mass spectrometry. *Biophys. J.* 79: 357-369.
- Brown, J.R. (1975). Structure of Bovine serum albumin. *Fed. Proc.* 34: 591-591.
- Carter, D.C., and Ho, J.X. (1994). Structure of serum albumin. *Adv. Prot. Chem.* 45: 153-203.
- Casals, C., Varela, A., Ruano, M.L.F., Valiño, F., Pérez-Gil, J., Torre, N., Jorge, E., Tendillo, F., and Castillo-Olivares, J.L. (1998). Increase of C-reactive protein and decrease of surfactant protein A in surfactant after lung transplantation. *Amer. J. Respir. Crit. Care Med.* 157: 43-49.
- Chapman, D., Urbina, J., and Keough, K.M.W. (1974). Biomembrane phase transitions. *J. Biol. Chem.* 249: 2512.
- Chi, L.F., Fuchs, H., Johnston, R.R., and Ringsdorf, H. (1994). Inhomogeneities of phase separated langmuir-blodgett films studied by atomic force microscopy. *Journal of Vacuum Science & Technology B: Microelectronics and Nanometer Structures.* 12: 1967-1972.
- Chia, N-C., and Mendelsohn, R. (1996). Conformational disorder in unsaturated phospholipids by FTIR spectroscopy. *Biochim. Biophys. Acta.* 1283: 141-150.
- Clark, J.C., Wert, S.E., Bachurski, C.J., Stahlman, M.T., Stripp, B.R., Weaver, T.E., and Whitsett, J.A. (1995). Targeted disruption of the surfactant protein B gene disrupts surfactant homeostasis, causing respiratory failure in newborn mice. *Proc. Natl. Acad. Sci. USA.* 92: 7794-7798.
- Clements, J.A. (1957). Surface tension of lung extracts. *Proc. Soc. Exper. Biol.* 95:170-172.

- Cockshutt, A.M., and Possmayer, F. (1991). Lysophosphatidylcholine sensitizes lipid extracts of pulmonary surfactant to inhibition by serum proteins. *Biochim. Biophys. Acta.* 1086: 63-71.
- Cockshutt, A.M., Weitz, J., and Possmayer, F. (1990). Pulmonary surfactant-associated protein A enhances the surface activity of lipid extract surfactant and reverses inhibition by blood proteins in vitro. *Biochem.* 29(36): 8424-8429.
- Cortijo, M., Alonso, A., Gómez-Fernández, J.C., Chapman, D. (1982). Intrinsic protein-lipid interactions. Infrared spectroscopic studies of gramicidin A, bacteriorhodopsin, and Ca^{2+} - ATPase in biomembranes and reconstituted systems. *J. Mol. Biol.* 157: 597-618.
- Crouch, E. (1998). Collectins and pulmonary host defense. *Amer. J. of Respir. Cell Mol. Biol.* 19: 177-201.
- Dluhy, R.A., and Mendelsohn R. (1988). Emerging techniques in biophysical FT-IR. *Anal. Chem.* 60(4): 269-278.
- Dluhy, R.A., Reilly, K.E., Hunt, R.D., Mitchell, M.L., Mautone, A.J., and Mendelsohn, R. (1989). Infrared spectroscopic investigations of pulmonary surfactant. Surface film transitions at the air-water interface and bulk phase thermotrophism. *Biophys. J.* 56: 1173-1181.
- Doyle, R.L., Szaflarski, N., Modin, G.W., Wiener -Kronish, J.P., and Matthay, M.A. (1995). Identification of patients with acute lung injury: predictors of mortality. *Amer. J. Respir. Crit. Care Med.* 152: 1818-1824.
- Engel, A., and Müller, D. (2000). Observing single biomolecules at work with the atomic force microscope. *Nature Struc. Biol.* 9: 715-718.
- Enhoring, G. (1977). Pulsating bubble technique for evaluating pulmonary surfactant. *J. Appl. Physiol.* 43: 198-203.
- Enhoring, G., Hohlfeld, J., Krug, N., Lema, G., and Welliver, R.C. (2000). Surfactant function affected by airway inflammation and cooling: possible impact on exercise-induced asthma. *Eur. Respir. J.* 15: 532-538.
- Figge, J., Rossing, T.H., and Fencl, V. (1991). The role of serum-proteins in acid-base equilibria. *J. Lab. Clin. Med.* 117: 453-467.
- Flanders, B.N., and Dunn, C. (2002). A near-field microscopy study of submicron domain structure in a model lung surfactant monolayer. *Ultramicroscopy.* 91: 245-251.

- Fleming, B.D., and Keough, K.M.W. (1988). Surface respreading after collapse of monolayers containing major lipids of pulmonary surfactant. *Chem. Phys. of Lip.* 49: 81-86.
- Floros, J., and Phelps, D. (1997). Chapter 73: Pulmonary Surfactant. *Anaesthesia: Biologic Foundations*. Lippincott-Raven Publishers. Philadelphia.
- Fuchimukai, T., Fujiwara, T., Takahashi, A., and Enhorning, G. (1987). Artificial pulmonary surfactant inhibited by proteins. *J. Appl. Physiol.* 62(2):429-437.
- Galla, H-J., Bourdos, N., von Nahmen, A., Amrein, M., and Sieber, M. (1998). The role of pulmonary surfactant protein C during the breathing cycle. *Thin Solid Films.* 327-329: 632-635.
- Galántai, R., and Bárdos-Nagy, I. (2000) The interaction of human serum albumin and model membranes. *Int. J. Pharm.* 195: 207-218.
- Giancola, C., De Sena, C., Fessas, D., Graziano, G., and Barone, G. (1997). DSC studies on bovine serum albumin denaturation: effects of ionic strength and SDS concentration. *Int. J. Biol. Macromol.* 20: 193-204.
- Glasser, S.W., Burhans, M.S., Korfhagen, T.R., Na, C.L., Sly, P.D., Ross, G.F., Ikegami, M., and Whitsett, J.A. (2001). Altered stability of pulmonary surfactant in SP-C deficient mice. *Proc. Natl. Acad. Sci. USA.* 98(11): 6366-6371.
- Goerke, J. (1998). Pulmonary surfactant: functions and molecular composition. *Biochim. Biophys. Acta* 1408: 79-89.
- Goerke, J. (1974). Lung Surfactant. *Biochim. Biophys. Acta* 344(3-4): 241-261.
- Gomez-Fernandez, J.C., Goni, F.M., Bach, D., Restall, C., and Chapman, D. (1979). Protein--lipid interactions. A study of (Ca²⁺-Mg²⁺)ATPase reconstituted with synthetic phospholipids. *FEBS Letters.* 98: 224.228.
- Goodman, D.S. (1958). The interaction of human serum albumin with long-chain fatty acid anions. *J. Amer. Chem. Soc.* 80: 3892-3898.
- Griese, M. (1999). Pulmonary surfactant in health and human lung diseases: state of the art. *Eur. Respir. J.* 13:1455-1476.
- Griese, M., Dietrich, P., Potz, C., Westerburg, B., Bals, R., and Reinhardt, D. (1996). Surfactant subfractions during nosocomial infection in ventilated preterm human neonates. *Amer. J. Respir. Crit. Care Med.* 153: 398-403.

- Groniowski, J., and Walski, M. (1979). Further studies on the tubular myelin structure of extracellular alveolar lining layer. *Acta Medica Polona*. 20(1): 15-16.
- Gross, N.J. (1995). Extracellular metabolism of pulmonary surfactant: the role of a new serine protease. *Annu. Rev. Physiol.* 57: 135-150.
- Gustafsson, M., Griffiths, W.J., Furosjö, E., and Johansson, J. (2001). The palmitoyl groups of lung surfactant protein C reduce unfolding into a fibrillogenic intermediate. *J. Mol. Biol.* 310: 937-950.
- Haagsman, H.P., White, R.T., Schilling, J., Lau, K., Benson, B.J., Golden, J., Hawgood, S., and Clements, J.A. (1989). Studies of the structure of lung surfactant protein SP-A. *Amer. J. Physiol.* 257(6 Pt 1): L421-429.
- Hansma, H.G., Kim, K.J., and Laney D.E. (1997). Properties of biomolecules measured from atomic force microscope images: a review. *J. Struct. Biol.* 119: 99-108.
- Harbottle, R.R., Nag, K., McIntyre, S., Possmayer, F., and Peterson, N.O. (2003). Molecular organization revealed by time-of-flight secondary ion mass spectrometry of a clinically used extracted pulmonary surfactant. *Langmuir*. 19(9): 3698-3704.
- Holm, B.A. (1992). Chapter 27: Surfactant Inactivation in Adult Respiratory Distress Syndrome. Pulmonary Surfactant: from molecular biology to clinical practice. Ed.B. Robertson, L.M.G. Van Golde, and J.J. Batenburg. Elsevier Science Publishers: Oxford, England.
- Holm, B.A., Enhorning, G., and Notter, R.H. (1988). A biophysical mechanism by which plasma proteins inhibit lung surfactant activity. *Chem. Phys. Lip.* 49: 49-55.
- Holm, B.A., and Notter, R.H. (1987). Effects of hemoglobin and cell membrane lipids on pulmonary surfactant activity. *J. Appl. Physiol.* 63: 1434-1442.
- Holm, B.A., Notter, R.H., and Finkelstein, J.H. (1985). Surface property changes from interactions of albumin with natural lung surfactant and extracted lung lipids. *Chem. Phys. Lip.* 38: 287-298.
- Holm, B.A., Wang, Z., and Notter, R.H. (1999). Multiple mechanisms of lung surfactant inhibition. *Ped. Res.* 46(1): 85-93.
- Hosokawa, T., Sami, M., Kato, Y., and Hayakawa, E. (2003). Alteration in the temperature-dependent content release property of thermosensitive liposomes in plasma. *Chem. Pharm. Bull.* 51(11): 1227-1232.

- Ikegami, M., Whitsett, J.A., Jobe, A., Ross, G., Fisher, J., and Korfhagen, T. (2000). Surfactant metabolism in SP-D gene-targeted mice. *Amer. J. Physiol. (Lung Cell. Mol. Physiol.)*. 279: L468-L476.
- Jacobson, W., Park, G.R., Saich, T., and Holcroft, J. (1993). Surfactant and adult respiratory distress syndrome. *Brit. J. Anaesth.* 70: 522-526.
- Janshoff, A., and Steinem, C. (2001). Scanning force microscopy of artificial membranes. *Chembiochem.* 2: 798-808.
- Johansson, J. (1998). Structure and properties of surfactant protein C. *Biochim. Biophys. Acta* 1408(2-3): 161-172.
- Johansson, J., Curstedt, T., and Robertson, B. (1994). The proteins of the surfactant system. *Eur. Respir. J.* 7(2): 372-391.
- Kaganer, V.M., Mohwald, H., and Dutta, P. (1999). Structure and phase transitions in Langmuir monolayers. *Rev. Mod. Phys.* 71: 779-819.
- Keough, K.M.W., and Kariel, N. (1987). Differential scanning calorimetric studies of aqueous dispersions of phosphatidylcholines containing two polyeoic chains. *Biochim. Biophys. Acta.* 902:11-18.
- Keough, K.M.W., Parsons, C.S., Phang, P.T., and Tweeddale, M.G. (1988). Interactions between plasma proteins and pulmonary surfactant: surface balance studies. *Can. J. Physiol. Pharmacol.* 66: 1166-1173.
- Keough, K.M.W., Parsons, C.S., and Tweeddale, M.G. (1989). Interactions between plasma proteins and pulmonary surfactant: pulsating bubble studies. *Can. J. Physiol. Pharmacol.* 67:663-668.
- Keough, K.M.W., and Taeusch, H.W. Jr. (1986). Surface balance and differential scanning calorimetric studies on aqueous dispersions of mixtures of dipalmitoylphosphatidylcholine and short-chain saturated phosphatidylcholines. *J. Coll. Interf. Sci.* 109: 364-375.
- King, R.J., Clements, J.A. (1972). Surface active materials from dog lung I, II, III. *Amer. J. Physiol.* 223(3): 707-733.
- Larsson, M., Larsson, K., Nylander, T., and Wollmer, P. (2003). The bilayer melting transition in lung surfactant bilayers: the role of cholesterol. *Eur. Biophys. J.* 31: 633-636.

- Lewis, J., and Jobe, A. (1993). State of the art: Surfactant and the adult respiratory distress syndrome. *Amer. Rev. Respir. Dist.* 147: 218-233.
- Lis, J.S., Kauffman, J.W., and Shriver, D.F. (1976). Raman spectroscopic detection and examination of the interaction of amino acids, polypeptides, and proteins with the phosphatidylcholine lamellar structure. *Biochim. Biophys. Acta.* 436: 513-522.
- Liu, Y., and Chang, C. (2002). Inhibitory effects of fibrinogen on the dynamic tension-lowering activity of dipalmitoyl phosphatidylcholine dispersions in the presence of tyloxapol. *Coll. Polym. Sci.* 280: 683-687.
- Matalon, S., Benos, D.J., and Jackson, R.M. (1996). Biophysical and molecular properties of amiloride-inhibitable Na⁺ channels in alveolar epithelial cells. *Amer. J. Physiol.* 271: L1-L22.
- Matsudomi, N., Ohhita, T., Kohayashi, K. and Kinsella, J.E. (1993). α -Lactalbumin enhances the gelation properties of bovine serum albumin. *J. of Agric. Food Chem.* 41: 1053-1057.
- Mautone, A.J., Reilly, K.E., and Mendelsohn, R. (1987). Fourier transform infrared and differential scanning calorimetric studies of a surface-active material from rabbit lung. *Biochim. Biophys. Acta.* 896(1): 1-10.
- McEachren, T.M., and Keough, K.M.W. (1995). Phosphocholine reverses inhibition of pulmonary surfactant adsorption caused by C-reactive protein. *Amer. J. Physiol. (Lung Cell Mol. Physiol.)*. 13: L492-497.
- McMurchie, E.J., Teubner, J.K., and Gibson, R.A. (1983). Thermal phase transitions in sheep, rat and rabbit surfactant lipids detected by differential scanning calorimetry. *Comp. Biochem. Physiol. A Comp. Physiol.* 74(2): 295-299.
- Melton, K.R., Nesslein, L.L., Ikegami, M., Tichelaar, J.W., Clark, J.C., Whitsett, J.A., and Weaver, T.E. (2003). SP-B deficiency causes respiratory failure in adult mice. *Amer. J. Physiol. (Lung Cell Mol. Physiol.)*. 285(3): L543-549.
- Mendelsohn, R., Dluhy, R.A., Crawford, T., and Mantsch, H.H. (1984). Interaction of glycoporphin with phosphatidylserine: A Fourier transform infrared investigation. *Biochemistry.* 23:1498-1504.
- Mendelsohn, R., and Mantsch, H.H. (1986). Chapter 4: Fourier transform infrared studies of lipid-protein interaction. *Progress in Protein-Lipid Interactions 2*. Elsevier Science Publishers BV., London.

- Mouritsen, O.G., Ipsen, J.H., and Zuckermann, M. (1989). Lateral density fluctuation in the chain melting phase transition of lipid monolayers. *J. Coll. Interf. Sci.* 129: 32-40.
- Murray, J.F. (1977) Mechanisms of acute respiratory failure. *Amer. Rev. Respir. Dis.* 115:1071-1078.
- Nag, K. (1996). Association and interactions of lipids and proteins of pulmonary surfactant in model membranes at the air-water interface. *Ph.D. Thesis*, Department of Biochemistry, Memorial University of Newfoundland, St. John's, Newfoundland, Canada A1B 3X9.
- Nag, K., Boland, C., Rich, N., and Keough, K.M.W. (1990). Design and construction of an epifluorescence microscopic surface balance for the study of lipid monolayer phase transitions. *Rev. Sci. Instrum.* 61: 3425-3430.
- Nag, K., Harbottle, R.R., and Panda, A.K. (2000). Molecular architecture of a self-assembled bio-interface: lung surfactant. *J. Surf. Sci. Technol. (India)*. 16: 157-170.
- Nag, K., Harbottle, R.R., Panda, A.K., Hearn, S.A., and Petersen, N.O. (2004a). Physicochemical Mapping of Phase Heterogeneity in Biomembrane Films. *Microscopy and Analysis*. 18(1): 13-15.
- Nag, K., Harbottle, R.R., Panda, A.K., and Petersen, N.O. (2004b). Chapter 17: Atomic force microscopy of interfacial monomolecular films of pulmonary surfactant. in *Atomic Force Microscopy: Biomedical Methods and Applications*. Eds. P.C. Brag and D. Ricci. Humana Press, Totowa, N.J. 242: 231-243.
- Nag, K., Munro J.G., Hearn, S.A., Rasmusson, J., Petersen, N.O., and Possmayer, F. (1997a). Correlated atomic force and transmission electron microscopy of nanotubular structures in pulmonary surfactant. *J. Struct. Biol.* 126: 1-15.
- Nag, K., Munro, J.G., Inchley, K., Schurch, S., Petersen, N.O., and Possmayer, F. (1999). SP-B refining of pulmonary surfactant phospholipids films. *Amer. J. Physiol.* 277 (6 Pt 1): L1179-1189.
- Nag, K., Panda, A.K., Au, B.H., Heyd, D.V., Harbottle, R.R., Schoel, M., Petersen, N.O., and Bagatolli, L.A. (2002a). Biophysical studies of nano-structured interfaces as models of lung surfactant membranes. *Rec. Res. Dev. Biophys.* 1: 53-70.
- Nag, K., Pao, J-S., Harbottle, R.R., Possmayer, F., Petersen, N.O., and Bagatolli, L.A. (2002b). Segregation of saturated chain lipids in pulmonary surfactant films and bilayers. *Biophys. J.* 82: 2041-2051.

- Nag, K., Pérez-Gil, J., Ruano, M.L.F., Worthman, L.A.D., Stewart, J., Casals, C., and Keough, K.M.W. (1998). Phase transitions in films of lung surfactant at the air-water interface. *Biophys. J.* 74: 2983-2995.
- Nag, K., Rodriguez-Capote, K., Panda, A.K., Frederic, L., Hearn, S.A., Petersen, N.O., Schurch, S., and Possmayer, F. (2004c). Disparate effects of two phosphatidylcholine binding proteins, C-reactive protein (CRP) and surfactant protein A (SP-A) on pulmonary surfactant structure and function. *Amer. J. Physiol.* 287: L1145-L1153.
- Nag, K., Taneva, S.G., Pérez-Gil, J., Cruz, A., and Keough, K.M.W. (1997b). Combinations of fluorescently labelled pulmonary surfactant proteins SP-B and SP-C in phospholipid films. *Biophys. J.* 72(6): 2638-2650.
- von Nahmen, A., Schenk, M., Sieber, M., and Amrein, M. (1997). The structure of a model pulmonary surfactant as revealed by scanning force microscopy. *Biophys. J.* 72(1): 463-469.
- Notter, R.H. (2000). Lung Surfactants: Basic Science and Clinical Applications. Marcel Dekker Inc., New York, N.Y.
- Notter, R.H., and Finkelstein, J.N. (1984). Pulmonary surfactant: an interdisciplinary approach. *J. Appl. Physiol.* 57: 1613-1624.
- Notter, R.H., Holcomb, H., and Mavis, R.D. (1980). Dynamic surface properties of phosphatidylglycerol-dipalmitoylphosphatidylcholine mixed films. *Chem. Phys. Lip.* 27: 305-319.
- Otsubo, E., and Takei, T. (2002). Characterization of the surface activity of a synthetic surfactant with albumin. *Biol. Pharm. Bull.* 25(12): 1519-1523.
- Paananen, R., Postle, A.D., Clark, G., Glumoff, V., and Hallman, M. (2002). Eustachian tube surfactant is different from alveolar surfactant: determination of phospholipid composition of porcine eustachian tube lavage fluid. *J. Lip. Res.* 43: 99-106.
- Palaniyar, N., McCormack, F.X., Possmayer, F., and Harauz, G. (2000). Three-dimensional structure of rat surfactant protein A trimers in association with phospholipids monolayers. *Biochemistry.* 39(21): 6310-6316.
- Panda, A.K., Nag, K., Harbottle, R.R., Rodriguez-Capote, K., Veldhuizen, R.A.W., Peterson, N.O., and Possmayer, F. (2004). Effects of acute lung injury on structure and function of pulmonary surfactant films. *Amer. J. Respir. Cell Mol. Biol.* 30: 1-10.

- Panaiotov, I., Ivanova, Tz., Proust, J., Boury, F., Denizot, B., Keough, K.M.W., and Taneva, S. (1996). Effect of hydrophobic protein SP-C on structure and dilatational properties of the model monolayers of pulmonary surfactant. *Coll. Surf. B: Biointerfaces*. 6: 243-260.
- Pattle, R.E. (1958). Properties, function, and origin of the alveolar lining layer. *Proceedings of the Royal Society of London-Series B: Biological Sciences*. 148: 217-240.
- Pattle, R.E. (1955). Properties, function, and origin of the alveolar lining layer. *Nature*. 175: 1125-1126.
- Pérez-Gil, J., and Keough, K.M.W. (1998). Interfacial properties of surfactant proteins. *Biochim. Biophys. Acta*. 1408: 203-217.
- Peters, T. Jr. (1985). Serum Albumin. *Adv. Prot. Chem.* 37:161-245.
- Pison, U., Herold, R., and Schurch, S. (1996). The pulmonary surfactant system: biological functions, components, physicochemical properties and alterations during lung disease. *Coll. Surf. A: Physicochemical and Engineering Aspects*. 114:165-184.
- Pittet, J.F., Mackenzie, R.C., Martin, T.R., and Matthay, M.A. (1997). Biological markers of acute lung injury: prognostic and pathogenic significance. *Amer. J. Respir. Crit. Care Med.* 155: 1187-1205.
- Pugin, J., Verghese, G., Widmer, M.C., and Matthay, M.A. (1999). The alveolar space is the site of intense inflammatory and profibrotic reactions in the early phase of ARDS. *Crit. Care Med.* 27: 304-312.
- Poole, S., West, S.I., and Walters, C.L. (1984). Protein-protein interactions: their importance in forming of heterogeneous protein systems. *J. Sci. Food Agric.* 35: 701-711.
- Possmayer, F. (2004). Physicochemical aspects of pulmonary surfactant in fetal and neonatal physiology (3rd Ed.). Ed. Polin, R., Fox, W.W., and Abman, S.H. WB Saunders Company, Philadelphia, PA. pp. 1014-1034.
- Possmayer, F. (1990). The role of surfactant-associated proteins. *Amer. Rev. Respir. Dis.* 142(4): 749-752.
- Possmayer, F., Nag, K., Rodriguez, K., Qanbar, R., and Schurch, S. (2001). Surface activity in vitro: role of surfactant proteins. *Comp. Biochem. Physiol. A: Mol. Integ. Physiol.* 129: 209-220.

- Postle, T. (2000). The analysis of lung surfactant phospholipids by electrospray ionisation mass spectrometry-applications to disease states. *Appl. Cardiopulm. Pathophysiol.* 9: 286-289.
- Postle, A.D., Heeley, E.L., and Wilton, D.C. (2001). A comparison of the molecular species compositions of mammalian lung surfactant phospholipids. *Comp. Biochem. Physiol. A: Mol. Integ. Physiol.* 129(1): 65-73.
- Postle, A.D., Mander, A., Reid, K.B.M., Wang, J.Y., Wright, S.M., Moustaki, M., and Warner, J.O. (1999). Deficient hydrophilic lung surfactant proteins A and D with normal surfactant phospholipid molecular species in cystic fibrosis. *Amer. J. Respir. Cell Mol. Biol.* 20:90-98.
- Reilly, K.E., Mautone, A.J., and Mendelsohn, R. (1989). Fourier-transform infrared spectroscopy studies of lipid/protein interaction in pulmonary surfactant. *Biochemistry.* 28:7368-7373.
- Rice, W.R., Sarin, V.K., Fox, J.L., Baatz, J., Wert, S., and Whitsett, J.A. (1989). Surfactant peptides stimulate uptake of phosphatidylcholine by isolated cells. *Biochim. Biophys. Acta.* 1006: 237-245.
- Robertson, B., Van Golde, L.G., and Batenburg, J.J. (1992). Pulmonary Surfactant: from molecular biology to clinical practice. Elsevier. Amsterdam.
- Rosenoer, V.M., Oratz, M., and Rothschild, M.A. (1977). Albumin structure, function, and uses. Pergamon Press: Oxford, England.
- Schurch, S., Goerke, J., and Clements, J.A. (1976). Direct determination of surface tension in the lung. *Proc. Natl. Acad. Sci. USA.* 73: 4698-4702.
- Schurch, S., Possmayer, F., Cheng, S., and Cockshutt, A.M. (1992). Pulmonary SP-A enhances adsorption and appears to induce surface sorting of lipid extract surfactant. *Amer. J. Physiol.* 263(6 Pt 1): L210-218.
- Shelley, S.A., Paciga, J.E., Balis, J.U. (1984). Lung surfactant phospholipids in different animal species. *Lipids.* 19: 857-862.
- Shiffer, K., Hawgood, S., Haagsman, H.P., Benson, B., Clements, J.A., and Goerke, J. (1993) Lung surfactant proteins SP-B and SP-C, alter the thermodynamic properties of phospholipid membranes: a differential calorimetry study. *Biochemistry.* 32(2): 590-597.

- Spragg, R.G., and Lewis, J.F. (2003). Surfactant therapy in acute respiratory distress syndrome. In: *Acute Respiratory Distress Syndrome*. Ed. M.A. Matthay, Ch. 19., M.Dekker, New York, NY
- Sznajder, S.I. (1999). Strategies to increase alveolar epithelial fluid removal in the injured lung. *Amer. J. Respir. Crit. Care Med.* 160: 1441-1442.
- Taneva, S., and Panaiotov, I. (1984). Effect of surface pressure on mixed dipalmitoyl- lecithin-serum albumin monolayer composition. *Coll. Surf.* 10: 101-111.
- Taneva, S., Voelker, D.R., and Keough, K.M.W. (1997). Adsorption of pulmonary surfactant protein D to phospholipid monolayers at the air-water interface. *Biochemistry.* 36: 8173-8179.
- Veldhuizen, R., Nag, K., Orgeig, S., and Possmayer, F. (1998). The role of lipids in pulmonary surfactant. *Biochim. Biophys. Acta.* 1408: 90-108.
- Veldhuizen, R., Welk, B., Harbottle, R., Hearn, S., Nag, K., Petersen, N.O., and Possmayer, F. (2002). Mechanical ventilation of isolated rat lungs changes the structure and biophysical properties of surfactant. *J. Appl. Physiol.* 92: 1169-1175.
- Veldhuizen, R.A., Yao, L.J., Hearn, S.A., Possmayer, F., and Lewis, J.F. (1996). Surfactant associated protein A is important for maintaining surfactant large-aggregate forms during surface-area cycling. *Biochem. J.* 313 (Part 3): 835-840.
- Wang, Z., and Notter, R.H. (1998). Additivity of protein and nonprotein inhibitors of lung surfactant activity. *Amer. J. Respir. Crit. Care Med.* 158(1): 28-35.
- Ware, L.B., and Matthay, M.A. (2000). The acute respiratory distress syndrome. *New Engl. J. Med.* 342(18): 1334-1349.
- Ware, L.B., and Matthay, M.A. (1999). Maximal alveolar epithelial fluid clearance in clinical acute lung injury: an excellent predictor of survival and the duration of mechanical ventilation. *Amer. J. Respir. Crit. Care Med.* 159: Suppl: A694. Abstract.
- Warriner, H.E., Ding, J., Waring, A.J., and Zasadzinski, J.A. (2002). A concentration-department mechanism by which serum albumin inactivates replacement lung surfactants. *Biophys. J.* 82: 835-842.
- Watanabe, H., Kragh-Hansen, U., Tanase, S., Nakajou, K., Mitarai, M., Iwao, Y., Maruyama, T., and Otagiri, M. (2001) Conformational stability and warfarin-binding properties of human serum albumin studied by recombinant mutants. *Biochem. J.* 357: 269-274.

- Wetzel, R., Becker, M., Behlke, J., Billwitz, H., Bohm, S., Ebert, B., Hamann, H., Krumbiegel, J., and Lasmann, G. (1980). Temperature behaviour of human serum albumin. *Eur. J. Biochem.* 104: 469-478.
- Wirtz, H.R., Dobbs, L.G. (2000). The effects of mechanical forces on lung functions. *Respir. Physiol.* 119: 1-17.
- Wright, J.R. (1997) Immunomodulatory functions of surfactant. *Physiol. Rev.* 77:931-962.
- Wright, J.R., and Hawgood S. (1989). Pulmonary Surfactant Metabolism. *Clin. Chest Med.* 10(1): 83-93.
- Yu, S.H., Harding, P.G., Smith, N., and Possmayer, F. (1983). Bovine pulmonary surfactant: chemical composition and physical properties. *Lipids.* 18(8): 522-529.
- Yu, S.H., and Possmayer, F. (1990). Role of bovine pulmonary surfactant-associated proteins in the surface-active property of phospholipids mixtures. *Biochim. Biophys. Acta.* 1046(3): 233-241.

THE UNIVERSITY OF CHICAGO
LIBRARY
1100 EAST 58TH STREET
CHICAGO, ILL. 60637
TEL: 773-936-3000
WWW.CHICAGO.EDU

